Infection of bronchial epithelial cells with pre-grown *P. aeruginosa* biofilms at Air-Liquid Interface for testing nebulized anti-infectives *in vitro*

DISSERTATION

Zur Erlangung des Grades des Doktors der Naturwissenschaften der Naturwissenschaftlich-Technischen Fakultät der Universität des Saarlandes

von

Justus Constantin Horstmann

Saarbrücken
2022

Tag des Kolloquiums:	21.07.2022
Dekan:	Prof. Dr. Jörn Walter
Berichterstatter:	Prof. Dr. Claus-Michael Lehr
	Prof. Dr. Rolf Hartmann
Vorsitz:	Prof. Dr. Marc Schneider
Akad. Mitarbeiter:	Dr. Jessica Hoppstädter

Meiner Frau und meiner Familie gewidmet

In Gedenken an meinen Vater Dr. Michael Horstmann, einem herausragenden Pharmazeuten und passionierten Technologen

Die Daten dieser Dissertation sind durch den Autor (bis auf die in den Kapiteln erwähnten Ausnahmen) zwischen März 2017 und Juli 2020 am Helmholtz-Institut für Pharmazeutische Forschung Saarland (HIPS) entstanden unter der Betreuung von Prof. Dr. Claus-Michael Lehr, Professor für Biopharmazie und Pharmazeutischer Technologie an der Universität des Saarlandes sowie Gruppenleiter der Abteilung „Drug Delivery“ am HIPS, mit Unterstützung von Frau Dr. Cristiane Carvalho-Wodarz und Dr. Nicole Schneider-Daum als wissenschaftliche Mitarbeiterinnen.

I. Table of contents

II. Abbreviations

ASM_{mod}	modified artificial sputum medium
2-AA	2-aminoacetophenone
ALI	air-liquid interface
API	active pharmaceutical ingredient
AU	arbitrary units
CAP	community-acquired pneumonia
CF	cystic fibrosis
CFTR	cystic fibrosis transmembrane conductance regulator
CV	Crystal violet
CLSM	confocal laser scanning microscope
DDEL	Department “Drug Delivery” (HIPS)
DHQ	dihydroxyquinoline
DMSO	dimethyl sulfoxide
DPI	dry powder inhaler
EDTA	ethylenediaminetetraacetic acid
ELISA	enzyme-linked immunosorbent assay
FCS	fetal calf serum
HAP	hospital-acquired pneumonia
HIPS	Helmholtz-Institute for Pharmaceutical Research Saarland
HHQ	4-hydroxy-2-heptylquinoline
HMDS	hexamethyldisilazane
HQNO	4-hydroxy-2-heptylquinoline-N-oxide
IL-8	Interleukin-8
KRB	Krebs-Ringer buffer
LCC	liquid covered conditions
LDH	lactate dehydrogenase
MBEC	minimal biofilm eradication concentration
MEM	minimal essential medium
MIC	minimal inhibitory concentration
NAC	N-acetylcysteine
NEAA	non-essential amino acids
OC	overnight culture
OD	optical density
ON	over night
PBS	phosphate-buffered saline
PCL	periciliary layer
PQS	Pseudomonas quinolone signal
QS	quorum sensing
RT	room temperature
SD	standard deviation

SEM	scanning electron microscope
TEER	trans electrical epithelial resistance
TRIS	tris(hydroxymethyl)aminomethane
UV	ultra violet

III. Short Summary

Patients suffering from lung diseases as cystic fibrosis are especially at risk contracting chronic bacterial infections[1,2]. In anti-infective research, one of the alternatives to experiments on animals are novel *in vitro* models[3,4]. In contrast to traditional tests, that comprise bacteria and the agent in one well, novel co-cultures with mammalian cells help to get a deeper understanding of host-pathogen interactions[3,5].

This work is aimed at creating and testing a realistic *in vitro* bronchial model of a *P. aeruginosa*[6] biofilm infected patient and its treatment with anti-infectives as inhaled tobramycin.

In the first of two experimental parts, the technical procedure for depositing antibiotics on top of Transwell® inserts by using a device developed at HIPS is presented. The deposition of a metered dose is thereby controlled by the invested volume. The system is tested for its applicability for infection research by assessing toxicity on cells, amongst others.

The second part presents the development and testing of a biofilm infected *in vitro* model of the lung with cells growing at the air-liquid interface. Either tobramycin and a novel pathoblocker[7] was used for testing. On the basis of the previous thesis of Dr. Juntke[8,9], a chronic-like system could be established via multiple consecutive aerosolized treatments with tobramycin[4].

IV. Kurzzusammenfassung

Patienten, die an Lungenkrankheiten wie der Mukoviszidose leiden, sind besonders anfällig, bakterielle Erkrankungen zu entwickeln[1,2]. *In vitro* Modelle sind dabei eine der Alternativen zu *in vivo* Tierversuchen[3,4]. Anders als traditionelle Tests, die nur Bakterien und Antibiotika *in vitro* untersuchen, können neue Co-Kulturen mit humanen Zelllinien zum Verständnis der „Host-Pathogen Interaction" beitragen[3,5].

Diese Arbeit befasst sich mit der Erstellung und Testung eines möglichst realistischen *in vitro* Bronchialmodells eines mit einem *P. aeruginosa*[6] Biofilm infizierten Patienten und dessen Behandlung durch Inhalation von Anti-Infektiva wie z.B. Tobramycin.

Im ersten von zwei experimentell erarbeiteten Teilen wird ein neu entwickeltes System vorgestellt, mit dem man Antibiotika auf Transwell® Einsätzen als Aerosol applizieren kann. Die deponierte Dosis wird dabei durch das Volumen der zu vernebelnden Flüssigkeit kontrolliert. Die Eignung für ein entsprechendes Infektionsmodell wird unter anderem durch die Bestimmung der Toxizität auf Zellen geprüft.

Der zweite Teil befasst sich mit der Entwicklung und Testung eines mit Biofilm infizierten Modells der Lunge mit an der Luft ausgesetzten Bronchialepithelzellen. Dabei wurde neben Tobramycin auch ein neuartiger Pathoblocker[7] eingesetzt. Aufbauend auf die vorausgegangene Dissertation von Dr. Juntke[8,9] konnte durch konsekutive Applikationen von aerosolisiertem Tobramycin ein über mehrere Tage infiziertes Modell erreicht werden[4].

1 Introduction

Parts of this chapter have already been published in the following research papers or book chapters:

Horstmann, J.C., Laric, A., Boese, A., Yildiz, D., Röhrig, T., Empting, M., Frank, N., Krug, D., Müller, R., Schneider-Daum, N., de Souza Carvalho-Wodarz, C. and Lehr, C.-M. (2022) Transferring microclusters of P. aeruginosa biofilms to the air-liquid Interface of bronchial epithelial cells for repeated deposition of aerosolized tobramycin. *ACS Infect. Dis.,* 8 (1), 137-149. DOI 10.1021/acsinfecdis.1c00444 ([4])

Horstmann, J.C., Thorn, C.R., Carius, P., Graef, F., Murgia, X., De Souza Carvalho-Wodarz, C., Lehr, C-M. (2021) A custom-made device for reproducibly depositing pre-metered doses of nebulized drugs on pulmonary cells in vitro, *Front. Bioeng. Biotechnol*. 9, 9:643491. DOI 10.3389/fbioe.2021.643491 ([10])

Carius, P.*, Horstmann, J.C.*, de Souza Carvalho-Wodarz, C. Lehr, C.M. (2020) Disease Models: Lung Models for Testing Drugs Against Inflammation and Infection. In: Schäfer-Korting M., Stuchi Maria-Engler S., Landsiedel R. (Eds.), Organotypic Models in Drug Development. Handbook of Experimental Pharmacology. Springer, Cham. DOI 10.1007/164_2020_366 (*shared first authorship) ([3])

Schneider-Daum, N., Carius, P., Horstmann, J.C., Lehr, C.M. (2020) Reconstituted 2D Cell and Tissue Models. In: Hickey, A. J. and da Rocha S.R. (Eds.), Pharmaceutical Inhalation Aerosol Technology, Third edition, CRC Press. DOI 10.1201/9780429055201 ([11])

1.1 Bacterial infections in cystic fibrosis

Cystic fibrosis is a genetical disease based on the cystic fibrosis transmembrane conductance regulator gene. The CFTR protein, that is coded by this gene, is a channel transporting chloride and bicarbonate to the apical side of epithelial cells[12]. Its normal function to transport chloride ions to the apical side is hindered in patients suffering from CF, since the protein structure of the channel is misfolded[12,13]. In response, body fluids on apical sides of epithelia in many organs are osmotically thickened, leading to obstipation of pancreas tubes and gastrointestinal problems, since pancreatic enzymes are hindered to reach the gastrointestinal tract, to name an example[13]. Lung mucus, usually produced by goblet cells, is easily transported to the nasopharyngeal area by the so called “mucociliary escalator” in healthy individuals[12] (Figure 1.1 left). This transport mechanism, that works via a synchronic beating pattern of small cilia on the apical side of bronchial epithelial cells, is hindered in patients with CF. Mucus being more viscous in CF causes the cilia to be compressed, that normally beat the mucus layer towards the nasopharyngeal region in a less viscous medium, called the periciliary layer (PCL)[14] or airway surface liquid (ASL)[1]. Mucus is a very important biological barrier in the lung, consisting mainly of water (about 95%), forming a gel together with the glycoprotein mucin, but also consists of other factors as phospholipids, cholesterol, salts and other proteins[15]. It protects the epithelial cell barrier physically against all kinds of particles, but bacteria are also physically removed[1,14,16]. Epithelium is additionally protected by proteins in the mucus as defensins, immunoglobulins and lysozyme[15].

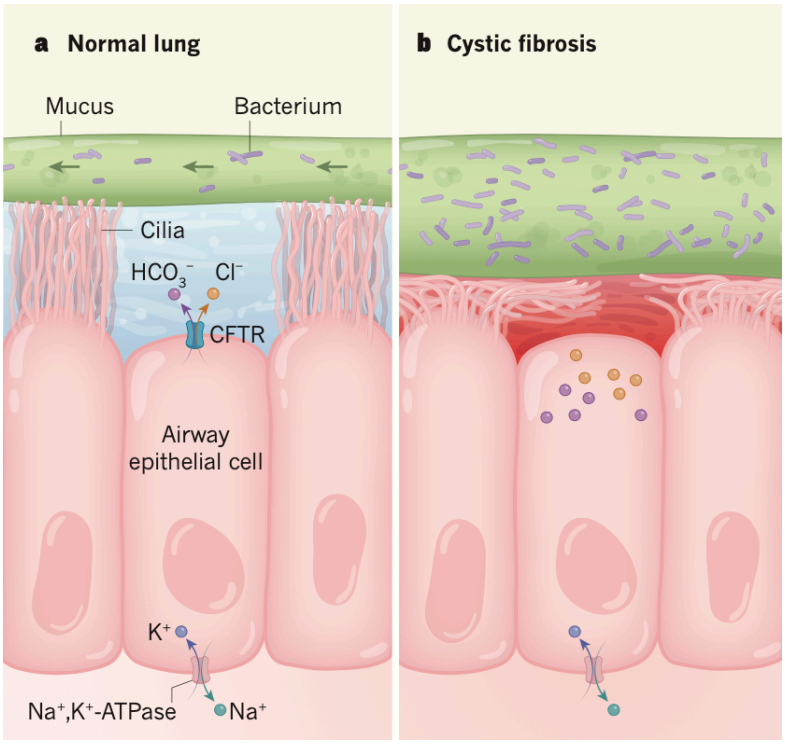

Figure 1.1: Cross section of bronchial epithelium of a healthy individuum (left, a) and an individuum suffering from CF (right, b). Mucus is transported by the cilia beating in a less viscous medium, the PCL (periciliary layer). CF causes the viscosity of mucus to increase, so that the mucus layer compresses the cilia, resulting in mucus to be not removed[14,17]. *Reprinted (adapted) by permission from Springer Nature Customer Service Centre GmbH: Springer Nature, Nature, Pore-forming small molecules offer a promising way to tackle cystic fibrosis, Sheppard D., Davis A., 2019*[17].

Subsequently, bacteria being ubiquitously present in the inhaled air are trapped in the mucus, but are not physically removed, when patients are infected with CF (Figure 1.1). In the course of the time, most patients acquire bacterial infections, that have to be treated with antibiotics. In CF patients, bacteria *P. aeruginosa* and *S. aureus* are predominantly abundant in infection increasing with age, underlining the importance of these species (Figure 1.2), but also other bacterial species can be identified as nontuberculous *Mycobacteria*, *H. influenzae* and *B. cepacia*[1,2,6].

Also patients without CF can acquire severe bacterial lung infections, as hospital-acquired (HAP) and community-acquired pneumonia (CAP)[18]. Predominantly, patients affected with CAP are infected with *Streptococcus pneumonia, Haemophilus influenzae* or *Mycoplasma pneumoniae*[19], but also *P. aeruginosa*[20].

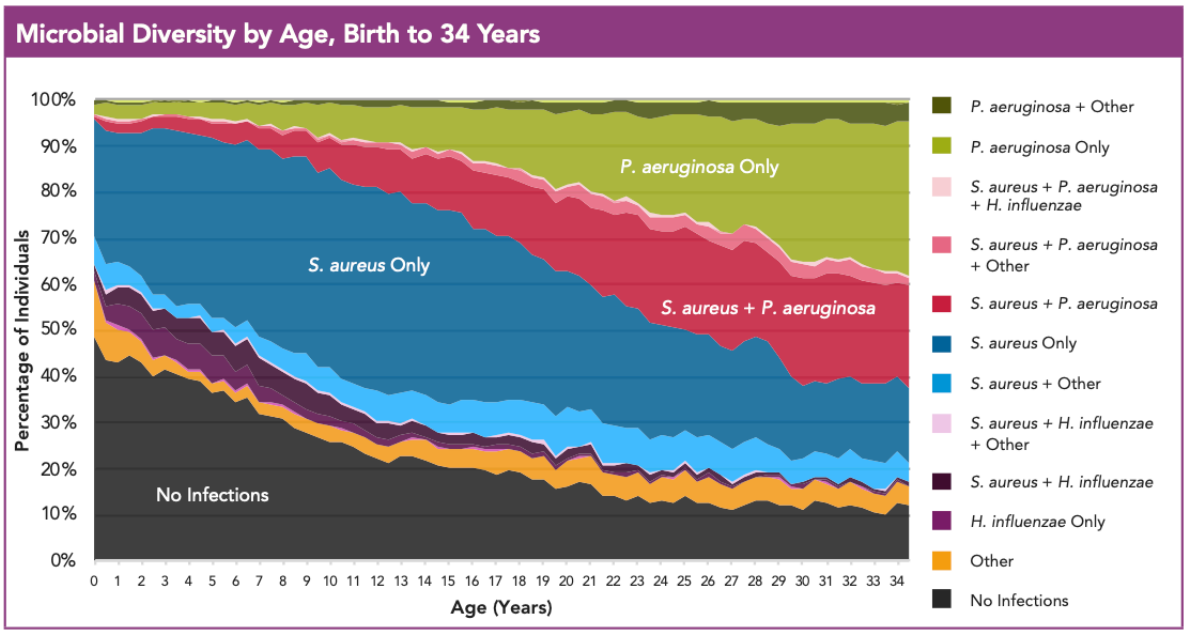

Figure 1.2: Microbial diversity of bacteria infecting CF patients from birth to 34 years. Number of patients without bacterial infection is continuously decreasing, whereas the prevalence of P. aeruginosa and S. aureus in patients is rising with increasing age. *With permission, Cystic Fibrosis Foundation Patient Registry 2018 Annual Data Report. Bethesda, Maryland. ©2019 Cystic Fibrosis Foundation*[6]

Bacteria, as the aforementioned, can build biofilms, that are generally formed when facing adverse conditions, i.e. no ideal growth conditions as adequate supply with oxygen and nutrients[1,21]. These stress situations force bacteria to form grouped colonies, that protect themselves by downregulation of growth and production of a protective matrix. Usually, biofilms (e.g., of *P. aeruginosa*) are formed on surfaces, starting with initial attachment of some planktonic bacteria, forming then clusters of bacteria building a protective matrix and finally disassembling again[22,23]. Depending on the location, these biofilms mature to build mushroom-like structures (on plastic surfaces[24]) or just clumps (as seen *in vivo* in human lung autopsies[21,24], see Figure 1.3). This inhomogeneous distribution of biofilm *in vivo* is somehow reminiscent of the biofilm presented later in Chapter 3 [4]. Typically, *in vitro* biofilms are cultivated not more than a couple of days, whereas *in vivo* biofilms can be in lungs for decades, provoking a chronic infection[21,25–27]. Mature biofilm is mainly characterized of the circumstance, that only outside bacteria have sufficient access to nutrients, whereas bacteria inside

those clusters lack nutrients as oxygen and iron, resulting in a stationary growth phase[22,28]. In the case of *P. aeruginosa*, communication of bacteria amongst each other is maintained via so called quorum sensing system, a complex structure of chemical molecules acting as signal molecules. This system is divided in the AHL (N-acylhomoserine lactone) and AQ (alkylquinolone) system[29]. A sender cell sends inducing signal molecules to control cell density or production of distinct molecules. These cause further production of signal molecules and virulence factors by acting as promoters together with the connecting proteins of the receiving cells[29]. The PQS (Pseudomonas Quinolone Signal, 2-heptyl-3-hydroxy-4(1*H*)-quinolone and the precursor HHQ (3-hydroxy-4-quinolone) work as autoinducers. Receiving cells can then produce molecules, for example elastases and pyocyanin, in order to defend and attack other cells like e.g. epithelial cells by using pqsR as transcriptional regulator[7]. Acting against the pqsR presents a straightforward target to reduce virulence of bacteria and to improve antibiotic efficacy[7,30,31]. Further information on a QS inhibitor counteracting biofilm formation using this pathway is given in chapter 3.3.8.

These biofilms are hard to eradicate once established, e.g. *P. aeruginosa* biofilms need up to 1000x increased antibiotic concentrations in comparison to planktonic bacteria to be eradicated[27,32], and patients chronically infected with biofilms of the most prevalent bacteria are often dying of these infections in the course of time[33]. There are several reasons for biofilms to be challenging to treat. First, there is a physical protection of biofilms, that surround themselves with a matrix consisting mainly of a mixture of polysaccharides, proteins, lipids and extracellular DNA[24,27,28]. This matrix and certain polysaccharides, as PSL, are shown to serve as a protection against antibiotics, causing biofilm bacteria to endure longer than planktonic cells, that is explained with electrostatic interaction forces with antibiotics[28,34]. Another important hallmark is the physiological protection of the biofilm and its bacteria. Whereas the availability of nutrients at the outer edge of biofilms is ensured, the interior of biofilms do not have access. Inside of biofilms, where nutrients are not abundant enough, bacteria can therefore become persisters that feature slow growth rates in order to keep being alive[28]. Nevertheless, this effect is decreasing the efficacy of antibiotics that

interact with the amplification of bacteria, as beta-lactam antibiotics[27,28]. These bacteria are genetically identical to the rest of the population and can switch back to the active phenotype with increasing nutrients and other agents as mannitol[26]. Last but not least, biofilms can increase the risk of bacterial resistance by facilitating exchange of resistance genes inside the clusters[27,28]. The fact, that biofilm formation (e.g. via extracellular polymeric substances) protects *P. aeruginosa* is generally entitled "adaptive resistance", whereas aggregation itself of bacteria facilitating gene transfer is called "acquired resistance". This is to discriminate from "intrinsic resistance", that *P. aeruginosa* reacts to subinhibitory concentrations of antibiotics by changing its own structural features in order to escape being eradicated[35]. This includes 1) outer membrane permeability (as mediated via porins), that prevents antibiotics to enter the bacterium, 2) efflux pumps, that actively transport antibiotics outside the cell (for example via ATP-binding cassette family transporters) and 3) inactivating enzymes (as the beta-lactamase against beta-lactam antibiotics)[28,35].

Figure 1.3: *P. aeruginosa* aggregates in a CF lung. Aggregates are not homogeneously distributed, but rather patched. *Reprinted from* [24] *with permission from Elsevier.*

1.2 Infection treatment of cystic fibrosis

The symptoms of cystic fibrosis are treatable in various ways to improve patient´s lives. One of the most challenging symptoms of CF is caused by the thick mucus, impeding breath. First of all, physical therapy helps to get rid of the excess mucus, e.g. via airway clearance techniques, using controlled breathing or chest physical therapy[36,37]. Inhaled hypertonic saline, inhalative NAC and DNase help thereby to physically decrease the viscosity of the mucus to better clear out the mucus[38,39]. Bronchodilators as salmeterol are also administered to improve breathing by relaxing the muscles[38].

Starting point of action for the general medicinal therapy is the misfolded CFTR protein, the reason for cystic fibrosis disease. Prominent representatives of "CFTR modulators" can either stabilize the conformation of the protein to enhance the traffic of chloride ions (so called correctors, as Lumacaftor) or improve the protein´s function (potentiators, as Ivacaftor)[38]. Recently, triple combinations of two potentiators and a corrector were FDA approved (Trikafta™)[40]. Ibuprofen and azithromycin are administered to reduce inflammation symptoms[38,39].

Nevertheless, the (chronic) infection with bacteria as described in chapter 1.1 is the most tragic consequence of this disease[3,4]. Still, antibiotics, that are administered orally and in severe cases via infusion, are penicillins, third generation cephalosporins or carbapenems in combination with an aminoglycoside or polymyxin to combat the most abundant CF pathogens[41]. In contrast, inhalable drugs as antibiotics have the advantage of being more precise, as the effective dose lands at the target organ instead being distributed in the first pass in the whole body, also reducing side effects[2,42]. To date, a variety of antibiotics is approved for inhalation by EMA and/or FDA, as aztreonam, tobramycin, colistimethate sodium, amikacin and levofloxacin[38,43,44].

All aforementioned antibiotics bear the risk of provoking resistance, and CF patients are still dying mostly in the age of around 30-40 years[6]. Therefore, new developments are in pre-clinical development in order to increase the efficacy against adaptive resistance by biofilms. Agents blocking QS pathways in order to reduce the production of virulence factors as pyocyanin and elastases are called pathoblockers[30,45]. Just

recently, a novel inverse pqsR agonist was introduced and could show increasing efficacy in co-administration with tobramycin[7]. Other strategies, as combating lectin structures of *P. aeruginosa* responsible for attachment and signaling, show reduction of biofilm mass without the use of antibiotics[46–48].

1.3 Modelling pulmonary diseases *in vivo* and *in vitro*

1.3.1 *In vivo* models

Traditionally, *in vivo* models are used to assess the efficacy and safety of all kind of drugs. To date, murine bacteria infected models are preferred to study long-term, chronic-like effects up to 7 days or even longer[49,50]. Nevertheless, immune reaction of mouse epithelia and also the very different lung anatomy compared to human beings is a drawback, since inhalable particles sizes reaching the human distal lung (≤ 5µm) are too large for those animals[4,51,52]. Additionally, authors are questioning the predictability of mouse models for drugs given to human beings itself, since the biological systems differ in a too large extent, leading to surprising adverse reactions in humans[53]. Rodents are nose-breathers[52], breath-controlled DPIs need special devices to bring the aerosol to the lungs, which is not physiological[4]. Still, pre-clinical trials using rodents are required for dose-finding and safety of excipients[52]. With increasing interest of the 3R community to replace, reduce and refine animal models, academia and industry try to find ways to design studies more and more ethically justifiable[54]. Reliable *in vitro* models – especially when human-based - that mimic organs as close as possible, are one of the possible solutions[52]. Even sophisticated *in vitro* models with many cell lines that are combined, are still less complex than *in vivo* models, giving at least the missing immune system. Nevertheless, this could also be an advantage in investigating single correlations[55].

1.3.2 *In vitro* models

1.3.2.1 Modelling Air-Liquid Interface and deposition *in vitro*

Submerging cells *in vitro* with a known concentration in order to test safety and efficacy has been done extensively in literature[56–58]. Undoubtedly, the physico-chemical properties of the lung are better simulated at the ALI conditions since the lungs are not filled with liquid in healthy state. In the following part, methods to model Air-Liquid Interface deposition and its prerequisites are presented, comparable to publications the author of this thesis being the first author or participated in[10,11].

Particles having an aerodynamic diameter of < 5-6 µm are less impacted in the nose, mouth or the trachea, but are inhaled into the deep lung[59]. Particles sedimenting on the lining fluid of the pulmonary surfactant face tremendously different dissolution premises, as these are often 1/10 larger than the surrounding fluid[60]. Meanwhile, it could be shown, that also *in vitro* tests are different when using ALI conditions in comparison to submerse conditions[61–63]. An example is presented by Bur et al. showing the drug concentration on the apical side of a permeable support being important for the transport. Particles that are deposited (resulting in probably very high local concentrations) are transported faster than the same dose at submerse conditions[64]. Additionally, lower doses are meant to more efficiently evoke a (toxic) response when deposited as an aerosol *in vitro*[65]. Other authors could not find a specific correlation, but a higher uptake into cells[66].

Many groups already applied aerosolized substances on cell cultures *in vitro*. Generally, there is a difference in the type of aerosol applied on *in vitro* cultures, which is typically either a nebulized aerosol (liquid/gas) or an aerosolized dry substance (solid/gas). It is to underline, that the deposition of aerosols in cell culture inserts has mainly two different purposes: First, the evaluation of toxic effects of inhalable noxae as cigarette smoke or other particles and second, the proof of efficacy of pharmaceutical substances[11].

Some groups started deposition with simple spraying of aerosols onto cell culture inserts, by using, for example, the MicroSprayer® device or the Dry Powder

Insufflator™ (PennCentury Inc, Wyndmoor, USA)[64,67]. These devices, that the company meanwhile stopped to market[68], are originally not purposed for the use on cell culture inserts and are therefore not straightforward in handling, as different apparats have to be build beforehand to deposit it[67]. On top, the dry powder apparently affects tightness of cells and disruptions of cell monolayers are reported[69]. Meanwhile, several groups tried to build own in-house devices to test individual hypotheses. Impactors that were originally made for aerosol classification[70] were re-constructed to include cell culture inserts. A prominent example is the multistage liquid impinger, that was modified by inserting a new second stage containing a hole in which a Transwell® insert was placed upside down[71]. Other devices include the twin stage impinger[72,73] or the Andersen Cascade Impactor[74,75]. While having the advantage to deposit quite well-defined particle sizes, these modified systems generally have the disadvantage to have a complicated setup and thus, a widely accepted use is not possible.

Other groups focused on the phenomenon that particles can be attracted by their charge. Jeannet et al. developed a device that works with a charged, humidified and pre-warmed aerosol[76]. Another group created an approach with a horizontal flow[77]. The commercial product Cultex® Electrical Deposition Device was developed to follow a comparable principle, that was, for example, employed by Yu et al. to deposit organic aerosols[78].

Besides the described modified impactors and electrostatic deposition devices, many corporations were interested in developing innovative machines. The majority of those were particularly involved to test toxicity of ambient inhalable noxae. One of the first visible was a group around Aufderheide et al., that developed a new device called Cultex® that was able to culture cells at the ALI conditions thereby principally allowing to be treated with an aerosol[79,80]. With this device, effects of ambient air pollutants as cigarette smoke[81], gaseous compounds[82] or diesel exhaust[83] were tested. Basically, permeable supports can be inserted into the device, thereby controlling basolateral medium flow and temperature. The aerosol is deposited on all inserts via cylindrical inlets and the inserts are placed in a row. Later, an updated version was presented called Radial Flow System® that features a ring on which inserts are placed[84,85]. This

enables a more coherent deposition of aerosol. So far, the emphasize of those applications lies within the assessment of toxicity[85].

In the field of nebulization of liquids, a new invented deposition system for aerosol clouds was further developed, characterized and enhanced to become now part of the Vitrocell® Cloud assortment[66,86,87]. This original device works with an Aerogen® nebulizer that sits in a hole on top of a transparent plastic chamber. This chamber is placed on an insert holder containing equipment to control the medium and a crystal quartz microbalance. The aerosolized solution sediments with a medium drop size of 5 µm onto the wells. Especially the Vitrocell® Cloud products were extensively used for comparable assessments to the Cultex® devices, as for example carbon nanotubes[88] or ultrafine particles[89]. Most importantly, these machines were also assessed for efficacy of potentially inhaled drugs, which is a so far quite underrepresented field[90,91]. Recently, a machine was published (Vitrocell® Cloud (Alpha) MAX) leading aerosol directly on each Transwell® insert[87,92].

Nevertheless, an important hallmark was not assessed so far, which is the application of a finite dose of drug. Patients suffering from pulmonary diseases need to inhale a distinct dose of drug in a short time frame. This is the fundamental difference to the chronic inhalation of ambient toxic substances, inhaled in lowest doses for up to decades of years. This problem was tried to be solved by inventing a device, that simulates the inhalation of pharmaceutical dry powders as budesonide[93,94]. The amount of drug in capsules in a Handihaler® was conducted via controlled airflow into the machine, simulating the process of disassembly of budesonide and lactose carriers via impaction to particles. In a subsequent step, the aerosol is led into a chamber enabling sedimentation of the resulting budesonide on Snapwell™ inserts. Using this device, metered dose deposition of API´s could be simulated for the first time on inflamed co-cultures[95,96]. On top, the treatment of bacteria could be simulated, notably without co-culture with epithelial cells[97]. Vitrocell® also produced a device called Vitrocell® Dry Powder Chamber, that has a comparable composition and uses Transwell® inserts[98].

Summarizing, it is important to apply drugs at the ALI as it is proven to be more comparable to *in vivo*[10,11]. A huge number of different approaches have been employed (Table 1.1). Nevertheless, a study of a device that is using an aerosol of the type liquid/gas that applies finite amount of drug on cells is not yet clearly presented. Therefore, a new device is tested and used to apply antibiotics on infected cells, presented in Chapter 2[10].

General classification	Device	Aerosol generation	Manufacturer/ Source	Mechanism of deposition	Specification	Deposition Efficiency	Cell type	Substance/formulation tested	Reference
Aerosol deposition without particle size differentiation	DP-4 Dry Powder Insufflator™	(DPI)	Penn-Century, Inc., Wyndmoor, USA	Impaction	spray deposition of aerosols on cell culture inserts in set distance	-	Calu-3	Micronized Salbutamol sulfate and Budenoside microparticles	[64]
						3-28%	Calu-3	Budesonide, Formoterol fumarate, sodium Fluorescein, Rhodamine 123 microparticles	[69]
	MicroSprayer® Aerosolizer IA-1C	Atomizer		Impaction		39% (inside cells)	A549	Polystyrene microparticles	[67]
						24-30 %	Calu-3	Budesonide, Formoterol fumarate, sodium Fluorescein, Rhodamine 123 solution	[69]
Modified impactors	Twin Stage Impinger (TSI)	(DPI)	Ph.Eur.	Impaction	single Transwell® insert located directly under second stage inlet	-	Calu-3	FITC-Dextran microparticles	[72]
						-	Calu-3	Salbutamol, Salbutamol sulfate microparticles	[73]
	Andersen Cascade Impactor (ACI)	Nebulizer , DPI	USP/Ph.Eur.	Impaction	Three Transwell® inserts inserted under stage 4 of an ACI	-	SAEC, Calu-3	FITC-Dextran suspension, Disodium fluorescein lactose microparticles	[75]
		Nebulizer, DPI, pMDI			8 Snapwell™ inserts on 3D printed, wetted stage that replace stage 4 or 5 of the ACI	-	Calu-3	Salbutamol sulfate solution and microparticles	[74]
	Multistage Liquid Impinger (MSLI)	DPI		Impaction	single Transwell® insert located directly under second stage inlet	-	Calu-3	PLGA microparticles	[99]
					two Transwell® inserts located shifted under inlet and upside down in stage 2 or 3	-	Calu-3	Salbutamol sulfate and Budenoside microparticles	[71]
Electrostatic deposition	NACIVT	Nebulizer, spark generator	Institute of Anatomy, U Bern, CH	Electrostatic deposition	Positive charged particles, humidified air-flow directed short-distanced on 24 Transwell® inserts	15% (Poly-styrene particles)	BEAS-2B, p. HBE cells, p. porcine lung macrophages	Polystyrene latex submicron particles suspension, silver nanoparticles	[76]
	NAVETTA	Atomizer	Vito NV, Mol, Belgium	Electrostatic deposition	Unipolar charged nanoparticles deposited via sideward air stream on 12 well plate	95%	A549 reporter cells	CuO nanoparticle suspension	[77]
	Cultex® RFS Compact+EDD	Aerosol generator	Cultex Laboratories GmbH, Hannover, D	Electrostatic deposition	Electrical Deposition Device produces positive charged particles to be deposited in Cultex® Radial Flow System	-	BEAS-2B	secondary organic aerosol from α-Pinene or D-Limonene	[78]
Deposition of non-metered (infinite) aerosol doses	Original Cultex® Device Cultex® RFS	Smoke machine		Impaction	smoking machine coupled to exposure chamber, ALI cond. under medium supply	-	HFBE-21	cigarette smoke	[81]
					See above, radial composition of exposure chamber, more consistent deposition	-	NHBE	cigarette smoke, e-cigarette aerosol	[85]

	Alice, Alice-Cloud Vitrocell® Cloud 12	Nebulizer	Helmholtz Zentrum München, Neuherberg, D	Cloud-settling, Sedimentation	droplet cloud entering exposure chamber, then distribution and settling on inserts	7%	A549	ZnO suspension	86
					See above, slightly changed nebulizer	17%	A549 reporter cells	Fluoresceine, Mannitol, Bortezomib solution	66
			Vitrocell® GmbH, Waldkirch, D			-	RPMI 2650	IgG Fab, IgG solution	90
	Vitrocell® 12/6 CF	Smoking robot		Impaction	Smoking robot VC1 attached to exposure module at ALI condition	-	EpiAirway	cigarette smoke, e-cigarette aerosol	100
	Vitrocell® 6 PT-CF	Nebulizer			PARI LC Sprint® nebulizer attached to exposure model, cells at ALI cond.	<7%	A549	Polystyrene submicron particles, carbon nanotubes	101
intermediate	Vitrocell® Cloud (Alpha) MAX	Nebulizer		(impaction), sedimentation	Deposition on single Transwell® inserts via cylinder inserts on cultivation machine	52%	A549, 16HBE14o-	Fluorescent particles	87,92
Deposition of metered (finite) aerosols doses	Vitrocell® Powder Chamber	DPI		Sedimentation	DPI connected at inlet to chamber and distribution of aerosol in 4 channels	-	-	Salbutamol sulfate microparticles	98,102
	PADDOCC	DPI	Biopharmaceutics and Pharmaceutical Technology, UdS, Saarbrücken, D	Sedimentation	separated air-flow control unit, aerosolisation and deposition unit, 3 Snapwell™ inserts	-	Calu-3	Salbutamol sulfate, Budenoside microparticles	93,94
						-	AT2 cells, pr. alveolar macrophages	IL-10 microparticles	95,96

Table 1.1: Selection of different devices for depositing aerosols onto ALI cultured cells. Devices are subdivided regarding their general method to deposit aerosols. Copyright (© 2019) from Pharmaceutical Inhalation Aerosol Technology, Chapter Reconstituted 2D Cell – and Tissue Models by Schneider-Daum, N., Carius, P., Horstmann, J.C., Lehr, C.M./Eds. Hickey, A. J. and da Rocha S.R.[11]. Reproduced (with minor adaptations) by permission of Taylor and Francis Group, LLC, a division of Informa LLC.

1.3.2.2 Infected *in vitro* models

In order to test new anti-infective compounds, the purpose of investigation needs to be identified first. If it is needed to dissect (patho)-physiological mechanisms and interplay with several cell types, sophisticated 3D-models or even animal models should be used[3]. To test delivery systems and safety/efficacy of an investigational drug, 2D *in vitro* cell cultures can already answer important hypotheses[3,4,11].

Traditional tests to prove the efficacy of novel antibiotics just include the microorganism and the agent, that eradicate the bacterium in well plates filled with broth or on agar plates with growth medium. These tests are still important to identify strong anti-infective agents, as they facilitate drug screening, accelerating hit identification[25,52,103,104]. Of note is the so called Calgary biofilm device, that is meanwhile a widely used test assay for testing agents on biofilms, that makes these tests very easy and reproducible[103,105–107]. Though, in the course of the regulatory process, methods are needed to proof not only efficacy but also need to comply with regulatory needs for higher complexity[108].

It has been proven, that ALI culture conditions matter (see chapter 1.3.2.1). So far, one of the very few studies on combatting *P. aeruginosa* at the ALI is from Loo et al[109]. Ciprofloxacin and Mannitol were brought into a formulation deposited at ALI conditions with an Andersen Cascade Impactor on well inserts with *P. aeruginosa* biofilm, proving the synergistic mode of action. But not only the air-liquid interface matters, most importantly, host factors need to be present. The simple presence of (human) mucus influences the efficacy of antibiotics by its mesh and interaction forces, reducing not only its efficacy, but also attenuate *P. aeruginosa* virulence[110,111]. It is also undoubtedly important that epithelial cells are present. Mammalian cells were shown to influence the efficacy of antibiotics, either to work better or worse[112]. Even very simple test systems show the necessity of including host cells to test anti-infectives, as they not only influence bacteria as shown, but also bring more information to the infection process: Bowler et al. used the Calgary Biofilm Device[103,105] to infect A549 cells grown submerse on the ground of well plates with *P. aeruginosa* biofilm and

planktonic bacteria. IL-8 release was significantly higher of cells infected with biofilm and planktonic bacteria were more virulent to the host cells[113]. These factors make the *in vitro* modelling of diseased patients and the search for possible novel anti-infectives quite challenging[3,114].

One of the first infected CF models clearly investigating the influence of epithelial cells were investigated by the O´Toole Laboratory. Anderson et al. found, that arginine increases the viability of CFBE41o- up to 8h in a submerse model. In this very important study, the authors could also find a relation between Type III secretion system of bacteria and viability of cells by adding subinhibitory amounts of tobramycin, attenuating the virulence of bacteria[5]. Interestingly, colleagues found the influence of CFBE41o- on the resistance of PA biofilms against tobramycin in comparison to biofilms grown on plastic, whereas increased biofilm amounts are explained with increased iron amount[115,116]. This model was used thereafter (with some modifications) in many continuing studies, for example to prove the combination of lactoferrin, that binds iron, and hypothiocyanite with aztreonam and tobramycin to be advantageous[117]. Lashua et al. could prove the addition of cationic peptides to inhibit biofilm growth and to increase biofilm eradication in combination with tobramycin, ciprofloxacin, meropenem and ceftazidime, whereas Price et al. could not show mannitol to have synergistic effects with tobramycin on the model, despite being argued before[118,119].

There are only very few *in vitro* infection models dealing with the very important point of chronic infections, as well as covering ALI conditions. There are infection models using *Haemophilus influenzae* and *S. aereus*, lasting some 4-7 days[120,121]. Very recently, a model using *P. aeruginosa* was able to be treated for 72h, with epithelial cells are staying alive[122]. The statement of an ALI model though is quite ambitious, since a volume of 20 µL was given on well inserts of an area of 0.33cm^2, which is a visible liquid layer.

All in all, the choice of the right infection model to study the success of treatment depends on the aim of the project[3,4]. Figure 1.4 gives a vast overview of some different cell culture approaches.

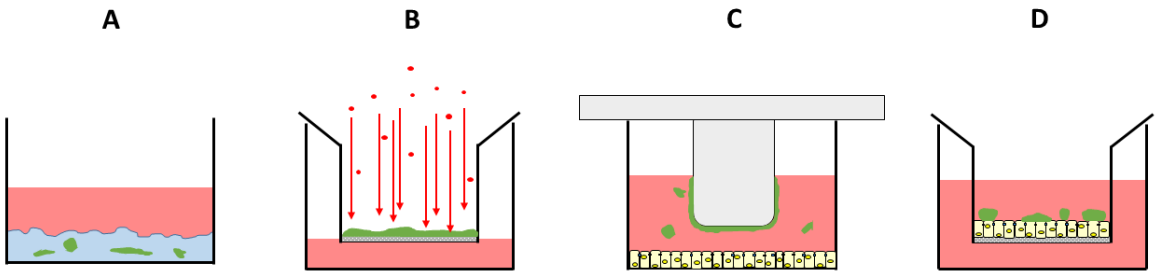

Figure 1.4: Brief overview of the most important cultivation methods to model infection *in vitro*. A). Mucus infected with bacteria in a well plate without host cells[110]. B) Deposition of Dry Powder aerosol on well inserts covered with biofilm, but without host cells[109]. C) Peg of a Calgary Biofilm Device covered with biofilm, indirectly infecting host cells[113]. D) Biofilm forming on top of submerse cultured epithelial cells[115]. Reprinted by permission from Springer Nature Customer Service Centre GmbH: Springer Nature, Disease Models: Lung Models for Testing Drugs Against Inflammation and Infection, Carius P., Horstmann J.C., de Souza Carvalho-Wodarz C., Lehr C.M.[3], Copyright © 2020.

1.4 Aim of this thesis

Numerous existing *in vitro* models to test anti-infectives have already been developed, as described previously. The benefits of using ALI conditions are thereby undoubted and methods, that realize deposition of agents on cell culture inserts, have already been tested, as exemplified in chapter 1.3.2.1.

Nonetheless, two very important aspects still need to be illuminated. The first is a deposition system, that allows to deposit reproducibly metered doses of aerosols on cell cultures, that is easy to clean and to be used at sterile conditions, enabling a sterile system for several days. A low production price has the advantage of purchasing many devices, that can be used at one experiment, saving difficult cleaning steps. Moreover, also small research groups have the possibility to test substances at ALI conditions.

The second step is the design of a relevant *in vitro* model of a biofilm-infected bronchial epithelium, that is kept at ALI conditions for more than a few hours to model chronic biofilm infections, i.e., of CF patients. It is tested, which conditions are necessary to create a chronic-like *in vitro* infection model.

By combining the deposition device of the following chapter 2 and the infected co-culture of chapter 3, a test system is created to analyze the impact of novel anti-infective, inhalable drugs in order to reduce the assessment of animal models in preclinical research.

2 Evaluation of a device to deposit reproducible doses of aerosolized drugs at the Air-Liquid Interface of filter-grown pulmonary epithelial cell cultures

The majority of this chapter has already been published in the following research paper:

Horstmann, J.C., Thorn, C.R., Carius, P., Graef, F., Murgia, X., De Souza Carvalho-Wodarz, C., Lehr, C-M. (2021) A custom-made device for reproducibly depositing pre-metered doses of nebulized drugs on pulmonary cells in vitro, *Front. Bioeng. Biotechnol*. 9, 9:643491. DOI 10.3389/fbioe.2021.643491 ([10])

Contributions to this chapter:

Dr. Chelsea Thorn (University of South Australia, Adelaide) imaged the deposition of sodium fluorescein and deposited particles to compare the deposition efficiency to free sodium fluorescein. Rudolf Richter (Workshop, Department of Physical Chemistry and Didactics of Chemistry, Saarland University, Saarbrücken) contributed the technical image of the device and produced the devices with support of Patrick Carius (HIPS, Saarbrücken). Pascal Paul (HIPS, Saarbrücken) contributed some replicates of deposition efficiency testing on Transwell® inserts and mass balance of sodium fluorescein in the device. Petra König and Jana Westhues (both HIPS, Saarbrücken) seeded Calu-3 cells on Transwell® inserts.
It is acknowledged that Dr. Florian Graef and Dr. Xabier Murgia created the first prototype and tested it (at HIPS). Also, Dr. Jenny Juntke used this device for her experiments using an anti-infective formulation on infected cells. These results were described in her PhD thesis and a publication[8,9].
All other experiments and the writing process were done by the author of this thesis.

2.1 Introduction

For the development of an infected pulmonary *in-vitro* model it seems to be important to include realistic circumstances as found *in vivo* in animals and humans (see chapter 1.3.2). This is, most prominently, the culture and treatment of cells at the ALI conditions, as initially discussed in more detail. The application of antibiotics at ALI conditions requires a system that efficiently and reproducibly directs the nebulized excipients on cell cultures. In literature, publications on the treatment of infected models at ALI conditions are still underrepresented, besides initial experiments on treatment of biofilms without cells[109] and on experiments using a smaller amount of liquid (20 µL in this case) on top of infected cells[122].

At any rate, the exact amount of drug needs to be given on cells - the difference between the systems is the amount of liquid on top (see Chapter 1.3.2). Nevertheless, it could be shown, that ALI conditions *in vitro* matter in terms of transport across the epithelium[64] and the degree of adverse reactions of the cells[65]. Apart from that, the ALI condition is generally accepted to be more *in vivo* like[60,123]. In order to build an infected model, that is on the one hand realistically grown at ALI conditions but on the other hand able to be treated for longer time than for couple hours, a method is needed that enables ALI conditions but also sterile conditions for longer treatment. As the application of considerable amounts of liquid is not acceptable, reduction to very small volumes showed the problem of unintentionally punctuating the cell membrane or a not acceptable distribution (data not shown). The use of dry powder deposition systems as the PADDOCC[93,94,97] or the Dry Powder Chamber[98] (as discussed in the introduction of this thesis) are unfortunately not suitable, since the construction properties do not allow the maintenance of sterile conditions for longer time periods, as these are very hard to be used under the sterile bench due to their dimensions and operation. For these reasons, it was clear to use a deposition system based on nebulization of a distinct amount of liquid, that is able to keep sterile conditions for longer time periods (3d). Due to practical considerations, commercially available deposition systems that were available in-house as the Vitrocell® Cloud system[66,86]

could not be used for treatment of the planned *in-vitro* model. First, the system is quite cost-intensive[87], which prevents the acquisition of several devices that can be used in the S1 and the S2 laboratory area for all necessary projects. Second, the use of the standard Vitrocell® Cloud device inside the sterile bench is very challenging due to the dimensions.

Therefore, the idea came up to use a device employed earlier at our group for deposition of $CaCl_2$ on Transwell® inserts[124]. Basically, it is a tapered plastic cylinder directly fitting on an Aerogen® Aeroneb® Nebulizer (of the types Aeroneb® Solo and Aeroneb® Pro). On the other side of the cylinder, a Transwell® insert of the size of 1.12 cm^2 can be placed. In this chapter, the device is thoroughly analyzed in order to identify its principal usability to deposit aerosolized drugs on cells, its limits and to find the optimal volume to be nebulized as described[10].

2.2 Materials and Methods

2.2.1 Dimensions and description of device

POM (Polyoxymethylene) was used to produce the cylindrical device at the workshop of Saarland University as described[10]. For shaping of the cylinder out of the block, a simple lathe can be used as well as a computerized numerical control lathe. The cylinder contains a bigger opening (2.57 cm diameter) to fit the Aeroneb® nebulizer, which is again connected to the Aeroneb® Lab control module with an AC/DC adapter (Aerogen®, Galway, Ireland). A rubber ring is inserted in a small cavity to ensure a safe connection and no aerosol to volatilize. A smaller, protruding outlet to fit exactly in a Transwell® insert (Corning™ Costar™, No. 3460, pore size 0.4 µm, Lowell, USA). Inside the device, the body is tapered towards the protruding outlet. The outlet fits into the Transwell® insert, with very small distance to the well walls (<1 mm). It can be ensured that the device is not touching the insert´s bottom by leaving 5.5 mm distance. The device can be principally also placed on 24-well plates, leaving 5.7 mm distance to the ground. It is very important to mention, that the device (as the nebulizer[125]) is autoclavable at 121 °C. Notably, experiments are able to be done via thoroughly spraying the device and nebulizer with isopropyl alcohol (70% in water v/v).

2.2.2 Deposition procedure

Deposition procedure was done as described[10]. The device is connected to the nebulizer and placed on a Transwell® insert or a 24-well plate. 100 µL PBS was initially nebulized three times in order to initialize the process and to ensure the swinging membrane in the nebulizer to work correctly. After each deposition step it needs to be taken care of remaining drops. This is ensured by disassembling the two parts and the either wiping the device and outlet of the nebulizer with a (sterile) tissue or to carefully knock them onto a (sterile) tissue. After reconnection, the next deposition can take place. 20 – 200 µL solution is pipetted onto the mesh of the nebulizer and is then nebulized. The end of a nebulization step is indicated by a small aerosol puff above the mesh of the nebulizer. Depending on the AC/DC converter, end of the nebulization is

indicated also by a light. As the end of the nebulization is not necessarily the end of deposition, the device is hold over the well for another 30 s (“settling time”, as standard condition, or as indicated) to ensure that the biggest part of the cloud is settled on the well ground. Before changing a concentration of solution or changing nebulized volumes, the system needs to be cleaned with (sterile) deionized water and wiped with (sterile) tissues. After the end of the experiment or if the complete agent is changed, also the nebulizer needs to be thoroughly washed with deionized (sterile) water and needs to be nebulized with 100 µL water for 3 times, as described[125].

2.2.3 Deposited materials and detection

Sodium fluorescein (Sigma, F6377, Munich, Germany) solution in PBS (Sigma, D8537, Munich, Germany) was nebulized at 2,5; 25; 100 or 250 µg/mL, as indicated. After deposition with the device as described[10], sodium fluorescein solution in PBS was measured at 485 nm excitation and 550 nm emission wavelength in a 96-well plate containing either 100 or 200 µL solution using a plate reader (Spectrophotometer Infinite M200 Pro, Tecan Trading AG, Männedorf, Suisse). Lipid liquid crystalline nanoparticles (LCNPs), as described elsewhere[126], were loaded with sodium fluorescein (3.5 mg/mL), were deposited exactly as the free drug and dissolved in 0.05% Triton-X to be quantified via fluorescent spectroscopy plate reader (Inspire multimode plate reader, Perkin Elmer).

2.2.4 Study of deposited mass and recovery of total deposited substance

Substance was either deposited in Transwell® inserts or in 24-well plates, as described[10]. In both, 200 µL PBS were filled prior to deposition. In Transwell® inserts, also 200 µL were filled in in the basolateral side in order to see a side deposition into the basolateral side. The basolateral liquid did not touch the Transwell® insert in order to prevent fusion with the apical side.

To determine the amount that was deposited on the inner walls of the device and to determine the amount on the mesh and the side walls of the nebulizer, the whole system was disassembled after end of deposition and placed on petri dishes. Nebulizer and device are washed with 3 mL PBS and resulting solution is measured spectrophotometrically. The resulting concentrations were calculated back using the following formula

$$\left(\frac{mass\ deposited}{mass\ invested}\right) * 100$$

“mass invested” is the mass of substance in the defined volume of liquid, which is either 20, 50, 100 or 200 µL. Further, “mass deposited” is either the mass in 200 µL in case of deposition in wells or 3 mL in case of washing in Petri dishes.

2.2.5 Analysis of influence of concentration, settling time and subsequent deposition

24-well plates filled with 200 µL PBS were used for analysis of factors that affect drug deposition as described[10]. Nebulization was done as described. To analyze the effect of diverse concentrations, either 2.5, 25 or 250 µg/mL sodium fluorescein was nebulized at either 20 or 200 µL invested volume and 30 s settlement time. To determine effect of settlement time, either 200 µL at 25 µg/mL or 20 µL at 100 µg/mL were nebulized and system was kept over the well for another 0, 30 or 60 s. Also, either 200 µL at 25 µg/mL or 20 µL at 100 µg/mL were nebulized one, two or three times into one well to evaluate dosing precision.

2.2.6 Analysis of homogeneity of deposited aerosol

Sodium fluorescein-LCNPs were used to prove the homogeneous distribution of deposited aerosol on Transwell® inserts[10]. System was used as described at 20, 50, 100 and 200 µL invested volume and inserts were left for 1h at RT. The inserts were cut out and mounted on microscope slides with coverslips to be imaged with the bottom side facing upwards. Imaging was done with an Olympus IX 53 inverted fluorescence

microscope (Olympus, Germany) together with a CoolLed pE-300 illuminator system with a 2x objective. Blank inserts served as a blank to subtract background. A heatmap was created with ImageJ showing intensities per pixel with red being highest and blue lowest intensity. The image was subdivided in 8 equal parts, and at the lines of all 8 parts intensity per pixel was plotted against the length. An average pixel intensity per length could be calculated using 3 different samples per volume that were correlated to the mean intensity. These were normalized per volume to one and 0 for highest and lowest values, each.

2.2.7 Analysis of barrier integrity and viability of epithelial cells

Here, the broadly used human bronchial epithelial cell line Calu-3 HTB-55 (ATCC®, Manassas, USA) was employed as described[10]. It is cultivated based on a weekly passaging rhythm using in-house passage numbers 35-55. The medium contained MEM (and Earle´s salts and L-glutamine) supplemented with 10 % FCS, 1 mM sodium pyruvate and 1 % non-essential amino acids (NEAA, all Gibco™, Thermo Fisher Scientific Inc., Waltham, USA). After 7 d of growth, cells were removed from T75 well using Trypsin/EDTA and Transwell® inserts were seeded with 1 x 10^5 cells. After 3 days, cells were cultured at the ALI conditions and experiments were done after 11-13 days. Deposition was done as described, but sterile conditions must be kept all the time by using sterile equipment. Nebulizer, device and all equipment as tweezers were sterilized with isopropyl alcohol 70% and experiment was done using a sterile bench enabling laminar flow. Basolateral medium was changed and well plates were stored on a heating plate at 37 °C. For deposition, a new 12-well plate was placed next to the heating plate and each single Transwell® inserts were inserted with a sterile tweezer. PBS was deposited as described. Then, inserts were placed back on the medium. As controls, inserts were used that did not face a deposition. As control containing dead cells, 1 % Triton-X 100 (Sigma-Aldrich, X100) was added to the medium. Cells were then incubated for 24 h at 37 °C and 5 % CO_2. After 24 h, basolateral medium was removed and centrifuged at 21250 x g to remove any small particles. Cytotoxicity is assessed via analysis of increased LDH release of cells, is that happening due to the compromised

cell wall. Via oxidation of lactate to pyruvate, LDH supports the reduction of NAD^+ to $NADH+H^+$, that is needed to reduce a tetrazolium salt to formazan[127]. LDH assay was done as described in manufacturer´s instructions (Roche, Cytotoxicity Detection Kit, Cat. No. 11644793001). Using a spectrophotometer (Thermo-Fisher™, Multiskan™ GO) color change was detected and cytotoxicity in % of the respective controls using the following calculation was calculated

$$\left(\frac{absorbtion\ sample - absorption\ untreated\ control(background)}{dead\ control - absorption\ untreated\ control\ (background)}\right) * 100$$

Viability was then calculated using

$$Cytotoxicity\ [\%] - 100 = Viability\ [\%]$$

Directly after removing medium, cells were submerged with 500 µL on the apical side and 1500 µL on the basolateral side with medium for 1 h. Then, TEER was measured with an electrical Volt-Ohm-meter (EVOM2, World Precision Instruments) with STX2 chopstick electrodes on heating plates. The values are corrected to values of blank inserts (90-120 Ω*cm^2) and to the area of the wells (1.12 cm^2).

2.2.8 Statistical analysis

Tests were done in triplicates, if not declared to be different. Either one-way or two-way ANOVA was used, as stated at each figure. Error bars indicate standard deviation (SD). Statistics were calculated and imaged using GraphPad Prism® 9.

2.3 Results and discussion

2.3.1 Technical dimensions and general use of the device

This device has originally been employed by Dr. Florian Graef and Dr. Xabier Murgia at HIPS at their respective PhD time. The former idea was to enlarge the deposition efficiency of the devices that have been employed before. The most comparable device to that time, the original Vitrocell® Cloud 6, had a deposition efficiency of about 17%[66], that needs to be divided by the number of wells, which is in this case six. So, about 3% of the invested mass lands on one insert, which is apparently only a small part of invested drug. When using expensive drugs, deposition efficiency needs to be enlarged. Therefore, a device was created, that is easy in handling and directly deposits on one well, which is assumed to increase deposition efficiency. To that time, no such device was on the market. The problem in depositing a known amount of liquid on cells is the missing connection between the outlet of a common-used nebulizer, as the Aeroneb® Pro nebulizer[125], and the bottom of the Transwell® inserts. If one would apply directly the nebulizer on top of a 12-well plate with inserts, this would cause problems in handling and reproducibility. First, there is no fixed application where to put the nebulizer, which could lead to deposition on wrong parts of the insert. Second, a lot of the nebulized cloud containing high effective drugs would be nebulized in ambient air or depositing uncontrolled on different other wells. Next, the distance to the well insert cannot be defined properly, that might result in different impaction forces on the well. In order to prevent this, a device needs to be built that ensures a stable connection between well and nebulizer as well as defining a proper distance. Next, a room is needed where the aerosol can distribute in, without having negative consequences for the applicator. This space, that is needed for sedimentation of an aerosol cloud was described in the ALICE or Vitrocell® Cloud system[86].

The resulting device was produced and developed together with Rudolf Richter from the Department of Physical Chemistry and Didactics at University of Saarland in form of an order from HIPS to the respective workshop of the department. The final device has the dimensions described in the technical image of Figure 2.1[10]. It is part of the

whole system that consists of the nebulizer with AC/DC adapter, the device described here and the well or Transwell® insert. It is made to exactly fit an Aeroneb® nebulizer, that is kept in connection with the device via a rubber ring that is inserted in a cavity 2 mm under the opening of the device (Figure 2.1). The shape of the inner body is tapered to the other outlet of the cylinder. The reason was the hypothesis, to better focus the aerosol to the outlet. The exit of the device is protruded for 12 mm and designed to be inserted into a 12-well Transwell® insert leaving no possibility for the aerosol to exit the well (Figure 2.1). It also can be placed easily on a 24-well plate insert. The distance to the well bottom is either 5.5 mm (Transwell® insert) or 5.7 mm (24-well bottom).

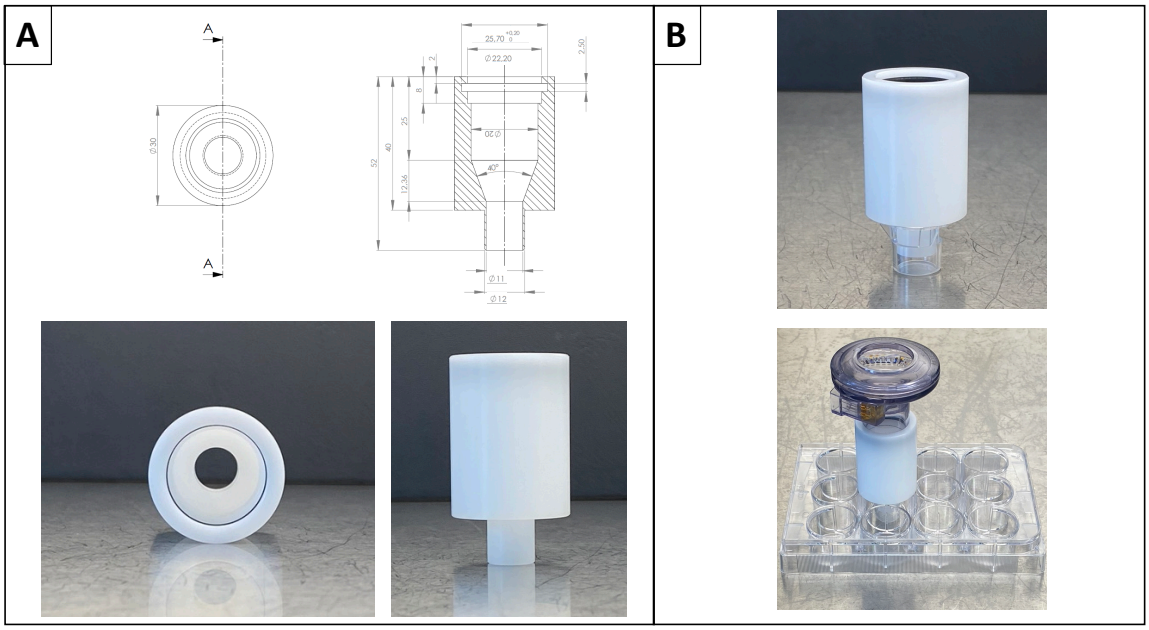

Figure 2.1: Overview and design of the deposition device and system. A) POM block is drilled to follow the imaged dimensions. Top view (left) and side view (right). B) Deposition device connected to Transwell® insert leaving some 5.5 mm space to the bottom (top image). The nebulizer connects well to the device and stably sits in the well insert (bottom image). Adapted from [10], © 2021 Horstmann, Thorn, Carius, Graef, Murgia, de Souza Carvalho-Wodarz and Lehr, Frontiers in Bioengineering and Biotechnology. Creative Commons Attribution License (CC BY). DOI: 10.3389/fbioe.2021.643491

2.3.2 Conditions that affect deposition of substance

Before the system can be actually used to deposit antibiotics on infected cells, a thorough characterization is needed to decide which conditions to choose for deposition[10]. This applies to the invested concentration, the invested volume and the number of deposition steps. Before starting the experiment, preliminary studies were done evaluating the ideal range for invested volumes, as volumes used in clinics (up to 5 mL) cannot be applied here only on Transwell® insert[125,128]. It turned out that volumes lower than 20 µL showed unacceptable, high standard deviations (data not shown). Thereafter, 20 µL showed deviations of about 22%, and these deviations have been decreasing until the higher end, which is defined at 200 µL (4.8 % SD, Figure 2.2). Higher invested volumes lead to emerging drops that can fall down onto the insert, resulting in a submerse-like state. Therefore, higher volumes were excluded. First, deposition efficiencies of increasing concentrations of the invested liquid were observed to be sure that concentration does not have an effect on deposition efficiency, three different concentrations (2.5, 25 and 250 µg/mL) were invested at two volumes (20 and 200 µL, Figure 2.2). As higher concentrations lead to higher deposited amount of substance, the deposition efficiency (Materials and Methods part) needs to be compared in order to detect a difference. The concentration had no measurable effect at either 20 or 200 µL ($p \geq 0.6$). This was so far expected, nevertheless, it shows that the substance can be measured precisely by the Tecan plate reader. It also proves, that comparisons of different doses and even of different substances are legit.

Next, the settlement time was evaluated, since this is a very important aspect of drug deposition *in vitro*[11,86]. Nebulization of the Aerogen® Nebulizer is finished after 3s (20 µL) or 30s (200 µL), but the nebulized cloud is still in the space inside the device, which can be clearly seen via disassembling. Therefore, the influence of the remaining settling cloud on the deposition efficiency has to be evaluated at both extreme volumes (Figure 2.2). 30s settlement time (or waiting time) has a significant influence on either 200 or 20 µL invested volume ($p=0.02$ vs. $p<0.001$, respectively). Further waiting until 60 s increased deposited amount, but not significantly at either volume ($p=0.78$ and $p=0.60$,

respectively). Notably, 20 µL invested volume showed a huge increase in deposition efficiency between 0 and 30s (ca. 2-5%), whereas this increase is not so pronounced with 200 µL invested volume (2.8 vs. 3.4 %). The reason is most probably the nebulization time. Higher volumes have time to already deposit while the nebulization itself is not yet finished, whereas this process is very limited at lower volumes. The amount of aerosol in the device settling down on the already deposited dose is relatively seen higher at lower volumes. Interestingly, this effect is only relevant at the first 30s, as there is no significant increase after 60s. As a tradeoff between necessary time to deposit substances and to keep the process as short as possible, 30s settlement time is a good agreement. Another group using the very recently emerged Vitrocell® Cloud MAX, that is comparable with regard to the chamber that the cloud is nebulized into, decided for a settlement time of one minute[92].

The deposition system is designed to exactly deposit finite amounts on drugs on cell culture inserts. Tentatively, it can be necessary to deposit a substance on a well more than one time, for example, if solubility aspects of the agent limit the invested dose and one deposition is not sufficient to reach the target dose. Deposition should be reproducible even with multiple applications. Thus, a study was performed with 20 and 200 µL, that was deposited in one well for one, two or three times at 25 µg/mL (200 µL) or 100 µg/mL (20 µL) at 30s settlement time (Figure 2.2). Both volumes could be applied reproducibly with a coefficient of determination of 0.942 (20 µL) or 0.8482 (200 µL). As expected, a multiple application of 200 µL is favored in terms of reproducibility, but it has to be considered that a measurable, and probably already visible, amount of liquid is deposited (>3% of 200 µL is about 6-8 µL, three depositions add up in more than 18 µL). In literature, so far only single depositions have been done. Here, multiple depositions bear the risk of resulting high standard deviations and higher liquid amount, but are possible with acceptable accuracy.

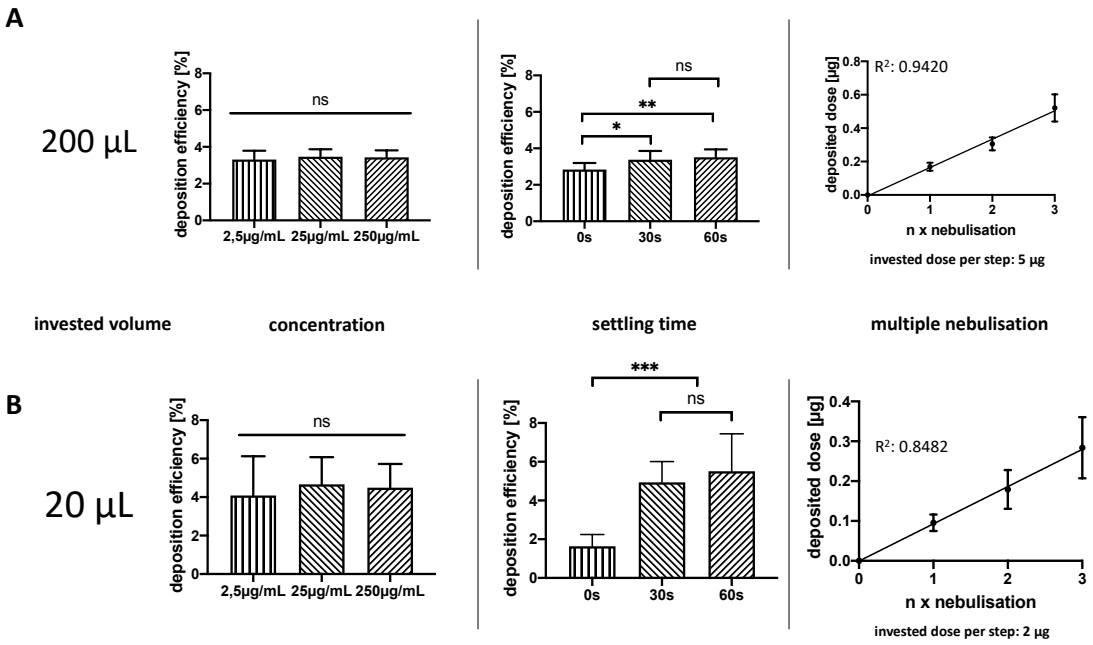

Figure 2.2: Characterization of the deposition system using sodium-fluorescein. A) Deposition of 200 µL at different concentrations (10-fold increasing), settling times (waiting time after deposition) and repeated depositions into one well are displayed from left to right. B) as in A), but 20 µL were used. Error bars are given as SD. One-Way ANOVA, Tukey´s multiple comparisons test, ns $p > 0.12$; * $p < 0.033$; ** $p < 0.002$; *** $p < 0.001$. N=9 of 3 independent experiments. Adapted from [10]. © 2021 Horstmann, Thorn, Carius, Graef, Murgia, de Souza Carvalho-Wodarz and Lehr, Frontiers in Bioengineering and Biotechnology. Creative Commons Attribution License (CC BY). DOI: 10.3389/fbioe.2021.643491

2.3.3 Linearity of dose at different volumes

As already clarified, doses of lower volumes have by tendency higher standard deviations than higher volumes. Also, higher deposition efficiencies with lower invested volumes in figure 2.2 attracted attention. Thus, a clear investigation on the linearity of dose deposition at various increasing volumes could be done[10]. Especially, it is to evaluate, if lower volumes have statistically higher deposition efficiency than higher volumes. Hence, 100 µg/mL sodium fluorescein in PBS is deposited on 24-well plates and repeated six times with each three replicates in order to have a broad set of data. The results are depicted in figure 2.3. Invested volumes of 20, 50, 100 and 200 µL, that could be all used for treatment on cell cultures, are investigated. Dose is

deposited very linearly by the used volume (R^2 factor of 0.9706, Figure 2.3 A). However, it was hypothesized, that deposition efficiency is enlarged with decreasing volume. Apparently, this is of no consequence for the linearity of deposited dose. By calculating the deposition efficiency, the underlying reason becomes clear (Figure 2.3 B). Deposition efficiency of 20 µL volume is by tendency higher than the efficiency of 200 µL (4.4 vs. 3.9 %, respectively). More prominently, the standard deviation differs by a lot between those two extrema (33.0 vs. 4.8 % standard deviation, respectively). This is also the explanation why there is no significant difference of deposited doses of the two extrema ($p = 0.36$). Possible reasons for the very high standard deviation could be pipetting errors of small volumes, but more prominently it could be assumed, that some of the liquid is driven to the apical side of the membrane via vibration. This is, relatively seen, a higher amount when nebulizing only small amounts of liquid. Due to this reason, deposition with lower volumes, as with 20 µL, cannot be recommended in this setting.

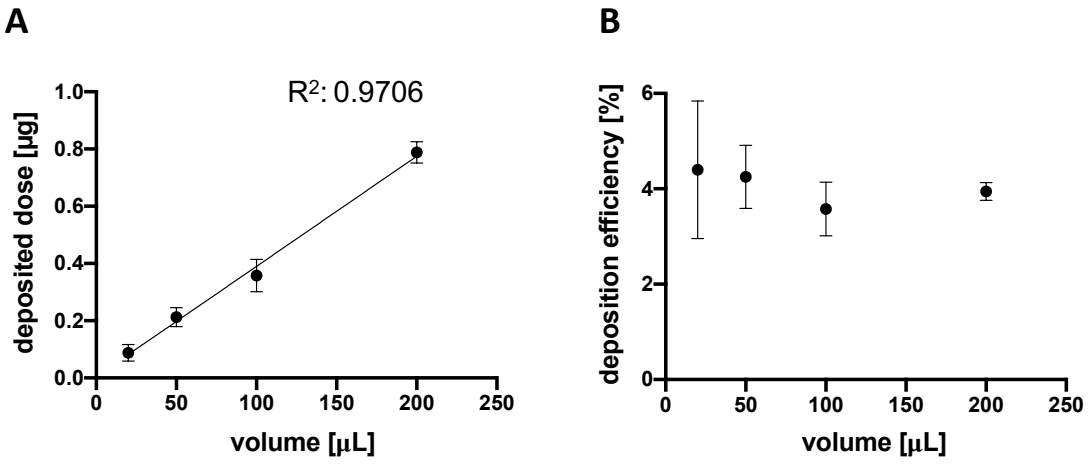

Figure 2.3: Deposited dose of sodium fluorescein per nebulized volume. A) Linearity of deposited dose with increasing volume. B) Deposition efficiency per invested volume. Error bars given as SD. N ≥ 18 of ≥ 6 independent experiments. Adapted from [10]. © 2021 Horstmann, Thorn, Carius, Graef, Murgia, de Souza Carvalho-Wodarz and Lehr, Frontiers in Bioengineering and Biotechnology. Creative Commons Attribution License (CC BY). DOI: 10.3389/fbioe.2021.643491

The deposition efficiency here seems to be quite modest, but compared to literature values it becomes very acceptable. A study using the Vitrocell® Cloud could show a deposition efficiency of 17 %, but on a plate, in that six Transwell® inserts are mounted[66]. Calculating it down to one insert, it is less than 3 %. However, this is a theoretical value based on literature. There have been better comparable studies depositing a dose directly on one insert, as for example a study by di Cristo et al. The group used the Vitrocell® Starter Kit, that is comparable to the usual devices offered by the company, but only features on insert for deposition[129]. By investing 125 µL of a 1 mg/mL particle suspension, deposited amount could be determined to be 0.71 µg/cm^2. Using this data, calculation of deposition efficiency per Transwell® insert (1.12cm^2) is possible. 0.64 % of the invested dose are theoretically landing on the insert. This is by far lower than what is achievable in this device. The reason could by the greater surface which surrounds the insert, as, for example, the bottom layer on the ground[87]. Also, it is of note that the dose was calculated with the included quartz crystal microbalance[129]. This might cause differences to the method described in this work. Notably, the same author did an earlier study without using any device. The Aerogen® nebulizer was just hold over the well insert and deposition was started[130]. Deposition efficiencies of up to around 90% were stated, but analysis was done via imaging of deposited substance in SEM and not via a spectrophotometrically analysis. This very high result seems to be a basis for further discussion. Recently, the Vitrocell® Cloud MAX has been evaluated. The device is not tapered towards the downstream end, enabling the analysis of bigger inserts. The group found a deposition efficiency of 52% onto 6-well permeable inserts[92]. Nevertheless, only 10 µL of liquid were used and the dimensions are different. As the 6-well inserts are roughly 4.5 times larger than the 12-well inserts, a deposition efficiency of about 12% could be a realistic comparable number. Also, a small SD of 1% seems to be very admirable, but needs to be further confirmed by other groups.

To summarize, volumes of 200 µL are favored in the here presented device, since the SD is by far smaller and the dose is therefore very reproducible.

2.3.4 Comparison of deposition in 24-well plates and Transwell® inserts

The analysis of deposition efficiency is simpler using 24-well plates, hence the plates as blocks are easier to use and purchase is less cost-intense. The aforementioned experiments have been done using this technique[10]. It was assumed, that there is no difference to the deposition in Transwell® inserts, as the space, in which the amount of substance is deposited, is very comparable (1.12 vs. 1.9 cm^2). Figure 2.4 A shows the comparison of deposition efficiency on Transwell® inserts and 24-well inserts at 20, 100 and 200 µL. Overall, no big difference is visible, only 20 µL seem to differ comparing to inserts ($p=0.01$)[10]. Even so, a statistical significance is not decisive. It matters most, that deposition efficiencies are somewhat in the same range. The exact doses have to be found in the unique experiments, that are done in each group on the basis of these results. All in all, experiments done on 24-well plates and Transwell® inserts can be compared. This is important for the antibiotic dose of tobramycin in chapter 3.

Instead of pure drugs and substances, pharmaceutical formulations are increasingly tested on cell culture as detailed in the Introduction and in Chapter 1. Liquid lipid crystalline nanoparticles (LCNPs), as described[126], are used to prove the ability of the device to reproducibly deposit sodium fluorescein bound in particle formulations. The LCNP bound sodium fluorescein is deposited in the range of about 4 % deposition efficiency (Figure 2.4 B). Again, 20 µL deposition efficiency deviates from the overall comparable values. This is an interesting feature, that lacks explanation so far. Though further trials need to be done to fully understand the fact, why 20 µL deviates by about $1/5^{th}$ of the deposition efficiency, it is to realize, that the overall efficiency is well comparable, and pharmaceutical formulations as well as free drugs can be used to deposit.

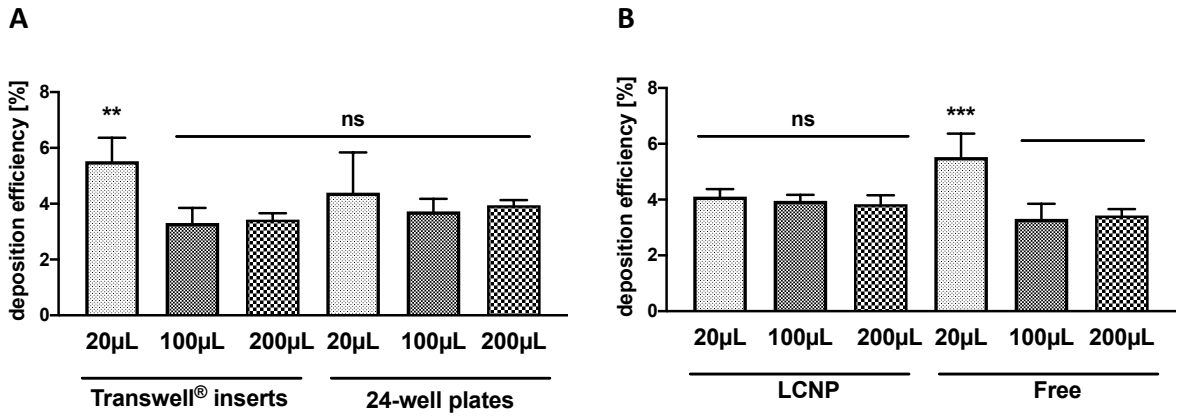

Figure 2.4: Comparable deposition of sodium fluorescein on Transwell® inserts and on 24-well plates, as well as free drug and formulation. A: Deposition of sodium fluorescein done either on 24-well plates or on Transwell® inserts. B: Deposited sodium fluorescein in LCNPs or as free substance in Transwell® inserts. Error bar represents SD. Two-way ANOVA, Sidak´s multiple comparisons test, ns $p > 0.05$; ** $p < 0.003$; *** $p < 0.001$. Transwell® inserts: N = 9 of 3 independent experiments, N = 6 of 2 independent experiments (100 µL). Wells: N = 18 of six independent experiments. Adapted from [10]. © 2021 Horstmann, Thorn, Carius, Graef, Murgia, de Souza Carvalho-Wodarz and Lehr, Frontiers in Bioengineering and Biotechnology. Creative Commons Attribution License (CC BY). DOI: 10.3389/fbioe.2021.643491

2.3.5 Recovered mass deposited in system

"Deposition" has been described as "deposition on well inserts", which was found to be around 4% using this device (Figure 2.3). Accordingly, around 96% of deposited substance was not found anymore. It is hypothesized, that most of the substance can be found in the device itself, as drops are already forming on the inner wells of the cylinder after having deposited 200 µL[10]. Thus, amount of remaining substance in the nebulizer, in the device and in Transwell® insert were determined using sodium fluorescein at the invested amounts of 20, 100 and 200 µL (Table 2.1). Interestingly, roughly a 1/5th of the deposited substance remained in the nebulizer (20 µL) that even further increased with higher volume. 34 % with 100 µL is even higher than the relative amount of 200 µL, which can be explained by having only 2 replicates at 100 µL which has to be kept in mind. Even though the amount of substance in the nebulizer was not expected, the deposition onto the inner walls of the device was expectably high and

also relatively increased with increasing volume (46, 55 and 63 %). Here it is proven why higher volumes than 200 µL are not possible to be nebulized. Notably, even using as low amounts as 20 µL and no visible drops are formed in the device, already half of the whole amount are deposited inside the device. Considering the combined deposited mass in all parts of the system, it stands out that ca. 20 % of the deposited dose of 20 µL is lost and not found in any of the parts, whereas deposition of higher volumes only loses some 6 % (not considering the SD). This is interesting, as this shows a relation to Figure 2.2 showing smaller volumes to need more time to settle down. Here, the same principle is assumed, with higher relative importance of a nebulized cloud. Relatively seen, more of the nebulized cloud is still in ambient air even after 30 s settlement time, and can therefore not be analyzed anymore. Finding comparable results in literature is quite challenging, this is mostly due to the fact that other devices are quite bulky and large and are therefore not suited for doing such tests, as depicted in the introduction of this thesis. The recently developed Vitrocell® Cloud MAX allows for doing such tests, thus finding 13% deposited in the nebulizer and 35% (probable value, not tested there) on the device´s wall and ambient air[92]. It is noteworthy to allude that only 10 µL and bigger well inserts were used in this study, as already discussed above.

	20 µL	**100 µL**	**200 µL**
Nebulizer	**20,52 ± 12,19**	**34,16 ± 2,83**	**27,45 ± 3,64**
Device	**45,84 ± 9,37**	**55,41 ± 3,32**	**63,03 ± 8,77**
Transwell	**5,52 ± 0,84**	**3,31 ± 0,54**	**3,43 ± 0,23**
Total recovery	**79,66 ± 9,02**	**92,88 ± 2,02**	**93,53 ± 8,51**

Table 2.1: Recovery of deposited sodium-fluorescein in the deposition system. 25 µg/mL were used at indicated volumes. Values in % of theoretical maximum amount, "Total recovery" being the combined masses of all compartments. SD is displayed, N=9 of three independent experiments (100 µL N=6 of 2 independent experiments). Adapted from [10]. DOI: 10.3389/fbioe.2021.643491

2.3.6 Imaging the deposited dose to confirm homogeneity

It was hypothesized, that lower volumes might spread better across the Transwell® insert, since lower volumes cause less drops to form. Judging by the heat map images (Figure 2.5), indeed a trend towards higher intensities could be found when comparing 200 and 20 µL. Interestingly, no distinct difference could be found when comparing the standard deviations of all normalized intensities of the deposited volumes (7%, 10%, 12%, 9%, for 20 to 200 µL, respectively). Comparing the normalized mean of all intensities at each volume, also no difference is observable (1.04, 1.02, 1.08, 1.07 AU, p=0.945, as in[10]). 200 µL seems to be even spread, also judging by the shape of its intensity curve (Figure 2.5). Arguing with this study, it apparently does not matter much, if a dose is deposited at smaller or higher volumes. Nevertheless, there is a difference regarding the volume deposited on the insert, that is limited to be still in ALI conditions. There is no specific limit considering the amount of liquid on the cell culture to call it “ALI conditions” or “submerse conditions” – though, volumes of more than 10 to 20 µL on a Transwell® insert of 1.12 cm^2 results in a confluent layer of liquid, foiling the definition of ALI conditions.

Likewise, it is also important to consider the material to be deposited. Cells feature a wet surface, whereas plastic is dry. This also impacts the studies on distribution of those aerosols and has to be reflected in future.

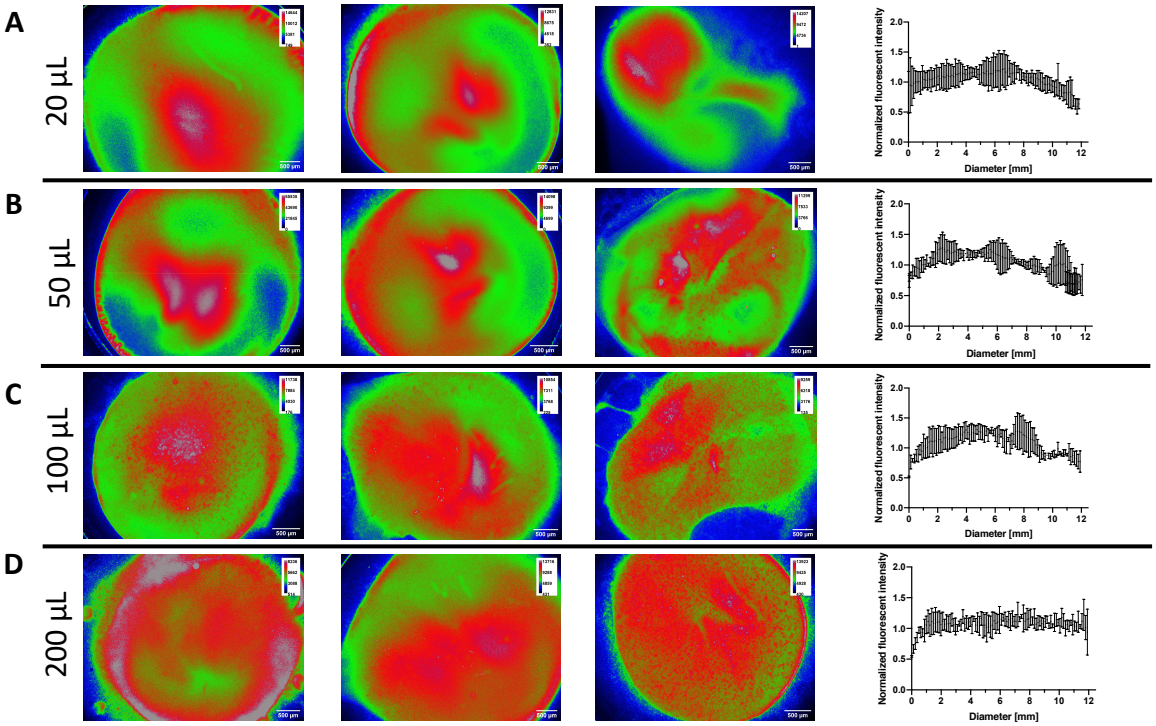

Figure 2.5: Analysis of distribution of sodium fluorescein loaded LCNPs on Transwell® inserts. A-D: Heat map distribution of 3 replicates of the respective volume nebulized into the device and deposited on inserts, blue giving the lowest and red the highest intensities, as shown. On the right side, the normalized fluorescence intensity is given per diameter length. N=3 replicates per volume. Adapted from [10]. © 2021 Horstmann, Thorn, Carius, Graef, Murgia, de Souza Carvalho-Wodarz and Lehr, Frontiers in Bioengineering and Biotechnology. Creative Commons Attribution License (CC BY). DOI: 10.3389/fbioe.2021.643491

2.3.7 Deposition of saline is safe for epithelial cells

Here, a method is described that deposits an aerosol of a (buffered) solution on cells. Studies on the Vitrocell® Cloud system, using a comparable method, did not find any harmful effects[86]. Thus, the here presented device should not be harmful, as an aerosol consisting of buffered saline is depositing on the cell surface. The device has the function of a spacer, that also could break the speed of the aerosol, comparable to other devices[66,86]. Nevertheless, the Calu-3 cell line is used here to prove the deposition to be safe for cells, because it is widely used and known, and it builds tight barriers[11,131]. Notably, it is not the CFBE41o- cell line, but in the following chapter, the control was always treated with KRB as the buffer, so that any possible adverse effect (which is not

expected) is equalized. On top, results can be partially transferred to other cell lines, because physical effects are studied here rather than receptor-based mechanisms.

Either 20 or 200 µL PBS were nebulized and the control did not face an aerosol. After deposition, cells were incubated further 24 h in order to see any adverse effects (as done in[10]). Basolateral amount of LDH was analyzed and calculated back to viability. Viability was maintained at 100% with 20 and 200 µL, respectively (Figure 2.6). Barrier integrity apparently dropped after 24h (Figure 2.6 B). Although all values dropped, TEER of about 300 Ω*cm^2 was maintained and did not differ between control and deposited samples (p=0.59). The reason for TEER values dropping are unknown. Cells were tested between days 12-13 after seeding, which is an in-house used protocol. Bacterial contamination could be excluded, no living bacterial cells were detected in medium samples after 24h as visualized under the light microscope. Mycoplasma controls are done on a regularly basis in-house and also did not show any contamination (data not shown).

Summarizing, epithelial cells tolerate deposition very well. This is important, as the epithelial cells are infected or inflamed before treatment and might be particularly vulnerable[95,96].

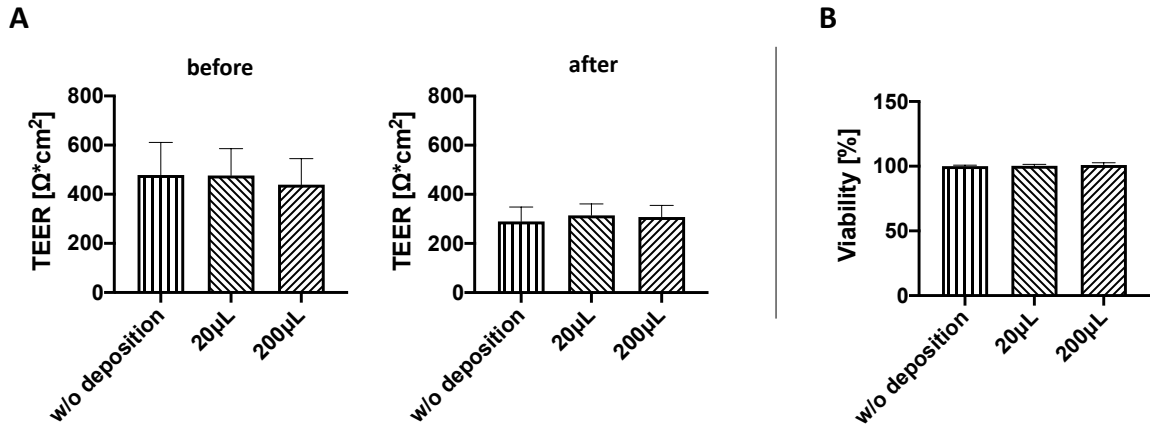

Figure 2.6: Calu-3 cells tolerate PBS deposition. A) TEER before deposition and after 24h. B) Viability of cells after 24h (measured via LDH). N = 9 of 3 independent experiments. Adapted from [10]. © 2021 Horstmann, Thorn, Carius, Graef, Murgia, de Souza Carvalho-Wodarz and Lehr, Frontiers in Bioengineering and Biotechnology. Creative Commons Attribution License (CC BY). DOI: 10.3389/fbioe.2021.643491

2.4 Summary and outlook

The question of how to apply antibiotics on cells at ALI conditions could be answered. An in-house developed device has the necessary characteristics to safely and reproducibly apply substances on cells, as already published[10]. It is straightforward in the design, as it only consists of a tapered POM cylinder and has many advantages in comparison to other devices. One of the main advantages is a relatively high deposition efficiency while not producing extraordinary costs. Hence, the device has not to be cleaned and dried after each deposition, but many devices can be used in parallel to simultaneously deposit different drugs. Such a procedure would help researchers, that already studied such simultaneous deposition [69,90,132]. Using the device, a homogeneous distribution of drug on the inserts can be realized. The handling is easy and personnel does not require technical know-how, only S1 or S2 cell culture approval. For the success of treatment of a long-term infected cell model, sterile application is needed. This is one of the easiest methods to apply drugs at the ALI under sterile conditions, as the device is easy to wash and wipe.

In future, imaging of the nebulized cloud via transparent devices or IT solutions could determine the characteristics of the process and prove the sedimentation process.

3 Development of a biofilm infected epithelial cell model at air-liquid interface

Parts of this chapter have already been published in the following research paper:

Horstmann, J.C., Laric, A., Boese, A., Yildiz, D., Röhrig, T., Empting, M., Frank, N., Krug, D., Müller, R., Schneider-Daum, N., de Souza Carvalho-Wodarz, C. and Lehr, C.-M. (2022) Transferring microclusters of P. aeruginosa biofilms to the air-liquid Interface of bronchial epithelial cells for repeated deposition of aerosolized tobramycin. *ACS Infect. Dis.,* 8 (1), 137-149. DOI 10.1021/acsinfecdis.1c00444 ([4])

Contributions to this chapter:

Harvesting cells of infected model and western blots in chapter 3.3.7.5. were done by Annabelle Laric (UKS, Homburg). Experiments shown in chapter 3.3.9.1 (addition of human mucus and ASM_{mod} on CFBE41o- cells) were done by Sarah Frisch, the prepared mucus samples were delivered by Benedikt Huck (both HIPS, Saarbrücken). Analysis of metabolomics was conducted by Nicolas Frank (HIPS, Saarbrücken), and analysis of alkylquinolones was done by Dr. Teresa Röhrig and Simone Amann (both HIPS, Saarbrücken). CLSM and SEM images of chapter 3.3.8.3 were partly taken by Dr. Annette Boese or Pascal Paul (both HIPS, Saarbrücken). Dr. Boese supported in testing biofilm susceptibility on well plates. Detection of tobramycin via LC-MS was done by Pascal Paul. For some infection experiments, the Transwell® inserts were seeded with cells by either Jana Westhues or Petra König (both HIPS, Saarbrücken). The group of Prof. Mustapha Si-Tahar (University of Tours, Tours, France) provided the PAK strains.
All other experiments and the writing process were done by the author of this thesis.

3.1 Introduction

The use of permeable supports, that enable bronchial epithelial cells as CFBE41o- to build a measurable tight barrier, offer the readout of changes to bacterial infection not only due to viability, but also via the transepithelial electrical resistance, which is still underrepresented in most studies. The state of bacteria is thereby crucial – planktonic bacteria may differ in many ways to their biofilm counterpart[23,24,133]. *In vivo*, the chronic infected patients suffer from biofilm infections, fast-growing planktonic bacteria are seldomly found[22]. Therefore, a test method to infect mammalian cells with bacteria rather being in the biofilm mode than in the fast-growing planktonic mode needs to be found. There have been publications, that try to exclusively infect mammalian cells with biofilm, for example by using peg-lids[113]. Nevertheless, a model needs to be found, that is constructed at the ALI conditions, as this status is proven to be more realistic than the submerse culture conditions[61–63,134]. A method that deposits the anti-infective formulation reproducibly onto an insert could be found already (chapter 2[10]). It could be proven, that the ideal invested volume is between 50 and 200 µL and a homogeneous deposition was reached. Most importantly, but expectably, the deposition does not harm epithelial cells.

Hence, the idea to transfer a ready-grown biofilm on top of cells growing at the ALI conditions, that was initially developed by Dr. Jenny Juntke[8,9], was employed here. Nevertheless, several very important proofs were still pending. First, the time for pre-growing biofilms needs to be carefully addressed to be as realistic as possible. Second, discriminating transferred bacteria between the biofilm and the planktonic mode of growth is extraordinary important for the model and needs to be defined, so that a valid biofilm model is present. On the other hand, optimal culture conditions are to be found. The presence of cells and the presence of ALI conditions in comparison to their counterpart in a bacterial infected model has, to the best of our knowledge, never been directly compared in this context.

Chronic-like *in vitro* infections with infection times of three days or more are, separate from few limited examples[120–122], seldomly available. Hence, it is planned to infect the

model for 24, 48 and 72h to compare the status of bacteria and of mammalian cells to decide, how long a model can be regarded as stable infected[4]. Last but not least, the influence of artificial or human mucus and the influence of a novel quorum sensing inhibitor can be tested on the characterized model.

3.2 Materials and Methods

3.2.1 Cultivation of cells

CFBE41o- cells (source of Dieter Gruenert, University of California, Oakland, USA) were employed for all infection studies (Material Transfer Agreement, UC control number 2003-21-0262, UC case number 2001-316). Cells were cultivated in T75 flasks at 37°C and 5% CO_2 in a weekly passaging rhythm using MEM Medium (Gibco™ Thermo Fisher Scientific, Waltham, USA) supplemented with 0.6 g/L glucose (Sigma, Munich, Germany), 1% NEAA and 10% FCS (both Gibco™ Thermo Fisher Scientific, Waltham, USA). Medium was changed every 2-3 days. For seeding Transwell® inserts (Cat. No. 3460, pore size 0.4 µm (Corning™ Costar™, Lowell, USA)), cells were detached with Trypsin/EDTA, centrifuged at 300 x g (Centrifuge 320R, Hettich), resuspended in medium and 5 x 10^4 cells were then seeded in 500 µL on the apical side. On the basolateral side, 1500 µL were filled and incubated for 2-3 days, then cells were cultured at ALI conditions using 500 µL medium on the basolateral side, as described[4]. After a total of 7 days cultivation, cells were used for infection studies, as TEER values have to be proven highest then (in-house)[8,9].

3.2.2 Bacteria cultivation

Bacteria cultivation was generally done as described[4]. In detail, *P. aeruginosa* strains PAO1 (DSM No. 22644, DSMZ, Braunschweig, Germany) and PA14 (DSM No. 19882, DSMZ, Braunschweig, Germany) were cultivated using Luria Bertani Broth (Sigma, Munich, Germany). PAO1-GFP (PAO1-GFP, ATCC 10145™, Manassas, USA) that contains a vector encoding the production of the Green Fluorescent Protein (GFPmut3), under the control of the promoter P_{lac} and equipped with resistance gene (*bla*) on a plasmid[135] was cultivated using LB medium containing 300 µg/mL ampicillin. PAK wt, PAK ΔpscF and PAK ΔfliCΔpscF (kind gifts of Prof. Mustapha Si-Tahar, University of Tours) was also cultivated using LB medium. 20 mL medium was filled in a 200 mL Erlenmeyer flask, and one colony of a LB Agar plate (not older than about 4 weeks, in

case of PAO1-GFP with 300 µg/mL ampicillin, stored for max. 10 days) containing single colonies of the respective bacteria was used to inoculate the broth. The flasks are incubated for 16 h overnight by shaking at 180 rpm at 37°C. For measuring the optical density, OC was centrifuged for 10 min at 3850 x g (Centrifuge 320R, Hettich). Supernatant was discarded and pellet resuspended with pre-warmed PBS. OD was measured with an UV meter (Thermo-Fisher™, Multiskan™ GO) in 1 mL cuvettes (either diluted 1:10 in PBS or undiluted, as indicated). Growth curves of bacteria were obtained by infecting 20 mL of LB medium with 1 colony of bacteria. 1 mL is withdrawn and measured via UV at each timepoint (diluted and recalculated when outside maximum absorbance). Medium is replaced thereafter.

3.2.3 Biofilm preparation

All bacterial strains were used to build biofilms. The washed bacterial suspensions were diluted to obtain mathematical OD 0.01. Standard 24-well plates were filled with 500 µL M63 medium, that has to be prepared freshly and to be used for 2 weeks. Dr. Jenny Juntke examined the optimal M63 recipe, that was based on existing recipes[8,136]. This medium was used here, as described[4]. M63 consists of 2 g/L $(NH_4)_2SO_4$, 13,6 g/L KH_2PO_4, 0,5 mg/L $FeSO_4$ x 7 H_2O, 4 g/L arginine and 246 mg/L $MgSO_4$ * 7 H_2O. The first three ingredients are autoclaved as a 5x concentrated solution and the latter ingredients are added as sterile filtered solutions under the sterile bench. 10 µL of OD 0.01 (corresponding to ca. 1 x 10^6 CFU) were used to infect one well of medium (200 µL for 24 h, 500 µL for 72 h, due to evaporation). Then, the 24-well plates were closed with BreathSeal foils (Greiner bio-one, Frickenhausen, Germany) and were incubated at 37 °C and humidity without shaking for 24 or 72 h.

3.2.4 Imaging of biofilms on abiotic surface

Light microscopic images were obtained as follows, compare[4]. 72h pre-grown PAO1 biofilm was washed 2x with deionized water and subjected to a 0.1% crystal violet solution (No. 61135, Sigma) in water in 24-well plates for 10 min. Then, wells were

washed 3x with water and either left in the well with water ("native biofilm on ground") or were scraped off with a 1000 µL pipette tip crosswise in 200 µL water and transferred in a new well ("transferred biofilm"). For imaging, these wells were centrifuged at 1460 x g for 10 min and supernatant was removed. Remaining biofilm on ground after scraping was also imaged with 200 µL water ("biofilm remnants on ground"). Images were obtained with a light microscope at 10x magnification (Axio Vert A.1, Zeiss, Jena, Germany).

For analysis at CLSM (TCS SP 8, Leica, Mannheim, Germany), biofilms of PAO1-GFP were used. Biofilm is grown for either for 24h, washed two times with PBS and was transferred on microscope slides to be imaged at CLSM. For 72h pre-grown biofilms on 24-well plates or on 24-well imaging plates (Miltenyi Biotec, Bergisch Gladbach, Germany), biofilm was washed once with PBS and subjected to 20 µg/mL Hoechst 33342 (Sigma, No. H3570) for 20 min (as in [4]). Then, staining was removed and replaced with PBS. Either biofilm was then imaged directly on the imaging plates ("native biofilm") or transferred via crosswise scraping of biofilm to an empty well of the imaging plate ("transferred biofilm"). Alternatively, 72h pre-grown PAO1-GFP biofilm was transferred in 200 µL PBS on Transwell® inserts without cells and after 1h at 37°C, supernatant was removed to have ALI conditions. The insert was imaged standing on a microscope slide at CLSM. Hoechst was imaged with UV light at 400 nm and PAO1-GFP Argon-Laser at 488 nm excitation.

3.2.5 Metabolomic analysis

Analysis was done as in [4]. Using 72 h grown biofilms, apical biofilm supernatant was removed. Then, the wells were filled again 400 µL fresh M63 (native biofilm). To model transferred biofilm, the 72h grown biofilm was transferred with 400 µL fresh M63 medium in a new well. Then, biofilms were either incubated for 1h in order to simulate the ALI infection on CFBE cells, or biofilms were incubated for another 24h. As a control, planktonic bacteria were obtained via inoculation of the same biofilm medium (20 mL M63) in an Erlenmeyer flask. The flask was inoculated with a PAO1 colony using

the same LB stock plate and incubated via shaking (180 rpm) at 37°C, overnight. After finishing respective incubation time, 400 µL of biofilms were centrifuged in plastic tubes at 21250 x g for 10 min. Likewise, 400 µL overnight culture was used after 16h incubation to ensure exponential growth (as usual), but using M63 medium to keep the same medium, which is important to later compare the features. Then, supernatant of the centrifuged vials was removed and resulting pellets were weighed. Methanol (1 mL) and 25 ng sulfadimidine as internal standard was given to the vials and was vortexed for 10 min. Dried pellets were then diluted in 100 µL methanol, of which 5 µL were used for analysis. Dionex Ultimate 3000 RSLC system coupled with a Bruker maXis 4G UHR-Q-TOF-MS were used and measurements were performed in duplicates. A linear gradient of 5-95% of acetonitrile (0.1% formic acid, B) in double distilled H_2O (0.1 % formic acid) was used to separate the sample. The flow rate was 0.6 mL/min at 45 °C on a Waters Acquity BEH C18 column (100 x 2.1 mm, 1.7 µm dp). For mass spectra, the centroid mode was used, with a range from 150-2500 m/z at 2 Hz scan rate. MetaboScape 4.0 was used as software. There, the minimal intensity threshold was set to 2.5 x 10^3 (maximum charge state of 3). For creating batch features, minimal group size was set to 6. All blank features were subtracted from analysis.

3.2.6 Susceptibility of PAO1 biofilm and planktonic bacteria to tobramycin

24-well plates were incubated with PAO1 to build biofilms for 72h incubation time, as described. 16h before the end of incubation, an overnight culture in LB medium in an Erlenmeyer flask was done, as described. After 72h, biofilms were washed once with PBS and incubated with increasing concentrations of tobramycin sulfate (Sigma-Aldrich, T1783, Munich, Germany) of either 0, 4, 8, 20, 50 or 100 µg/mL in 400 µL M63 and further incubated 24h, as done in [4]. Likewise, transferred biofilm was made by washing the 72h grown biofilm once, then transferring it to new wells and adding tobramycin to yield the same concentration at same volume. Overnight culture was seeded at the same CFU on wells (OD 0.01, 1:5 concentrated to match 10^8-10^9

CFU/mL) and was subjected to same treatment on 24-well plates. After 24h the wells were scraped off, supernatant was transferred to sterile plastic vials and vortexed for 5 minutes. CFU was counted then as described in 3.2.10.

3.2.7 Infecting epithelial cells with PAO1 biofilm and treatment at ALI

Before infection, basolateral medium of seven days grown CFBE41o- cells on Transwell® inserts is changed to medium supplemented with 0.4% arginine, as it was shown that cell survival is enhanced and cell monolayers are better preserved after infection[5,8,9]. Biofilm was grown for 72h, washed two times with KRB and transferred with 200 µL on epithelial cells. After 1h in cell incubator, biofilm parts are assumed to be settled and remaining liquid is discarded to rebuild ALI conditions.

Right thereafter, cells were treated at ALI conditions as described[4]. The described deposition device was used and deposition on cells was done exactly as described in Chapter 2. For treatment, tobramycin sulfate (Sigma, Germany) was used. A dose of about 10 µg on cell inserts was ideal, as proven in initial experiments (data not shown). As the deposition efficiency was initially calculated being 3.45 ± 0.23% with 200 µL invested volume in the given circumstances, the value was rounded to 3% and calculated back to the necessary dose of 10 µg. Hence, ca. 333.33 µg tobramycin sulfate is needed in 200 µL invested volume, adding up to a concentration of 1,6 µg/mL. This dose was used throughout all experiments and always made by producing a sterile-filtered stock of 16.6 mg/mL in KRB, that was frozen and stored for not longer than three weeks at -20°C. Right before experiments, vials were thawed and diluted with sterile KRB. For evaluating and proving to have the correct dose to kill bacteria, concentration of the 200 µL volume was varied 10-fold (0.16, 1.6, 16,6 mg/mL, chapter 3.3.4). Nevertheless, thereafter used concentration was always 1.6 mg/mL. The deposited dose was analyzed with the system used as described in 200 µL PBS in 24-well plates, finding 1.6 ± 0.09, 14.8 ± 0.16 and 102.0 ± 4.89 µg, respectively (n=3). Tobramycin sulfate was analyzed with LC-MS (Dionex UltiMate 3000 Binary Rapid Separation UHPLC System (Thermo Scientific, USA) and TSQ Quantum Access Max

(QQQ, Thermo Scientific, USA)), equipped with a Zorbax Eclipse xdb C-18 column (5 µm, 50*4,6 mm, Agilent, USA) + C18 guard column. The Flowrate was 0,7 mL/min, and 3 µL was used as injection volume. Eluents were acetonitrile (eluent A) and water (eluent B), both supplemented with 0.1 % trifluoracetic acid, 0.1% pentafluoropropionic acid and 0.1% heptafluorobutyric acid. The was a gradient of eluents A and B featuring a starting ratio of 20:80 first, then from 1 to 3.5 min, ratio was changed to 70:30. Between 3.5 and 4.5 min, the ratio was restored to 20:80. 2,97 min was the retention time. Electrospray-Ionization was employed (positive Ion Mode) and the SRM (Selected Reaction Monitoring) of the ion 468.184 (parent Ion) à 324.09 m/z and 205.16 m/z (fragments).

3.2.8 Biofilm pre-treatment with ciprofloxacin

As a proof of concept, biofilm infection of cells was done with biofilms that were subjected to a pre-treatment with ciprofloxacin before transfer on cell model. Therefore, 72h grown biofilm was washed, pre-treated with 500 µL of 1 µg/mL ciprofloxacin (Fluka Analytical, 17850-25G-F, Germany) in KRB for 1h and washed again once to compare to non-treated biofilm incubated for another 1h with only KRB (as indicated). Then, biofilms were scraped off as described and placed on cells. As control, planktonic bacteria were seeded at an OD of 0.01 and concentrated 1:2 and 200 µL were put on cells for 1h prior to restoring ALI conditions as described. Planktonic bacteria had comparable CFU as biofilm bacteria as illustrated.

3.2.9 Comparison of different culture conditions

In order to compare the influence of cells on treatment, empty permeable supports were used and inserts that are seeded with epithelial cells as described. Both were infected and treated after 1h as described above.

The influence of submerse conditions was checked via using epithelial cells grown on Transwell® inserts that were infected and treated at ALI conditions in the same way as

described[4]. One group of inserts was thereafter submerged with 500 µL on the apical side and 1500 µL on the basolateral side and incubated for another 24h.
To find out differences from biofilm to the planktonic state of growth for infection of cells, biofilm and planktonic bacteria infected epithelial cells as described. 200 µL planktonic bacteria in KRB were seeded at OD 0.01 and a concentration of 1:5, which matches the concentration of biofilm bacteria in suspension of about 10^8-10^9 CFU/mL.

3.2.10 Analysis of CFU

Generally, suspensions containing bacteria are always vortexed for 5 minutes to destroy biofilm clumps. In case of infected cells, 500 µL cold sterile distillated water was poured onto the ALI grown cells to destroy mammalian cells (compare[137]) and basolateral medium was removed. After 30 minutes and 4 °C, attached cells were scraped off the Transwell® insert, shortly mixed with a pipette on the well and put into plastic vials, as done in[4]. Then, these suspensions are diluted in 10-fold dilution steps on 96-well plates in PBS containing 0.05% Tween 80 (Sigma, Germany). Drops of 20 µL of the expected countable dilutions were placed on LB Agar plates in triplicates and incubated for ca. 20 h at 30 °C. Colonies were thereafter counted visually. Plates were left at room temperature for another 20h in order to find new emerging colonies. By the dilution and the initial amount of liquid, the original number of bacteria was calculated.

3.2.11 Analysis of barrier function

Tightness of barrier was assessed via transepithelial electrical resistance (TEER) at the end of respective incubation via adding 500 µL medium on the apical side and 1500 µL on the basolateral side[4]. Permeable supports were further incubated for 1 h. Using an epithelial Voltohmmeter (EVOM, World Precision Instruments, Sarasota, Florida) and STX2 Chopstick electrodes, TEER was measured by sticking the two electrodes in the apical and basolateral compartment without injuring the cells on a heating plate at 37

°C. The resulting value was corrected by area of the insert (1.12cm^2) and the value of the blank insert (as described).

3.2.12 Cell viability

Mammalian cell viability was assessed via release of LDH as described in Chapter 2 and in[4]. Notably, presence of lower doses of bacteria do not disturb the assay, as confirmed by other authors before[5,117]. Nevertheless, high amounts of bacteria disturb the assay, so that a color reaction does not take place[137,138]. In that case, complete destruction of cell layers was confirmed via imaging. To confirm, that LDH is destructed by overgrowing PAO1 bacteria, 24-well plates were filled with normal medium, medium plus 1U of LDH per mL (LDH (Rabbit muscle), 10127230001, Roche, Mannheim, Germany) as done in Montefusco, Horstmann et al[137]. Medium or medium with LDH was diluted to OD 0.01 (approximately 1x10^8 CFU of PAO1-GFP) and incubated for 20h at 37°C. Afterwards, LDH was detected as described in Chapter 2.

3.2.13 Imaging of biofilms on cell surfaces

Confocal images of biofilms on epithelial cells were obtained using PAO1-GFP as in[4]. CFBE41o- were pre-stained with Hoechst 33342 prior to infection. 200 µL at a concentration of 5 µg/mL in KRB were used and incubated for 20 min apically. Then, cells were washed once and infection was done as described. After incubation, the cells were not washed and paraformaldehyde 3% was added apically (100 µL) and on the basolateral side (1500 µL) and incubated at 4°C overnight. Then, liquid was carefully removed, the membranes were cut out and mounted upside down on a microscope slide using DAKO® mounting medium (DAKO, S2023, Carpinteria, USA). and a glass coverslip. Images were visualized using CLSM (TCS SP 8, Leica, Mannheim, Germany). Hoechst was imaged with UV light at 400 nm and PAO1-GFP was imaged with 488 nm excitation (Argon Laser).

SEM images were done using PAO1 bacteria and CFBE41o- cells that were not colored as in[4]. Transwell® inserts were fixed in paraformaldehyde 3% as described before

(over-night) and dehydrated using ethanol 400 µL apically at a concentration row of 30-40-50-60-70-80-90-96-100% (2x), each for 10 min. This was followed by addition of 200 µL hexamethyldisilazane (No. 44191, Sigma-Aldrich, Munich, Germany) over night, that evaporated in a fume hood. Samples were mounted on aluminum stubs with carbon discs and sputtered with gold (Quorum Q150R ES, Quorum Technologies Inc., Laughton, UK). Samples then were imaged using SEM (EVO® HD15, Zeiss, Jena, Germany) under vacuum conditions.

3.2.14 Cytokine detection

ELISA was done to analyze amount of cytokine (Interleukin 8 (IL-8)) according to manufacturer´s protocol (No. 88-8086-22, Invitrogen, Carlsbad, USA), as in[4]. Frozen aliquots stored at -80 °C were used (aliquots remaining from LDH detection after centrifugation). Samples were thawed at room temperature and diluted 1:10 in Elisaspot reagent to be directly placed on the wells.

3.2.15 Transport experiment

As an additional experiment, 48h incubated cells were either infected and treated at t=1h or both t=1h and 24h or were not infected and only subjected to KRB deposition. The infected co-culture was done as explained above. All inserts were measured TEER as described. Then, the cells were washed twice with KRB and submerged with KRB containing 10 µg/ml tobramycin sulfate in order to prevent further growth of bacteria and incubated another hour to measure TEER. Sodium fluorescein working solution was prepared at 10 µg/mL in KRB with 10 µg/mL tobramycin sulfate. KRB on Transwell® inserts was removed and replaced with 520 µL working solution and 1500 µL basolateral KRB. As control, EDTA (Sigma, Germany) was added at 16mM in working solution as above. Right after the start, 20 µL of apical volume was removed and sampled at start and at the end of the experiment and diluted in 180 µL KRB. 200 µL from the basolateral side was removed and refilled with fresh KRB at t=0, 20, 40, 60,

90, 120, 180, 240 min. Plates were placed on a shaker (IKA MTS 2/4, Staufen, Germany) at 200 rpm while incubation at 37 °C. Resulting samples were put into a 96-well plate, saved from light and were read at 485 excitation and 530 nm emission in a Tecan plate reader (Spectrophotometer Infinite M200 Pro, Tecan Trading AG, Männedorf, Suisse) as described.

Apparent permeability values were calculated using following well known formula, that is often used in-house[7,139,140]:

$$p_{app}\ (cm * s^{-1}) = \frac{J}{A * c_0}$$

With c_0 being the initial concentration of the donor (µg/cm^3) and A the area of the Transwell® insert (1.12 cm^2). Flux *J* is the cumulative mass in µg transported across the cells versus the time in s (with mass <10% of total mass).

3.2.16 Western blot

After finishing respective incubation of infected cells (24, 48 and 72h post infection), the wells were frozen at -20 °C. Then, samples were thawed at RT and remaining liquid was carefully removed. Epithelial cells on inserts were then lysed with 300 µL lysis buffer for 5 min at 4 °C (150 mM NaCl, 20 mM Tris-HCl, 1 mM EDTA, 1% Triton X-100, 1 mM Na_3VO_4, 10 mM 1,10-phenanthroline monohydrate, 1 mM PMSF,) plus complete Inhibitor (1x, Roche, Heidelberg, Germany). Then, the resulting liquids were further assayed at university clinic in Homburg. Samples were centrifuged at 14000 x g for 15 min and resulting supernatants were analyzed via reducing SDS-PAGE (40 µg total protein per lane (bicinchoninic acid (BCA) assay, ThermoFisher, Dreieich, Germany). Afterwards, substance was put onto nitrocellulose membranes (Bio-Rad, Feldkirchen, Germany). Blocking was done with 5 % (w/v) non-fat dry milk in TBS for 1h. Primary mouse monoclonal antibody (against human E-cadherin (250 ng/ml, BD Biosciences, Germany) in 1 % BSA in PBS was subjected to the probes overnight. Chemiluminescence of HRP (Western Lightning® Plus-ECL, Perkin Elmar, USA) was measured, after incubation with HRP-coupled secondary antibody (GE Healthcare,

Solingen, Germany) for 1h, using LAS-3000 (Fujifilm, Dusseldorf, Germany). The resulting signals were quantified with Aida imaging Software (Elysia-raytest GmbH, Straubenhardt, Germany). The 120 kDa fraction intensity was plotted in % of control intensity of respective triplicates (compare with[4]).

3.2.17 Influence of QS inhibitor on epithelial cells

Infection of CFBE41o- at ALI was done as described. Here, an additional experiment was done. After 1h infection, PAO1 biofilm suspension was removed, and pqsR inverse receptor agonist compound 4[7] was applied on infected cell model as treatment after 1h. This treatment was applied as 100 µL solution in KRB at 10 µM concentration, diluted from a 2 mM stock in DMSO (kind in-house gift of the authors of [7]), resulting in a 1:200 dilution of DMSO stock in KRB (0.5 %). If this treatment was combined with tobramycin, 200 µL tobramycin sulfate 1,6 mg/mL was nebulized before on infected cells as described.

48h post-infection, 200 µL KRB was added to the apical side and the apical liquid as well as the basolateral medium was transferred to plastic vials. For analysis, the equivalent amount of acetonitrile (plus HHQ-d4 as internal standard) was added to the samples. These were then thoroughly vortexed for 5 min and centrifuged at 21250 x g for 15 min. Resulting supernatant was then transferred to vials and analyzed via LC-MS/MS (Dionex Ultimate 3000 HPLC system plus TSQ Quantum Access MAX (both Thermo Fisher Scientific, Waltham, USA), as done before[7]. A Zorbax Eclipse XDB 80 Å C18 5µm column was used (4.6 x 50 mm column, Agilent, Santa Clara, USA). Eluent A: H_2O with 0.1% trifluoroacetic acid, 0.1% heptafluorobutyric acid and 0.1% pentafluoropropionic acid. Eluent B: Acetonitrile with 0.1% trifluoroacetic acid, 0.1% heptafluorobutyric acid and 0.1% pentafluoropropionic acid. Measurement with isocratic flow 50% of eluent A at 0.7 mL/min. Spray voltage 3500V, vaporizer emperature 370 °C, positive ionization mode. Data acquisition using Xcalibur software. PQS: precursor ion 260.048 m/z, product ions 145.958 and 174.927 m/z. HHQ: precursor ion 244.050 m/z, product ions 158.944 and 171.943. HQNO: precursor ion

260.036, product ion 158.908. DHQ: Precursor ion 161.971 m/z, product ion 115.979 m/z. 2-AA: precursor ion 136.016 m/z, product ion 91.048 m/z.

3.2.18 Addition of human mucus and artificial mucus on cells

This additional method was initially introduced by Dr. Xabier Murgia[141], with small modifications continued by Dr. Jenny Juntke[8,9]. Human mucus was obtained from tracheal tubes of patients at Klinikum Saarbrücken gGmbH. The method was ethically approved by the Ethics Commission of the Chamber of Medicine Doctors of Saarland (File number 19/15). In order to provide sterile mucus for cell culture, mucus disks were produced before experiments. Approximately 30 g visually clean mucus from tubes was placed per disk on Teflon® sheets and was frozen at -80 °C. Thereafter, disks were freeze-dried (Alpha 2-4 LSC, Christ, Germany) overnight and put under UV light for 1h under sterile conditions. Each batch was tested for microbial growth and only used on cells if sterile.

Mucus disks were added on CFBE41o- cells grown on Transwell® inserts for 6d at ALI conditions (one day less as described before) and 50 µL CFBE Medium was placed apically on the disks. The plate was agitated at 200 rpm on a shaker (IKA MTS 2/4, Staufen, Germany) in the incubator at 37 °C and 5 % CO_2 overnight. On the next day, excess medium was carefully removed. As control, 50 µL of sterile artificial mucus was used as described by Huck et al.[16]. Briefly, it contains of water, porcine stomach mucin, deoxyribonucleic acid, diethylenetriaminepentaacetic acid, NaCl, KCl, Trizma base, casein hydrolysate, egg yolk emulsion and poly(acrylic) acid to adjust viscosity comparable to human mucus. This formula is called “modified artificial sputum medium (ASM_{mod})”. In order to provide sterile artificial mucus, the mucus without egg yolk emulsion was autoclaved at 121 °C and sterile filtered egg yolk emulsion was added thereafter. Each batch was tested for bacterial contamination.

As further control, 50 µL medium was added on CFBE41o- cells over night as well. After incubation, all samples are submerged with medium (1500 µL basolateral and 500 µL apical) and TEER was measured after ca. one hour, as described.

3.2.19 Artificial mucus addition on cells and infection

Infection experiments was done as described, with 72h PAO1 biofilm growing in M63 before the experiment. In the here done additional experiment, instead of 200 µL PAO1 biofilm suspension in KRB, 200 µL biofilm suspension in ASM_{mod} was transferred on cells, with CFBE41o- with and without ASM_{mod} as control. As infected control, cells were infected with biofilm in KRB as described. After 1h, liquid was removed, but ASM_{mod} on cells remained (mostly) on cells, since it was too viscous to remove. Inserts were then treated with deposited KRB or tobramycin dose as described.

3.2.20 Statistical analysis

Experiments were generally done in triplicates in at least three independent experiments (or as indicated). Either Two-Way ANOVA or One-Way ANOVA has been chosen, that is indicated according to the data set. Tukey´s multiple comparisons test was generally done, or as indicated. P values are defined as: ns $p>0,12$; * $p<0,033$; ** $p<0,002$; *** $p<0,001$. Generally, mean and standard deviation are given, others are indicated. All experimental graphs were imaged and analyzed with GraphPad Prism® 9.

3.3 Results and discussion

3.3.1 Biofilm and evaluation of a method to transfer

3.3.1.1 Characterization of PAO1, PAO1-GFP and PA14

P. aeruginosa, as many other bacteria, consists of various strains and variants. The strain PAO1 was used in many *in-vitro* models of infection and can by assumed as one of the most prominent strains of *P. aeruginosa*[118,142–144]. Also, a previous study, which is aimed to be continued here, has been done with the same strain[8,9]. Nevertheless, this PAO1 strain is derived from a wound infection[145], which is technically not the location of infection to be modelled in this work, but, as a normal *P. aeruginos*a strain, it is able to build biofilms as commonly known[146,147]. Alternatively, a genetical modified PAO1 expressing a green fluorescent protein (GFP) is used (PAO1-GFP). It is resistant to a concentration of 300 µg/mL ampicillin, that is used for cultivation of it[135]. LB agar plates to obtain single colonies of PAO1-GFP to infect LB medium are also made with ampicillin and stored for max. 10 days. PAO1-GFP has been used in our group before[8,9,137]. Another used strain in this study is PA14, that also has been used frequently in literature[5,148,149]. A quality control for all overnight cultures has been the continuous observation of the medium (macroscopically) and bacteria (via light microscope). After about 15h, the medium must look turbid and slightly greenish. Each overnight culture is visualized under light microscope to check morphology of bacteria. Both bacteria should share the morphological structure as possible to see by light microscope and should be moving due to the flagella.

In order to further characterize the bacteria, a growth curve was done to evaluate the ideal timepoint to work with bacteria. As commonly known, bacteria growth is divided in the lag phase, log phase, stationary phase and death phase[150]. Bacteria first do not proliferate and accommodate to their environment, but then start to grow exponentially, when they find ideal circumstances. This lag phase endures about 3h in the present PA strains (Figure 3.1). PAO1 is cultivated as described in materials and methods section. Bacteria start to proliferate very fast until about 10-15 h after seeding

(Figure 3.1). In this setup, a plateau phase is not visible, since bacteria continue to grow, but it is assumed that 15h is a good timepoint to have a) enough bacteria and b) bacteria still being in a proliferating state. Therefore, no overnight cultures were used being older than 15h.

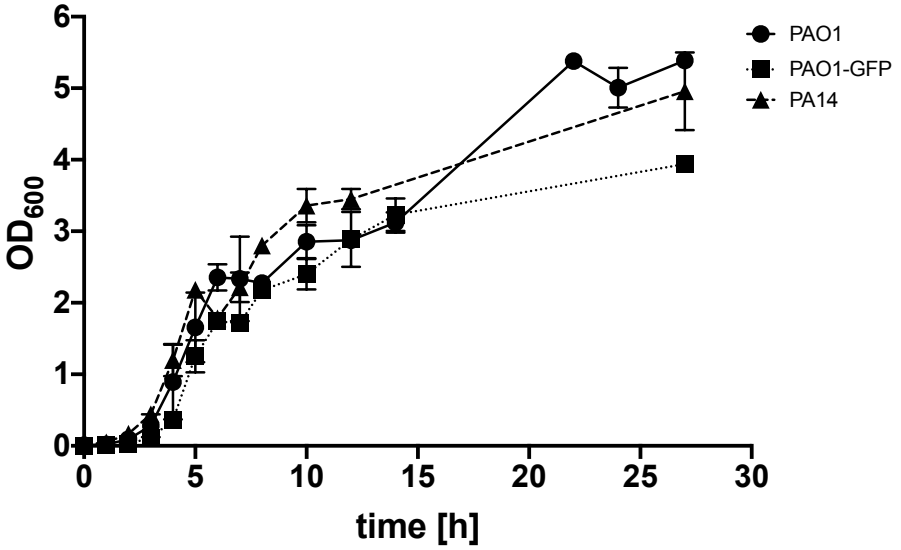

Figure 3.1 Growth curve of PAO1, PAO1-GFP and PA14 as grown in Erlenmeyer flasks. N=6 of two independent experiments (PAO1), N=3 of one experiment (PAO1-GFP, PA14).

3.3.1.2 Characterization and transfer of 24h grown biofilms

Pseudomonas aeruginosa builds biofilms on surfaces, as on stones, wet surfaces but also on urinary catheters, as being well known[144]. Biofilms are also able to be formed on cells *in vitro*, as shown by several works already demonstrated in the introduction of this thesis[5,116]. A preliminary study by Dr. Jenny Juntke, which partly serves as basis for this work, showed epithelial cells to be destroyed when cultured with planktonic PAO1[8]. As the time frame for obtaining a mature biofilm is very limited, the idea was taken up to pre-form a biofilm on plastic wells to transfer it on cells. This has the advantage of having both: healthy cells and a mature biofilm[8]. It could be shown, that biofilms are on top of epithelial cells. Nevertheless, the procedure of the biofilm transfer could not be fully characterized. In order to learn the method and to prove the

reproducibility, a very comparable protocol was employed to pre-grow PAO1 biofilms for 24h (Figure 3.2).

200 µL M63 medium supplemented with arginine was used to grow biofilms using an initial inoculum of about 1 Mio. bacteria (10 µL of 1 x 10^8 CFU/mL, Figure 3.2 B). After 24h growth at static conditions at 37°C, the biofilm grown in M63 of the recipe best suited for this procedure is formed preferably on surfaces as shown by studies of Dr. Jenny Juntke[8]. Biofilm on the ground and on the well walls is macroscopically visible. Turbid, mostly greenish supernatant is removed and washed two times (Figure 3.2 C). Then, the biofilm is scraped off crosswise together with one circular move via a 1000 µL pipette tip in 200 µL liquid, and transferred to another surface (Figure 3.2 D to E).

To prove reliability of this process, the biofilm was stained with 0.1 % crystal violet solution comparable to a known protocol[136]. With even two washing steps, PAO1 biofilm firmly attaches to the ground as shown by a bright blue color. M63 is apparently facilitating this process in comparison to other media, as proven by initial experiments and Dr. Juntke´s comparison of biofilm media[8]. After scraping process, less biofilm is visible on the ground, but being still a huge amount as seen by eye (Figure 3.2 D). Transferred biofilm on empty wells is stainable and shows a biomass being successfully pipetted, as it could be successfully stained (Figure 3.2 E).

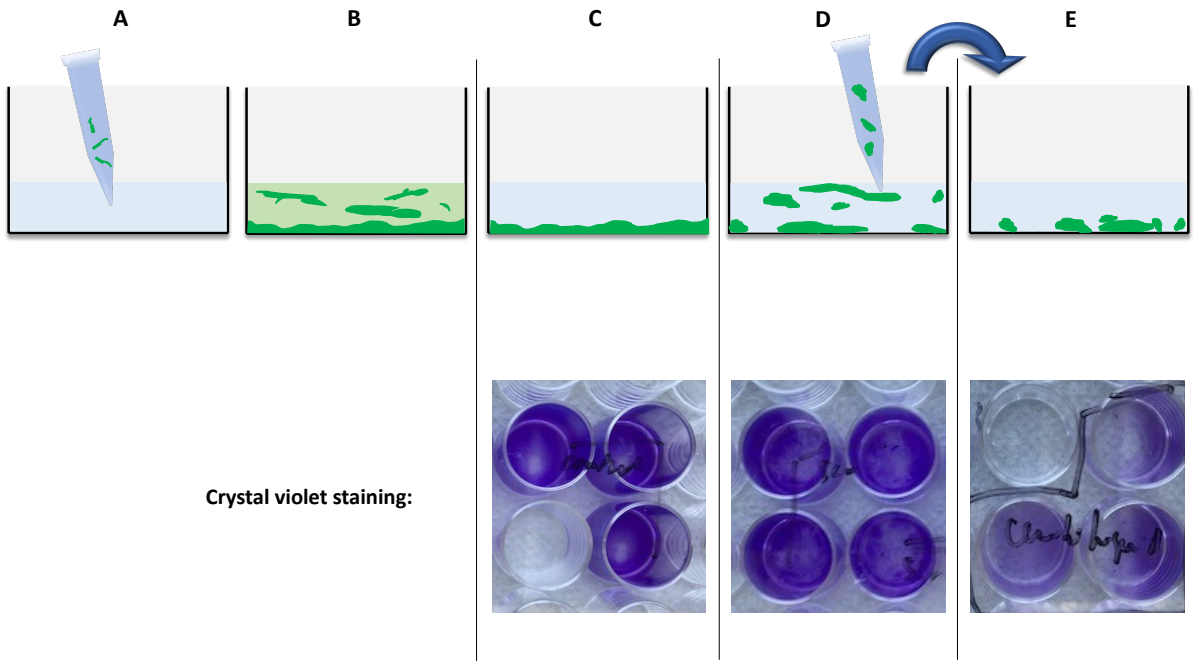

Figure 3.2: General transfer procedure for biofilms formed by *P. aeruginosa* (in this case 24h pre-grown). (A) M63 Minimal medium, 200 µL per well in 24-well plate, inoculated with 1 Mio. Bacteria. (B) After 24h: Biofilm and free-floating bacteria. (C) Supernatant washed two times with PBS. (D) Attached biofilm on ground is scraped off (crosswise) with 200 µL PBS. (E) Transferred biofilm suspension settled onto a surface (here plastic well). Below the schemes, representative macroscopical images of dried, CV-stained biofilms are shown.

The biofilm transferred shows a CFU being about 1 x 10^9 CFU/mL (Figure 3.3 A), which is about 3 times higher than the initial inoculum. Bacteria have grown and built biofilm structures as imaged by CV staining. Even so, the CFU is highly deviating, showing a span between 11 and 8 $\log_{10}$ CFU/mL, which could be a problem infecting cells reproducibly.

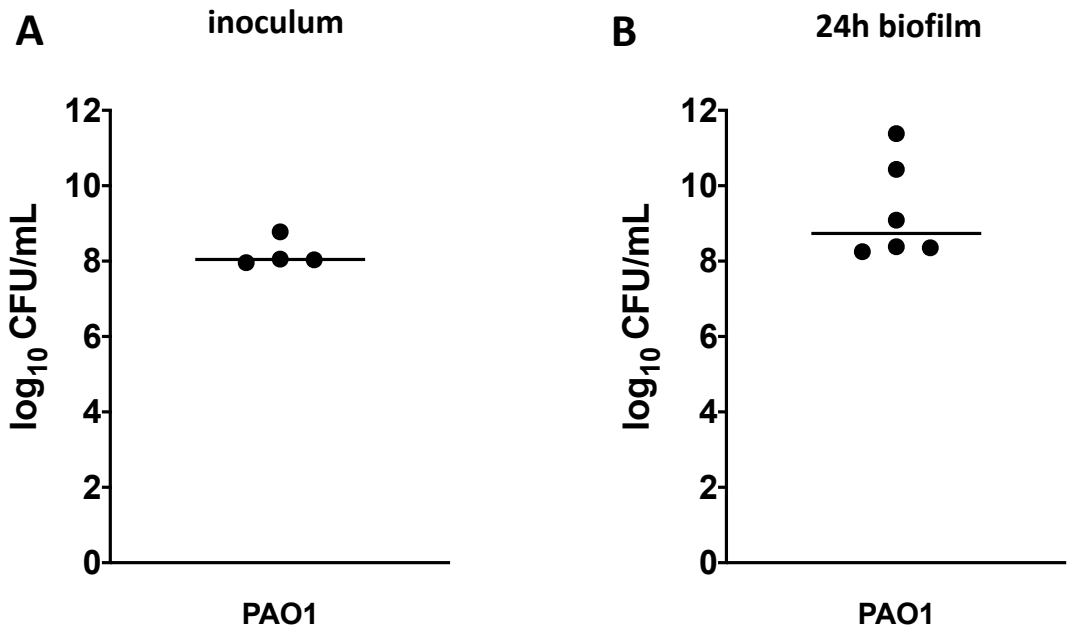

Figure 3.3: CFU of the initial starting inoculum for PAO1 (A) and 24h PAO1 biofilm (B). N=6 of 3 individual experiments, inoculum N=4 of 2 independent experiments. Line showing mean of individual values.

Biofilm mass as imaged in Figure 3.2 was evaluated via absorption. It could be shown, that the washed biofilm on the ground shows most biofilm mass, followed by the remains of scraped biofilm on the ground (76 % of control, Figure 3.4). Transferred biofilm mass only features 18 % of the control. Adding this amount to the remaining biofilm mass, a theoretical amount of about 94% is reached, which comes close to the 100 % of real remaining biofilm, proving somewhat the plausibility of 18% transferred biofilm mass. To date, no comparable studies are found to contextualize those values. Preliminary experiments were made in-house to enlarge the mass of transferred biofilm by using plastic cell scrapers. These scrapers were suited to better remove the biofilm, but the biofilm could not be transferred because it sticks to the plastic. Therefore, the method of using 1000 µL pipette tips employed by Dr. Jenny Juntke was approached in this study and following studies of this thesis.

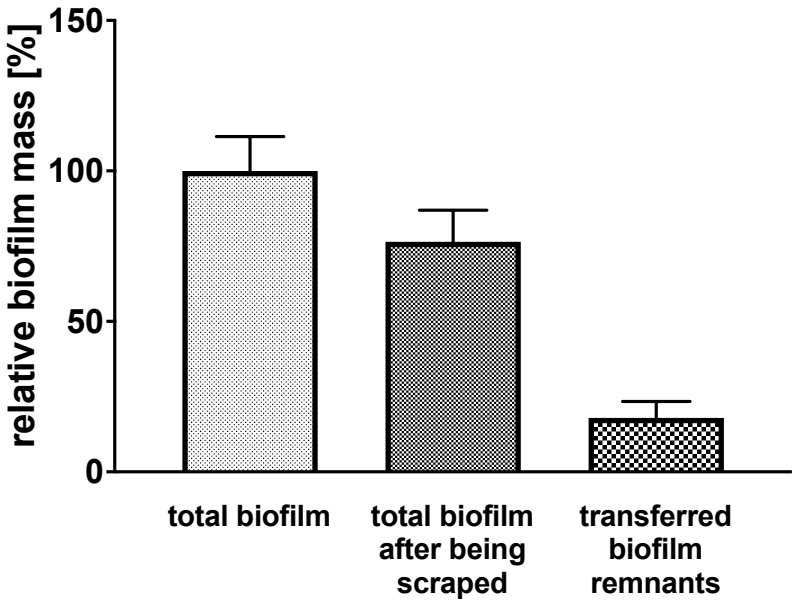

Figure 3.4: Relative biofilm mass of 24h grown PAO1 biofilm. Biofilm mass analyzed via crystal violet staining. Mean and SD. N=9 of 3 independent experiments.

Dr. Jenny Juntke showed colored biofilm parts of PAO1-GFP to be transferred as imaged under confocal microscope[8]. To verify the reproducibility of this procedure, scraped 24h pre-grown PAO1-GFP biofilm was transferred onto glass slides to show biofilm parts as expected. Figure 3.5 shows these aggregates consisting of the transferred biofilm suspension after visualization on glass surfaces. These parts are about 20-30 µm in diameter, which is quite small but could be realistically a part of a biofilm matrix as reported *in vivo* and *in vitro*[22,151]. Unlike as in the named literature, this aggregate is pinched between two glass slides, so the original diameter is likely to be smaller. Generally, only very few biofilm-like aggregates were found under the confocal microscope, superposable to the macroscopic view on the 24-well plates showing only some slight biofilm structures. Even though, it is very probable, that these parts are biofilm parts, having a suited biofilm suspension was still somewhat questionable, as the number and mass of found biofilm parts is quite low. An option is to grow the biofilm for more than 24h, as this is also more comparable to *in vivo*[22,24,152]. The hypothesis is, that biofilm will mature and be more visible.

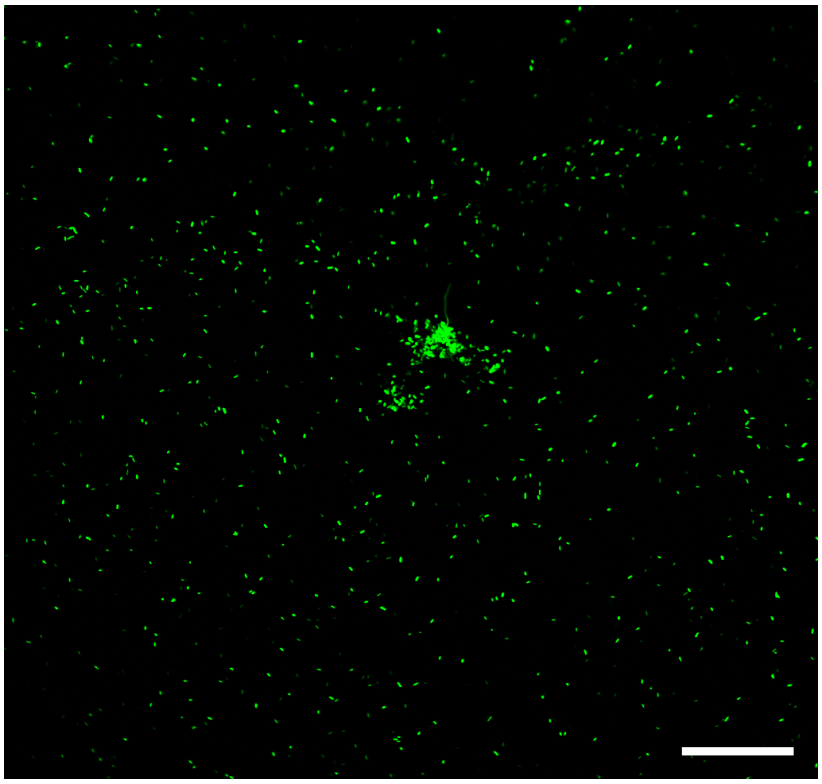

Figure 3.5: PAO1-GFP transferred 24h grown biofilm suspension shows small aggregates perceived as biofilm. Suspension transferred on a microscope slide imaged at CLSM. Scale bar 50 µm.

3.3.1.3 Characterization and transfer of 72h grown biofilms

Biofilms differ from their grade of maturation and maturation times of up to 10 days *in vitro* are reported[23]. Several groups employed maturation times of more than 24h[25,152,153]. *In vivo* biofilms are formed in the course of longer time periods, even years, as described in the introduction[21,22]. Therefore, the growth time is tried to be increased, as this reflects the *in vivo* biofilm better than the 24h biofilm due to higher grade of maturation as shown. Additionally, it was hypothesized, that longer growth times lead to bigger biofilm parts. Biofilms were started by inoculating M63 medium in 24-well plates as shown in Figure 3.2, but preliminary experiments revealed, that the biofilm dries even in the cell incubator with high humidity (90-95% relative humidity[154]). Therefore, the biofilms were started with 500 µL instead of 200 µL M63 and placed near of additional plates providing further humidity in the incubator. With

these modifications, the well bottoms were completely covered with liquid even after 72h.

After incubation time, these biofilms feature a very slimy texture and are mostly greenish and turbid. A visible slimy texture stays on the well bottom even after washing 2x with PBS. By scraping off this texture, biofilm parts become clearly visible (Figure 3.6 D). After staining those biofilms with crystal violet 0.1% as described, the transfer process is visualizable. Biofilm on ground (Figure 3.6 A) is very even and homogenous. This homogenous layer is now, that the biofilm is mature and apparently more cohesive, nearly completely destroyed after scraping off its surface with a pipette (Figure 3.6 B). Transferred biofilm suspension is detectable by eye with stained parts being in the former empty receptor well (Figure 3.6 C). This is perceived as a proof for biofilm mass being present and successfully transferred onto a new surface, as described in [4].

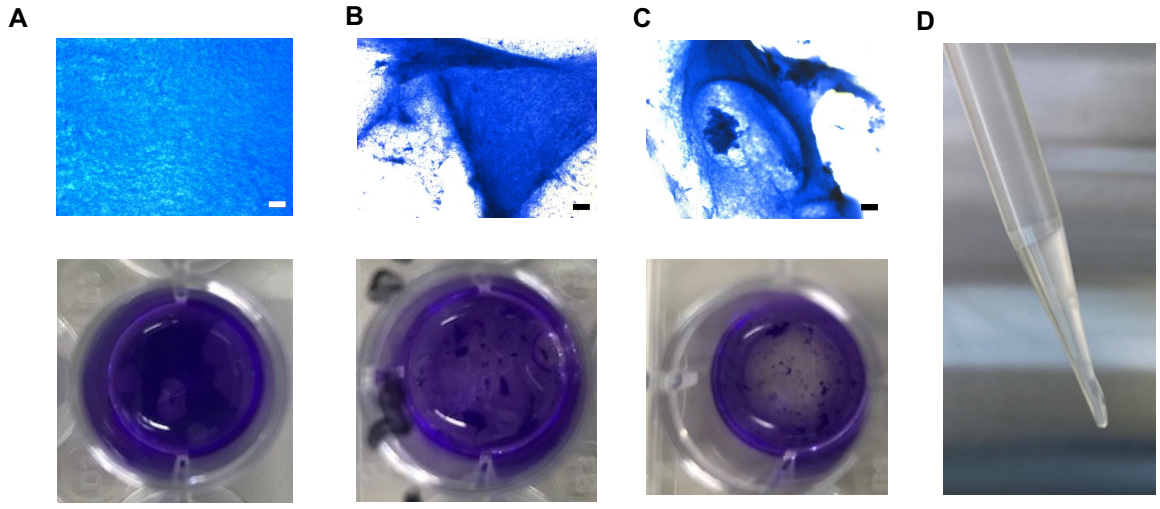

Figure 3.6: 72h pre-grown biofilm stained with crystal violet 0.1% on 24-well plate. Microscopic (above) and macroscopic (below) images are shown to explain biofilm transfer process corresponding to presented 24h-grown biofilm. (A) 72h-grown biofilm on the bottom of the well. (B) Biofilm remnants on the bottom of the well after scraping off biofilm partially. (C) Transferred biofilm suspension transferred on a new well. (D) Macroscopic image of the 1000 µL pipette tip with transferred biofilm suspension, without staining. Biofilm parts are visible with bare eye. Scale bar: 100 µm. Adapted with permission from [4]. ©2021, American Chemical Society.

Growing biofilms for 72h is apparently helping to increase biofilm mass, as the biofilm parts are now visible by eye, in contrast to the 24h biofilm (image not shown). Therefore, it seems to be straightforward to further analyze the 72h biofilm instead of the 24h grown biofilm. Transferring very comparable PAO1-GFP bacteria on blank Transwell® inserts could give insight, if biofilm parts stay on the well even after removal of supernatant (Figure 3.7). The biofilm parts are ubiquitously seen under the confocal microscope and are quite capacious, as being partly longer than 200-300 µm, which makes this method a promising tool to infect cells with biofilm. Furthermore, as the crystal violet solution stains the complete biofilm[136], a stain discriminating between free floating bacteria and the biofilm matrix would help to see if the biofilm itself is completely destroyed or if it is partially still intact. Therefore, PAO1-GFP bacteria were grown on a 24-well imaging plate for 72h and stained with Hoechst 33342 (as described in materials and methods and in[4]) to counterstain the eDNA of the biofilm matrix, that is interacting with Hoechst 33342[155]. This stain has been shown to be the best stain in this setting, as tested in preliminary experiments.

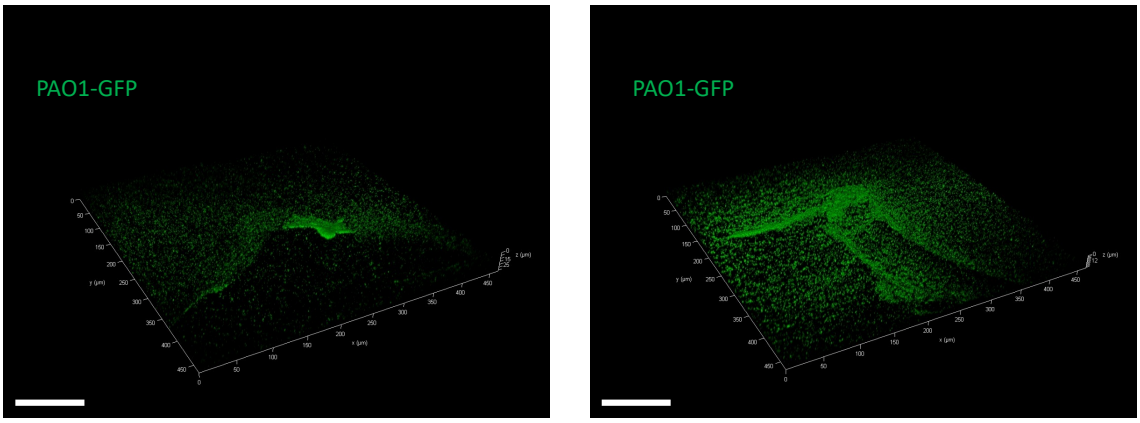

Figure 3.7: CLSM images of transferred 72h PAO1-GFP biofilms on top of Transwell® inserts. Biofilm suspensions were transferred in 200 µL PBS and supernatant was removed after 1h settling time. Scale bar 100 µm.

Figure 3.8 shows the results after staining. Native biofilm is firmly attached to the ground as seen macroscopically. The PAO1-GFP bacteria build a layer of mushroom-like structures, that are quite known to build on various surfaces *in vitro*[25,115,116]. Hoechst 33342 stains bacteria, as it is colocalizing with the GFP emission, but also stains nonspecifically a small part above the bacterial cell layer that is supposed to be eDNA (Figure 3.8 A). In subfigure B, the already transferred biofilm suspension is depicted, that differs from the biofilm on the ground. Most prominently, biofilm matrix as stained by Hoechst 33342 is not colocalizing any more with the PAO1-GFP bacteria[4]. The matrix circumvents the bacterial cells in the middle, showing that the matrix went off partially. Biofilm structure is expectably destroyed by scraping with the pipette. Nevertheless, the matrix seems to be still present, surrounding the biofilm clumps. Furthermore, one of the most important aspect of the biofilm is the state of growth, that is characterized by low physiological activity[22,28]. If this effect is also present in transferred biofilms needs further prove, which is provided by upcoming experiments.

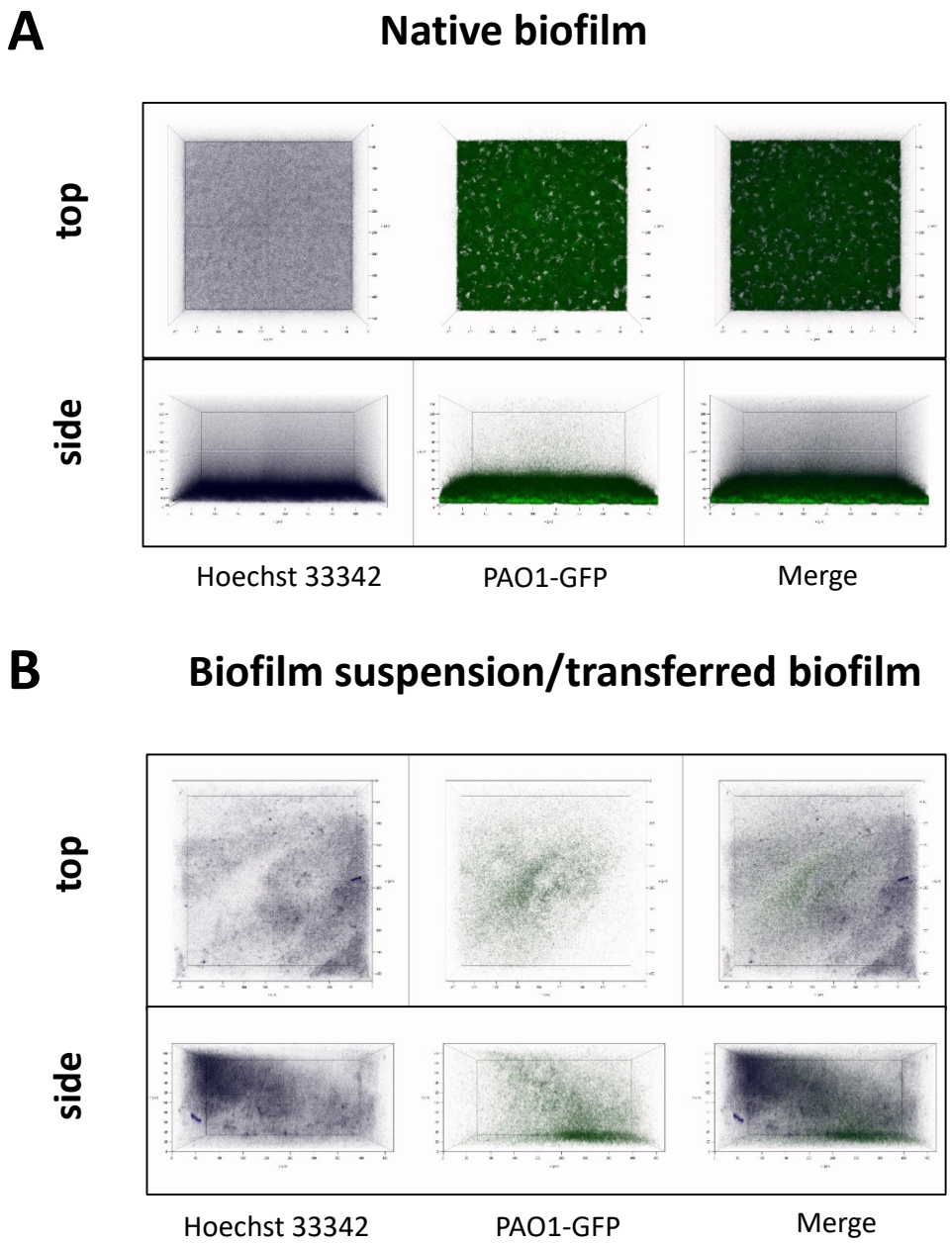

Figure 3.8: CLSM images of native/transferred PAO1-GFP biofilm. A: Grown on the bottom of the well, B: Biofilm, that was scraped off from biofilm grown as in A) and transferred in an empty well. Biofilms were stained with Hoechst 33341 to mark extracellular DNA. Adapted with permission from [4]. ©2021, American Chemical Society.

72h pre-grown biofilms are hypothesized to show a very high and variable number of CFU due to the long growth phase. Unexpectedly, the opposite is true (Figure 3.9), as already shown comparably in[4]. CFU of 72h biofilms is comparable to CFU of 24h-grown biofilms (9.2 vs. 8.7 $\log_{10}$ CFU/mL, respectively). Of all 72h-grown biofilms, a total of 69 values, only 13 values are beyond $\log_{10}$ 9.3-8.7 CFU/mL. Only 4 values can be perceived

as “outliers”, as they are way beyond the SD. This was most probably an artefact that happened while diluting and plating the CFU, such a high deviation due to a very high bacterial burden in the well itself is perceived as rather not probable. Given the fact, that a quite impressive number of 38 individual experiments were done with each a new 72h-grown biofilm counted individually, these values prove the reproducibility of the transferred biofilm and its usability for infection experiments.

Comparing CFU of biofilms grown on plastic to prove its reproducibility was not extensively done in literature. Ceri et al. compared the mass of biofilms grown on plastic tips to prove the usability of a new biofilm testing device called “Calgary biofilm device”[103,105]. The group could not find a statistical difference on the mean CFU of biofilms per peg, either after 4 or 24h of growth, whereas a tendency towards higher variability could be seen with increasing time, as well as a higher number of CFU per se. The deviation of CFU values was shown to be around 1 log, which is in best agreement with the here shown values, nevertheless, around 80% of the here shown values are inside a limit of only 0.6 logs, covering many more individual experiments as in literature used. Hence, the transferred biofilm is perceived as well reproducible.

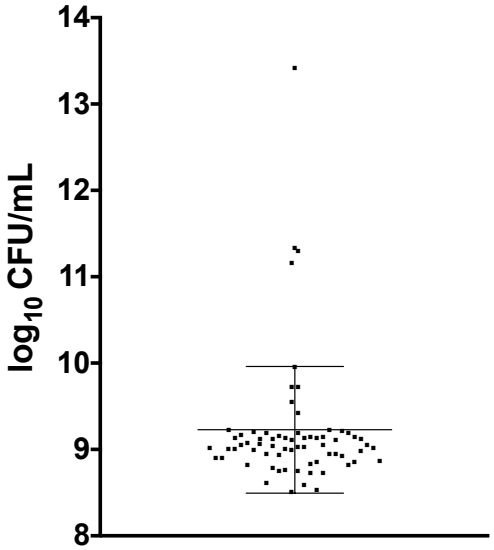

Figure 3.9: CFU of transferred 72h biofilm of all done experiments between 09/18 to 07/20. Some of the data are shown in[4]. 69 replicates of 38 independent experiments. Line shows mean, and error bar shows standard deviation.

The reason for choosing PAO1 as model bacterium was explained above. Nevertheless, it is important to compare the biofilm forming capacity of PAO1 to other PA strains in terms of CFU and biofilm mass. This would further prove the ability of PAO1 being the optimal PA strain for establishing biofilms to infect the cells with. Even PAO1-GFP, that was used for imaging (Figures 3.5, 3.7, 3.8), is not considered to be different to PAO1, the strain needs also to prove its comparability to the PAO1 reference strain. PA14 as a well-known strain was also used as a comparison, as shown in[4]. Genetically modified PA bacteria could show differences to PAO1 in biofilm forming capacity. Likewise, attenuated strains could be beneficial for building a model that is longer stable since bacteria being less pathogenic to epithelial cells. Having this in mind, PA strain called PAK and some genetically modified strains, that came from Prof. Mustapha Si-Tahar (University of Tours) as a kind gift, were also tested for its ability to form biofilms in the same setting.

Several modifications of the original PAK wild type[156] were sent. The strain PAK ΔpscF is deficient in one of the most important pathogenic bacterial structures, the Type 3 Secretion System, as it contains an in-frame partial deletion in the gene pscF coding for the major needle protein[157–159]. Attenuated strain PAK ΔfliC contains an in-frame deletion of the fliC gene. This PAK bacterium is deficient in the flagella protein attenuating virulence and possibility to colonize on surfaces[160]. PAK ΔfliCΔpscF was created via introducing a plasmid partially deleting pscF gene in PAK ΔfliC[157,158]. Overnight cultures of these three strains are shown in figure 3.10. Compared to PAO1, PA14 or PAO1-GFP, these overnight cultures are in our experiments rather yellowish than green, which could be an indicator for lower pyocyanin and pyoverdine production.

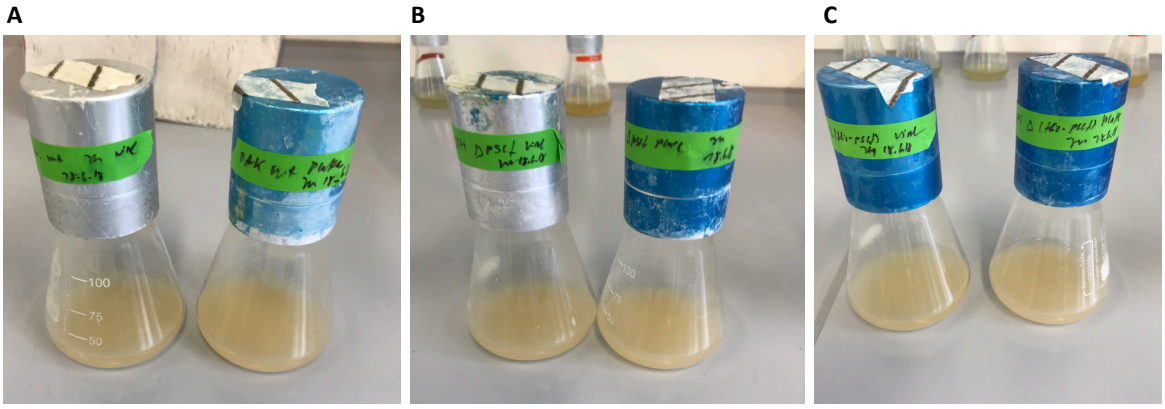

Figure 3.10: Overnight cultures of attenuated PAK strains (kind gift from Prof. Si-Tahar, University of Tours). (A) PAK wild-type, (B) PAK ΔpscF, (C) PAK ΔfliCΔpscF.

There are no obvious reasons for different biofilm forming capacities, but attenuated strains could be hindered in biofilm formation, especially PAK ΔfliCΔpscF, as it carries a deletion in the fliC gene which is important for colonization[160].

Biofilms were grown in M63 medium as described and directly compared to each other (Figure 3.11). CFU of biofilm after 72h of all named strains is very comparable, with PAO1 being significantly higher ($p<0.001$) than all PAK strains, but only in a range of 1 log, which is not a big difference regarding to a biological system growing for 72h. Interestingly, the biofilm mass of PAO1 measured via crystal violet staining is significantly different to all other strains that were analyzed (Figure 3.11 B). PAO1 biofilm mass was set to 100 %, and strains PAO1-GFP, PA14 and PAK wild-type show about 60% of it, which does not result in a visually seen difference in practice. Even though there is a difference in biofilm mass, there is no difference in CFU. Therefore, PAO1-GFP is meant to be as comparable as it can still be used to obtain reasonable images. As explained in the introduction of this thesis, biofilms consists of a matrix, that's ingredients are not yet completely uncovered, but mostly consisting of extracellular DNA, proteins and polysaccharides as Psl[161]. Different bacterial strains do apparently differ in biofilm mass creation of at least one of these ingredients, which is most probably due to genetical changes. Attenuated strains PAK ΔfliCΔpscF and PAK ΔpscF show even less biofilm mass, with ΔfliCΔpscF reaching some 10% of the biofilm

mass of PAO1. As hypothesized, this might be due to the reason, that there is a deletion in the fliC gene responsible for colonization[160]. PAO1 is proven here to form biofilms in the given situation with the given M63 recipe best. This is another important reason for choosing PAO1 for infecting epithelial cells instead of different PA strains.
Nevertheless, it could be very interesting to use at least the PAK wt and PAK ΔpscF strains for future infection experiments, as they build reasonable amounts of biofilms.

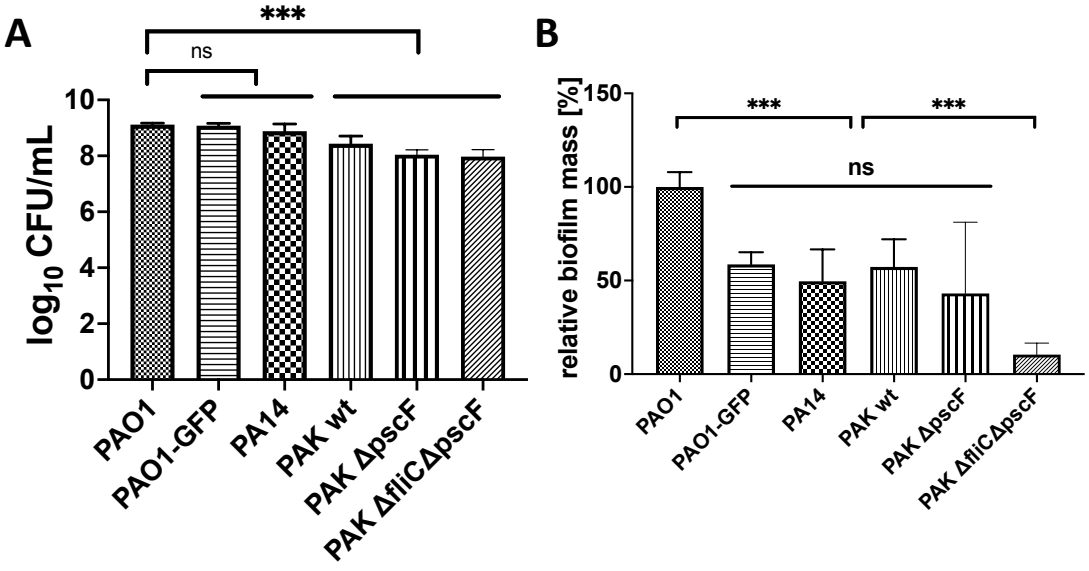

Figure 3.11: Analysis of 72h-grown biofilms of PAO1, PAO1-GFP, PA14 and (attenuated) PAK strains. (A) CFU of biofilms after 72h. (B) Biofilm mass analyzed via crystal violet staining relative to PAO1 biofilm mass. Bars show mean and SD. One-Way ANOVA, Tukey´s multiple comparison test, ns $p>0.12$; * $p<0.033$; ** $p<0.002$; *** $p<0.001$, N=9 of 3 independent experiments. Adapted with permission from [4]. ©2021, American Chemical Society.

3.3.1.4 Metabolomic analysis

It could be shown that PAO1 and PAO1-GFP 72h pre-grown biofilms are transferable and biofilm matrix can be stained (Figures 3.7 and 3.8). The method to transfer biofilm on cells *in vitro* has, to the best of our knowledge, not been performed yet outside the institute[8,9] and might lead to doubts, if the transferred biofilm shows the same characteristics as native, untouched biofilm.

Therefore, we sought to use a method that generally distinguishes between the biofilm and the planktonic mode of growth. Metabolomic studies have been used in previous studies on bacteria to identify profiles of bacteria[162–164]. Here, metabolites formed by either the planktonic or biofilm bacteria are analyzed via LC-MS and features are compared to analyze similarities or differences, as done in[4].

Biofilms were grown for 72h and transferred on new 24-well plates, to be further incubated for 1h or for 24h. As a comparison, biofilms were not transferred but only medium was changed. This was then finally compared to planktonic bacteria normally grown over night in a shaker (as explained in materials and methods part).

Venn diagrams showing the different features (characteristic for each condition) clearly indicate the strong comparability of transferred biofilm and native biofilm (Figure 3.12). Whereas about 80% of native and transferred biofilm features are identical, only 51% of the features of transferred biofilm and planktonic bacteria are same. The same is true after further incubation of 24h, however, the values are shifted. Now, nearly 100% of the features of transferred and native biofilm are same, but also 75% of transferred biofilm and planktonic bacteria (Figure 3.12 B). The features after 1h incubation are more realistically to evaluate than those after 24h. This is, since the later employed procedure to transfer biofilm on cells to incubate for 1h, as the planktonic bacteria, is more comparable (see chapter 3.3.2 and following). Transferred biofilm clearly differs from the planktonic cells.

In literature, planktonic bacteria directly infected epithelial cells, arguing that a biofilm is formed on the cells that is pre-mature, about 4-6h[115,116,119]. Another study even proved biofilm differences in gene regulation in contrast to planktonic bacteria via a method using gene microarrays under subinhibitory tobramycin treatment[5]. This is not done in the present experiment, since a universal discrimination between two states of growth was achieved by checking a huge set of data, and not by comparing certain details of a huge proportion. It is known for longer that biofilms are different to planktonic bacteria and even change their phenotype during growth, which makes it important to have mature biofilms[133]. It is interesting, that the biofilm apparently still shows the characteristics of a native biofilm, even though it was mechanically

disrupted. The metabolomic study is therefore rated as a straightforward technique to obtain a simple “yes or no” answer.

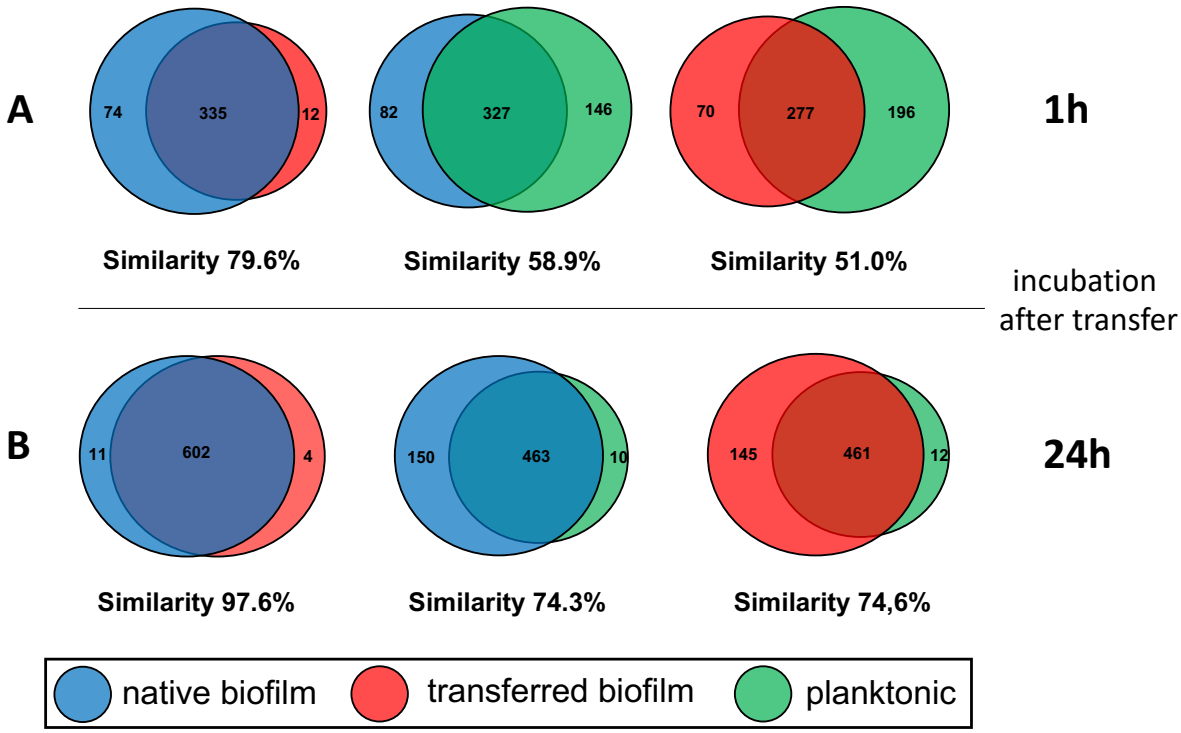

Figure 3.12: Venn diagram showing metabolomic features of 72h PAO1 biofilm that are grown natively on wells, transferred biofilm suspension and planktonic bacteria. Numbers in circles showing specific features for respective growth condition and percentage of similarity below. (A) Biofilms transferred and further incubated for 1h. (B) Biofilms transferred and further incubated for 24h. Experiments on 24-well plates without host cells. N=3 of one experiment. Adapted with permission from [4]. ©2021, American Chemical Society.

3.3.1.5 Antibiotic resistance of native and transferred biofilm

One of the most problematic characteristics of the biofilm mode of growth is the antibiotic tolerance which can increase necessary antibiotic to eradicate bacteria up to 1000 times the MIC[27,105]. Therefore, the question needs to be answered, if more tobramycin is needed to eradicate biofilm compared to planktonic bacteria and if transferred biofilm also features same characteristics, as shown in[4].

Either native biofilm, the biofilm suspension or a suspension of planktonic bacteria were treated with increasing tobramycin concentrations on plain 24-well plates for

24h. Results plotted as CFU vs. tobramycin concentration is shown in Figure 3.13. Native biofilm and transferred biofilm are comparably reduced over time, whereas planktonic bacteria are mostly killed at already 4 µg/mL, which is in range with previously done studies on MIC (data not shown) and literature values[27]. Transferred and native biofilms are reduced with increasing tobramycin concentration, but still viable bacteria can be counted at concentrations of 100 µg/mL (2,9 and 6 $\log_{10}$ CFU/mL, respectively). Planktonic PAO1 were completely eradicated with 50 µg/mL. This can be seen as a proof for transferred biofilm having comparable tolerance to tobramycin as native biofilm. Nevertheless, transferred biofilm is apparently more reduced (about 2 logs) as native biofilm. Most probably this is a matter of initial CFU. As shown in Figure 3.6, big parts of biofilm, that was scraped, still remains on the ground after transfer. For 24h pre-grown biofilm it could be shown, that 80% of the native biofilm remains on the ground after scraping (Figure 3.4). The native biofilm CFU could be therefore underestimated and initial CFU be not as comparable as shown in Figure 3.13. However, a study comparing both native and transferred biofilm for its susceptibility to treatment has not been found after intensive literature research. So far, only biofilms without comparison to planktonic bacteria were treated with antibiotics to show the increased tolerance to treatment by estimating the MBEC[103,152]. Other authors did not use CFU to show the reduction of biofilms, but rather optical methods as fluorescently labeled bacteria[25,165]. This experiment serves as a last proof, that a mature biofilm is transferred on cells and therefore, a model of chronic infection can be realized. All experiments are done to prepare a complete model that consists of nearly all components as *in vivo*. That is, human bronchial epithelial cells grown at the ALI conditions, a chronic biofilm, that infects these cells and treatment of this chronic infected model using a device to reproducibly apply anti-infectives to cure the infection[4,10].

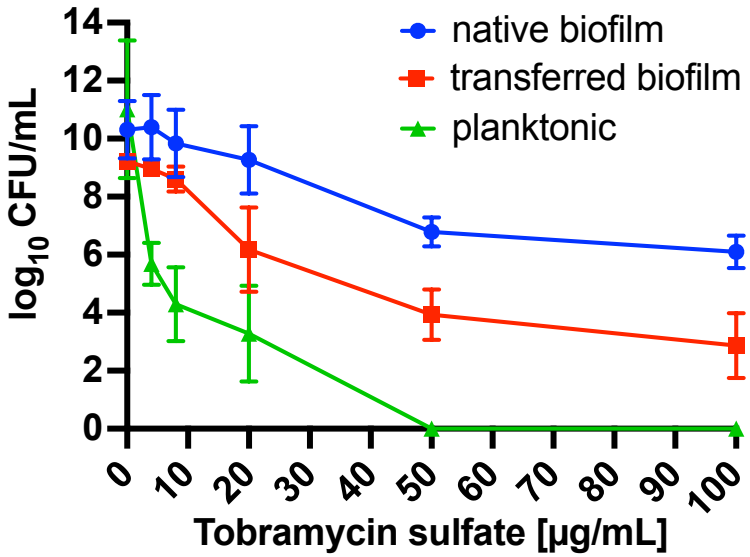

Figure 3.13: PAO1 biofilm grown natively and transferred biofilm suspension show comparable resistance to tobramycin. CFU of PAO1 treated with tobramycin sulfate on 24-well plates on plastic without cells in increasing concentrations. N=9 of three independent experiments. Adapted with permission from [4]. ©2021, American Chemical Society.

3.3.2 Use of CFBE41o- cell line and protocol of infection

In the paragraphs before, the cultivation of bacteria was shown, including the well-known phenomenon of biofilm production on plastic. It could be shown, that biofilm bacteria have different metabolic properties and react differently to treatment by tobramycin, which is also known. Nevertheless, it has never been shown that these properties remain after transfer of scraped and transferred biofilm suspension. As a continuation of an initial project started at HIPS DDEL by Dr. Jenny Juntke[8,9], pre-grown biofilm was used to infect epithelial cells rather than planktonic bacteria to realistically simulate a chronic bacterial infected (cystic fibrosis) bronchial epithelium at the air liquid interface.

For infection, the well-known cystic fibrosis cell line CFBE41o- was used[166,167], as published[4]. Originally, these are bronchial epithelial cells of a CF patient that were transformed using the SV40 large T antigen based origin-of-replication defective pSVori- plasmid[166,167]. The cells have been characterized, finding a barrier-forming polarized structure with tight junction proteins as ZO-1, claudin-1 and occludin[167]. This

cell line has been already employed for earlier studies of Dr. Jenny Juntke, who carefully characterized the cell line, coming to the result to recommend use, since it was found to be more resistant against infection than the comparison cell line Calu-3[8]. The following part shows why three culture conditions are most important. First, this is the biofilm form of growth (which has been already mainly characterized), second the air-liquid interface conditions of treatment and third the long-term chronic like infection process.

The two already denoted procedures are combined in a convergent process[4]. First, the cells are seeded seven days before the experiment. Then, while cells have been set to ALI by removing apical medium and reducing basolateral medium to 500 µL, a PAO1 biofilm is made in M63 medium three days before the experiment. At the day of the experiment, all used media are pre-warmed, and basolateral medium of cells is changed as described in materials and methods. Biofilm is scraped off with 200 µL KRB as described and transferred with a 1000 µL pipette onto the cells. The inoculum of about 1 x 10^9 PAO1 bacteria per mL is comparably high[119,142], but though very reproducible between the single experiments (Figure 3.9). (Infected) cells are then put back into the incubator at 37 °C and 5 % CO_2 for one hour. In this time, the biofilm settles down on cells, but it is noteworthy that infection starts right after addition of bacteria (t=0h).

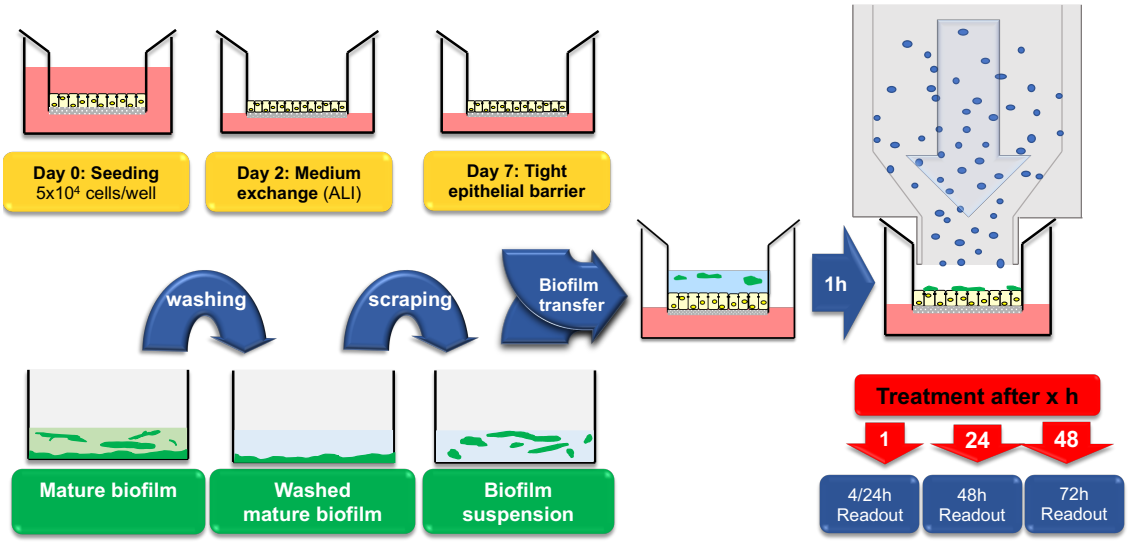

Figure 3.14: CFBE41o- cells and PAO1 biofilm are merged in a convergent process and infected cells are treated at ALI with described device (Chapter 2). Reprinted with permission from [4]. ©2021, American Chemical Society.

After one hour, the supernatant is carefully removed and ALI conditions are restored. The CFU per mL is, compared to initial CFU count of biofilm suspension, slightly reduced after 1h on cells and removal of supernatant (about 8 $\log_{10}$ CFU/mL, Figure 3.15). This is probably due to free floating bacteria, that are not attaching to the cells and accordingly removed. Bigger biofilm parts are most likely settled due to its size and weight. Comparing the biofilm transfer on blank filter inserts without any cells, no difference can be found to the CFU count on cells ($p=0.14$). This shows, that cells apparently do not feature special attachment forces to bacteria.

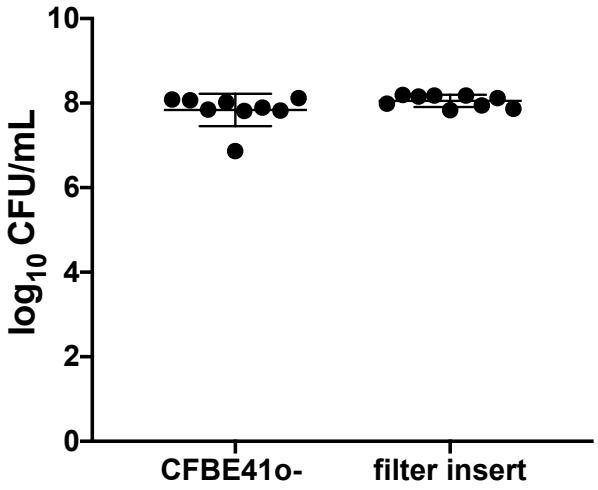

Figure 3.15: CFU count of PAO1 biofilm remaining on cells after 1h compared to PAO1 biofilm on blank filter inserts. N=9 of 3 independent experiments. Bars show mean and standard deviation. No difference can be seen using an unpaired t-test (p=0.14).

Figure 3.16 shows the situation right after removal of supernatant, supporting the assumption to have bigger biofilm clusters on cells (as described in[4]). Along single bacteria spots, also bigger agglomerations of bacteria can be found, that measure some 10 to 40 µm in diameter.

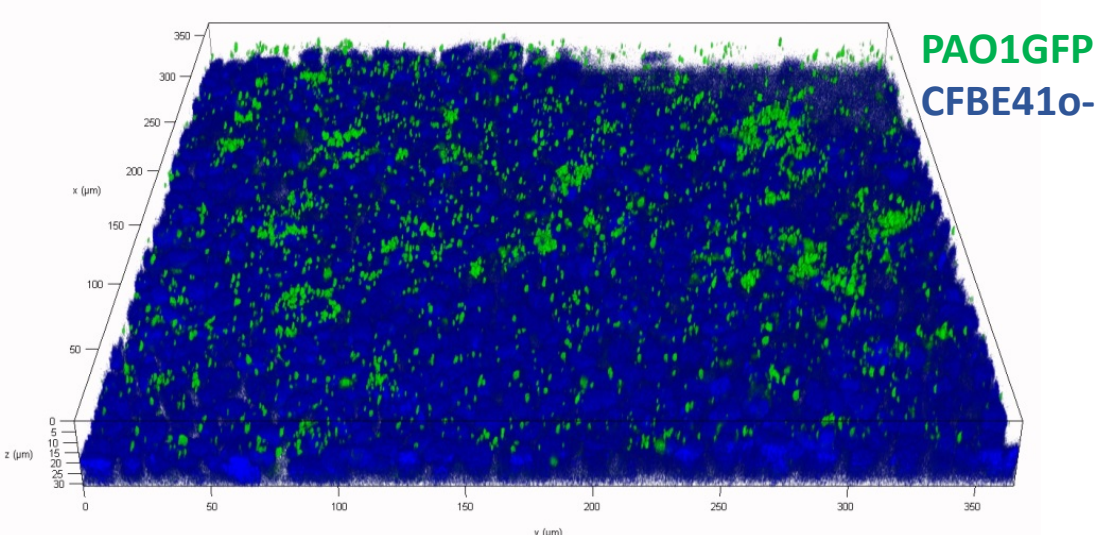

Figure 3.16: Confocal image of CFBE41o- cells (blue) and PAO1-GFP biofilm (green) 1h after transfer. Adapted with permission from [4]. ©2021, American Chemical Society.

Also, the PAO1 strain biofilm on cells was imaged. Initial experiments using different dyes to stain the biofilm on cells (e.g. calcofluor white stain or crystal violet stain) did not show usable results, as these dyes ubiquitously stain all biological membranes. So, SEM images of samples after 1h were done using water-free samples (Figure 3.17), as shown in [4]. Biofilms are quite huge in size (around 30 µm) and also feature characteristic holes in the extracellular matrix. The epithelial cells can be clearly seen, which are still in a good shape and not yet attacked by bacteria. Comparing those images to literature, a good correlation can be seen, yet, no group has been transferring whole biofilms on cells so far. Though, PAO1 biofilms grown on cells for 20h could be imaged, featuring comparable results[146,151]. The size of biofilm parts is comparable to the confocal images, supporting the results. In literature, *in vivo* biofilm clusters have shown a comparable size, too, which supports this approach to some extent[22].

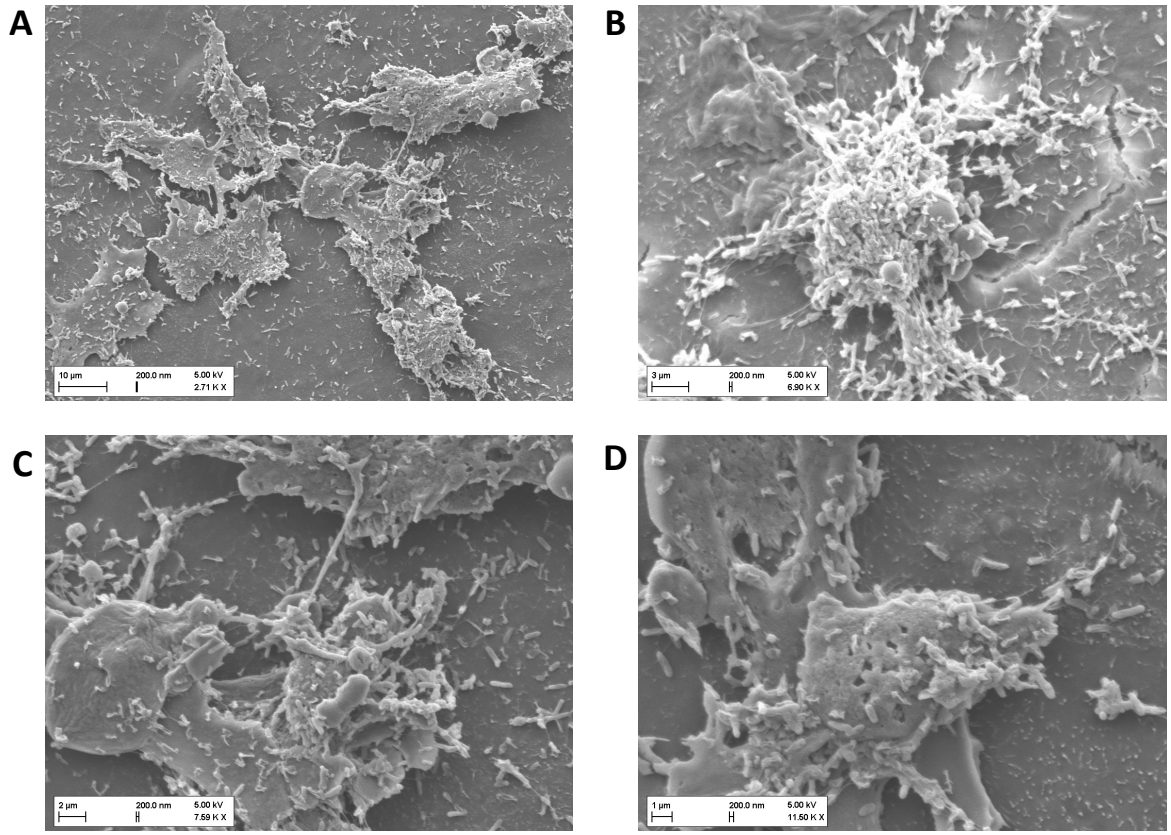

Figure 3.17: SEM image of transferred PAO1 biofilm onto CFBE41o- cells 1h after transfer. A: Cell boundaries are visible at smaller magnifications. B-D: With higher magnifications, extracellular matrix and the characteristical holes are better visible. Subfigure A adapted with permission from [4]. ©2021, American Chemical Society.

The method of transferring PAO1 biofilms on cells seems to be a promising approach to infect cells, since the biofilms can be seen on cells and the CFU did not change much after transfer. The timepoint 1h after infection is a good timepoint to already treat the bacteria, as a comparable model treated at later timepoints (4h) could not withstand the infection of PAO1[8]. As shown in Figure 3.14, cells are treated after 1h with the deposition device presented in chapter 2. Nevertheless, further optimization of making the biofilm less virulent for cells, so that a treatment can be carried out later than 1h, or that the model itself survives longer to model chronic infection, would be favorable.

3.3.3 Pre-treatment of biofilm and infection with planktonic bacteria

Since CFBE41o- cells were shown not to withstand the infection for a longer time period (>1-4h), the biofilm is apparently too virulent for cells. To reduce pathogenicity, the O´Toole group has already tried to treat biofilms with tobramycin in advance, proving reduced cytotoxicity against CFBE41o- cells[5]. Other groups have already shown, that ciprofloxacin can act as a quorum sensing inhibitor, possibly reducing virulence against cells[168]. In this additional study, it was analyzed, if a subinhibitory concentration of 1 µg/mL ciprofloxacin reduces virulence of biofilms without changing the initial CFU of inoculum.

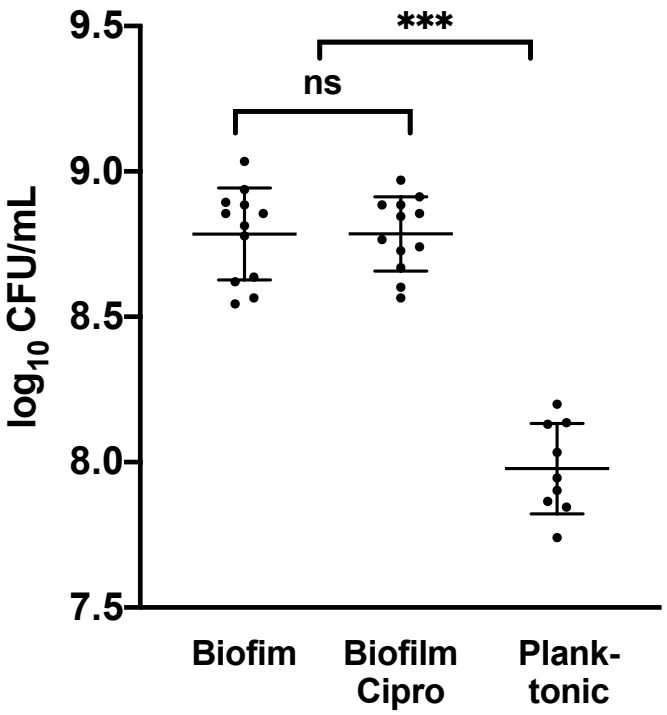

Figure 3.18: CFU of 72h pre-grown PAO1 biofilm, biofilm pre-treated with 1 µg/mL ciprofloxacin (Biofilm Cipro) and planktonic bacteria used for infecting the cells. N=9-12 of 4 independent experiments. Bars show mean and standard deviation. One-Way ANOVA, Tukey´s multiple comparison test, ns $p>0.12$; * $p<0.033$; ** $p<0.002$; *** $p<0.001$.

Biofilm that has been growing for 72h (as explained) was not directly washed and transferred to infect cells at ALI, but was subjected to either KRB with 1 µg/mL ciprofloxacin or only KRB still being in the 24-well plates. After 1h, biofilms were

washed once and were transferred. As comparison, planktonic PAO1 was used. Figure 3.18 shows the biofilms after growth for 72h and pre-treatment compared to planktonic bacteria. No statistically significant difference in CFU was found between untreated and pre-treated PAO1 biofilm ($p<0.001$). This proves the sub-inhibitory concentration of ciprofloxacin not to change CFU count and therefore to be comparable. Nevertheless, it was technically not possible to completely reach same CFU count by diluting PAO1 overnight culture of planktonic PAO1, which proved to be some 0.8 logs less than biofilms (Figure 3.18). Even so, the number of CFU is still in the same magnitude, which was rated in discussion within the institute as acceptable given the circumstances of a biological system.

To evaluate the effect on cells, it´s TEER values were measured after 1 and 6 h of incubation (Figure 3.19). Already after 1h, TEER of infected cells is significantly reduced compared to control ($p=0.002$ and 0.004, "Biofilm" and "Biofilm Cipro", respectively) and $p<0.001$ with planktonic (Figure 3.19 A). After 6h, TEER is not measurable any more (Figure 3.19 B). Nevertheless, no macroscopical changes can be seen, medium is not yet turbid and appears to be still red, not yellowish, that would be a hint at bacterial overgrowth.

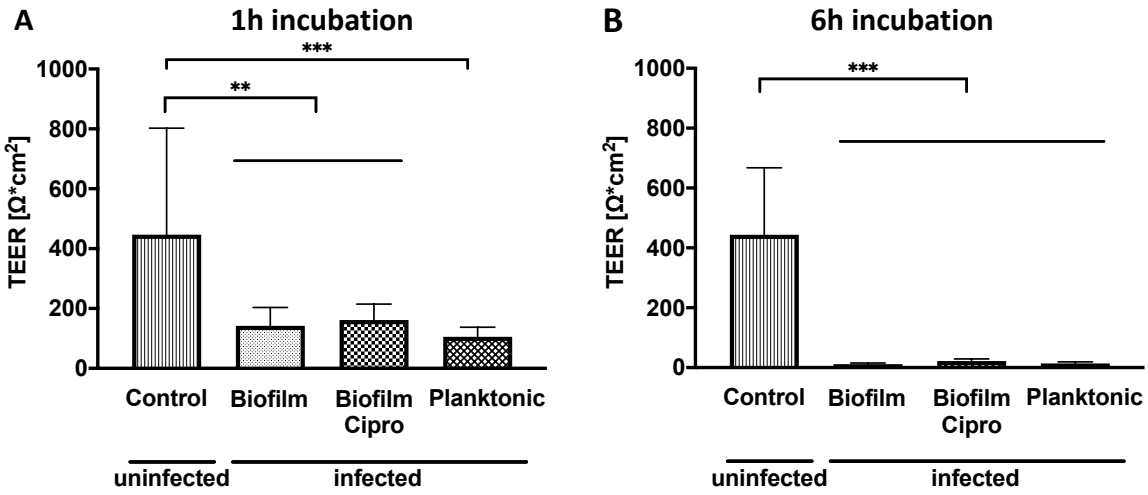

Figure 3.19: Barrier integrity of CFBE41o- infected with PAO1 biofilm, biofilm pre-treated with 1 µg/mL ciprofloxacin (Biofilm Cipro) and planktonic bacteria. N=9 of three independent experiments. Bars show mean and standard deviation. One-Way ANOVA, Tukey´s multiple comparison test, ns $p>0.12$; * $p<0.033$; ** $p<0.002$; *** $p<0.001$.

The fact that medium is not yet overgrown with bacteria, and the relatively short time period of 1 and 6h post-infection makes it possible to analyze viability via LDH test kit. Longer infection times cause LDH to be disrupted[137,138]. By LDH release, viability can be calculated as described. After 1h of infection, viability of all conditions is very comparable and cells are about 100% viable (Figure 3.20 A). After 6h, infected cells have already been significantly compromised (Figure 3.20 B). About 40% of the cells infected with biofilm or planktonic bacteria are still viable after 6h. However, 60% of cells infected with biofilm pre-treated with ciprofloxacin are viable. This is a statistically significant difference to the other groups ($p<0.001$).

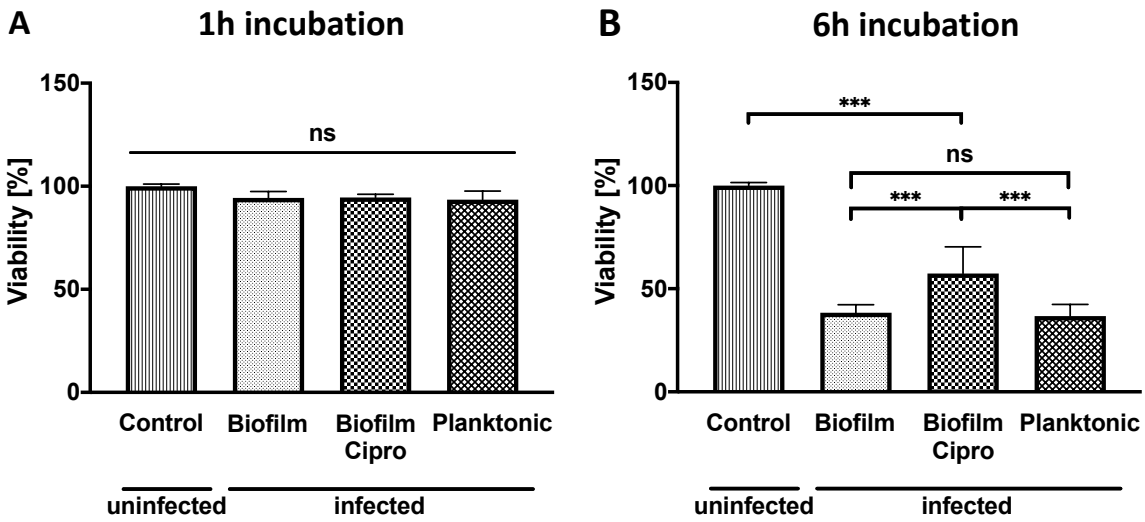

Figure 3.20: Viability of CFBE41o- infected with PAO1 biofilm, biofilm pre-treated with 1 µg/mL ciprofloxacin (Biofilm Cipro) and planktonic bacteria. N=9 of three independent experiments. Bars show mean and standard deviation. One-Way ANOVA, Tukey´s multiple comparison test, ns $p>0.12$; * $p<0.033$; ** $p<0.002$; *** $p<0.001$

Ciprofloxacin was before proven to reduce virulence factors in PAO1[168]. The authors of the study used even a lower concentration of 0.25 µg/mL, finding a reduction in growth curve with higher concentrations. Virulence factors as elastase, protease and alginate were proven to be reduced or completely vanished[168]. However, the authors did not show the protective effect on human cells as was proven in this experiment. Anderson

et al. proved this protective element on cells, yet with tobramycin, finding less cytotoxicity on CFBE41o-[5].

Nevertheless, especially the weak response in TEER values shows that a treatment by antibiotics is necessary as early as possible. Otherwise, TEER values are gone, as already found by Dr. Jenny Juntke with younger biofilms[8,9]. The hypothesis, that biofilm can be made less pathogenic on cells via pre-treatment with sub-inhibitory antibiotics could only be partly proven. The effect on epithelial cells could be proven in the given setting, but it is not strong enough, as shown by TEER. Additionally, as changes in virulence factor production has been proven[168], the test system pre-treated with ciprofloxacin could influence the results of other anti-infectives to be tested on the model, that should be exclusively measured as treatment induced effects and not model specific effects, e.g., QS molecules. Due to these reasons, the idea of pre-treatment was waived and not further assessed for creating the test system.

3.3.4 Choice of antibiotic and dose finding studies on model

Due to the aforementioned results it is obvious, that a treatment with a higher dose is necessary and has to be applied on the model as early as possible, i.e., after 1h, as discussed[8,9]. In-house studies could find, that ciprofloxacin nanoparticles basically were able to treat PAO1 infection on cells at ALI[8,9]. Nevertheless, tobramycin is a well-known glycopeptide antibiotic having been used in clinic for inhalation and being available as dry powder formulation[43,44] (chapter 1). In order to model a chronic *P. aeruginosa* biofilm infected patient *in vitro*, which is a complex and demanding project per se, a rather simple approach to model the inhalation of tobramycin is achieved by first using a tobramycin sulfate solution.

For treating the infected cell culture inserts with antibiotics, the deposition device as thoroughly explained in chapter 2 was employed. First of all, a suitable dose to be deposited on the infected model needs to be defined, as explained in[4]. By theoretical considerations, a dose of 10 µg was tried to achieve, as a preliminary experiment showed good results at a concentration resulting in 10 µg mass (data not shown).

Deposition experiments with sodium fluorescein showed a deposition efficiency of >3 %. Therefore, this value (3%) was used to calculate the dose needed (resulting in a value of 333 µg to be invested, which is about 1.6 mg/ml in the case of 200 µL). In order to confirm the dose depositing on wells, 200 µL tobramycin sulfate was invested at 0.16, 1.6 or 16.6 mg/mL, with resulting 1.6 ± 0.09, 14.8 ± 0.16, 102 ± 4.89 µg dose deposited in the wells, respectively (Figure 3.21). This is, especially for the 1.6 mg/mL invested concentration, higher than expected, nevertheless, the initial deposited amount of fluorescein was higher than 3%, falsifying initial deliberation. In this very chapter, these 10-fold increasing doses are referred to “1/10”, “1” and “10”, for simplification purposes.

In all experiments, a concentration of 1.6 mg/mL tobramycin sulfate was used, except the following part of this chapter.

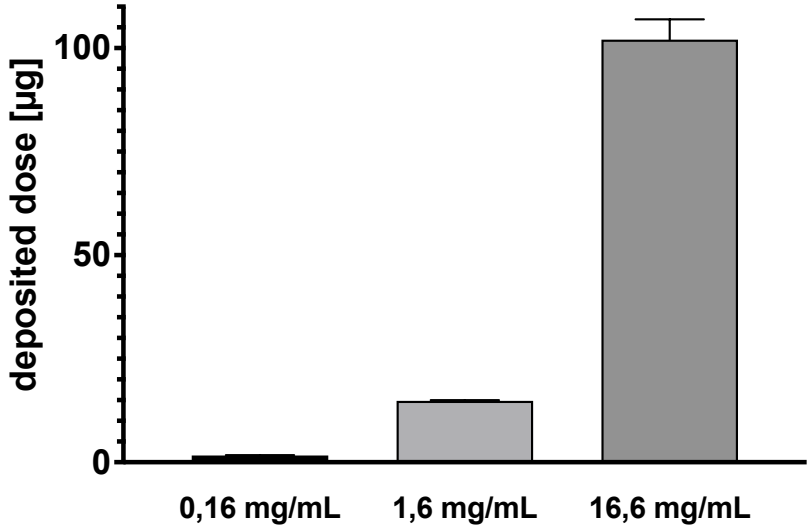

Figure 3.21: Deposited dose of tobramycin for treatment of the infected model. 200 µL tobramycin sulfate nebulized at given concentrations. N=3 of one experiment

As patients suffer from infection that is often not cured by treatment[144], cells and biofilm need to be in a co-culture even after treatment. A total eradication of biofilm is not the aim, as bacteria still need to be present for assessing the state of cell and bacteria in co-culture for a longer time period. The invested concentration was reduced

and increased by 10-fold, as described[4], to define the best dose and to address cytotoxicity on cells.

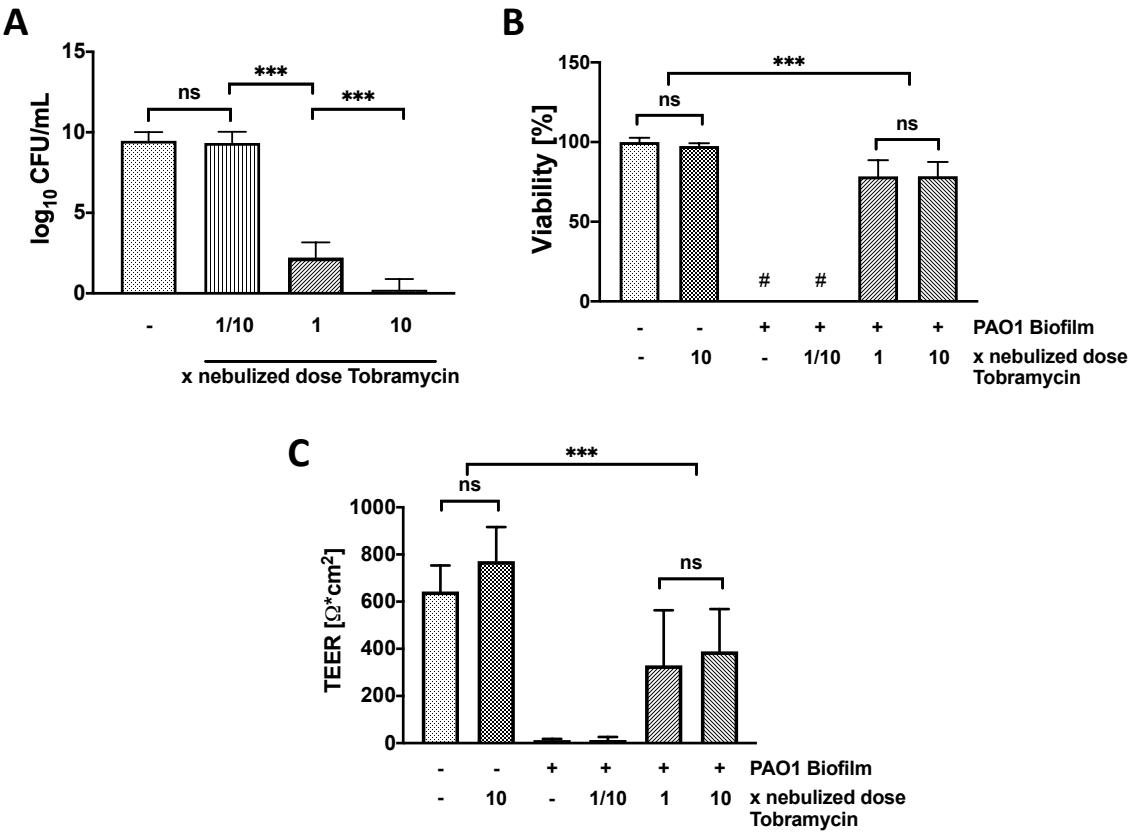

Figure 3.22: Dose finding studies on infected cell model and cytotoxicity of highest dose of tobramycin sulfate after 24h incubation. (A) CFU after 1/10th, 1-fold or 10-fold of the respective dose of tobramycin sulfate. (B) Viability determined via LDH release after indicated dosing of tobramycin sulfate. (C) TEER values of infected and not infected cells at given tobramycin doses. # LDH detection could not be done due to overgrowth of bacteria, lysed cells confirmed with light microscope. One-Way ANOVA, Tukey´s multiple comparison test, ns $p>0.12$; * $p<0.033$; ** $p<0.002$; *** $p<0.001$, N=9 of 3 independent experiments. Subfigure A and B adapted with permission from [4]. ©2021, American Chemical Society.

The actual 1-fold dose of tobramycin (14.8 ± 0.16 µg) showed a significant reduction of CFU down to 2.2 $\log_{10}$ CFU per mL, which is a good reduction, but bacteria are still present, which is very important for further evaluation, as bacteria need to be present for evaluation of pathogens (Figure 3.22 A). Surprisingly, 1/10th of the dose did not have any effect on the CFU on the apical side of Transwell® inserts. Increasing the 1-

fold dose 10-fold (102 ± 4.89 µg) did not lead to total eradication of bacteria, but significantly less bacteria are on the well plates ($p<0.001$). Meanwhile, the highest applied dose was not toxic at all to cells as expected[5] (Figure 3.22 B). Infected cells that were not treated or only with $1/10^{th}$ of the dose, could not be tested for LDH release, as the bacteria being overgrown after 24h apparently destroyed all LDH molecules, as described in literature[137,138]. Figure 3.23 shows a separately done experiment to proof LDH destruction of bacteria, that was published by the author of this thesis together with Carlos Montefusco-Pereira[137]. Medium containing LDH and medium that contained LDH and PA bacteria was incubated for 24h. After incubation, the LDH was not detectable in wells with bacteria, but in those without infection, which proves the bacteria being responsible for the loss of LDH. Nevertheless, this only takes place in wells with bacteria being overgrown, so when no treatment is present and bacteria have at least 8-12h time to grow, as another study confirmed[138]. Likewise, low amounts of bacteria do not disturb the analysis. Light microscope revealed in every single experiment the infected and not treated cells being completely disrupted after 24h latest (data not shown).

Viability of wells that were infected and treated with 1 or 10x of the dose did not differ and maintained about 80% (Figure 3.21 B). TEER values are very comparable to the results of viability. Infected wells and wells treated with a 10^{th} of the dose decreased to around 10 $\Omega*cm^2$ (Figure 3.21 C). TEER of wells treated with 1 or 10x the dose is significantly reduced compared to the uninfected control, but maintaining a level of around 300 $\Omega*cm^2$ in this dataset, which is still to be rated as a tight bronchial barrier[169,170]. Accordingly, the highest dose is not toxic to cells as shown in viability and TEER values only non-significantly increased with treatment (772 vs. 643 $\Omega*cm^2$, Figure 3.21 B, C).

This study paved the way towards further assessment of efficacy. A dose of about 14.8 ± 0.16 µg has been proven to be not toxic to cells. The TEER values are not different from each other when treated with 10-fold different doses ($p=0.91$). This is the reason for following controls to not include tobramycin sulfate any more but only KRB, as TEER is not changed to control. A 10-fold lower dose was not able to kill bacteria and to save

viability of cells. In comparison to 10-fold higher dose, either viability and TEER values were not changed, but CFU was reduced. No studies could be found in literature that did a comparable study at comparable circumstances (besides[4]). Since the one-fold dose, being 14.8 ± 0.16 µg, did not eradicate all bacteria, and still saves TEER values, this dose was used for all further experiments and is from now on called just "dose".

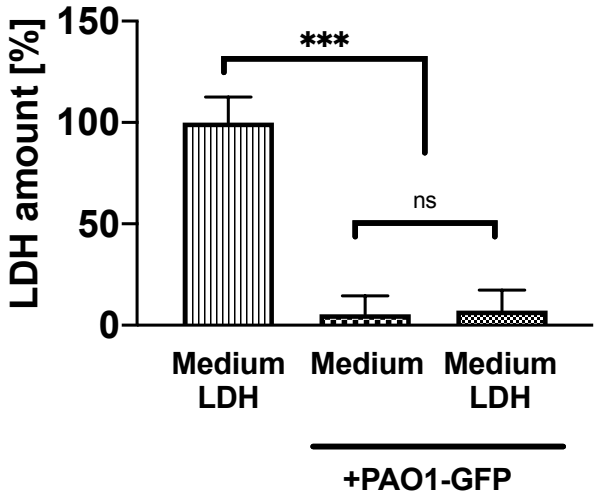

Figure 3.23: LDH is reduced after infection with PAO1 bacteria (here the comparable strain PAO1-GFP). LDH = 1U LDH/mL. N=8-9 of 3 individual experiments. One-Way ANOVA, Tukey´s multiple comparison test, ns $p>0.12$; * $p<0.033$; ** $p<0.002$; *** $p<0.001$, N=9 of 3 independent experiments. This is adapted (with permission) from Montefusco-Pereira, C. V., Horstmann, J. C., Ebensen, T., Beisswenger, C., Bals, R., Guzmán, C. A., Schneider-Daum, N., Carvalho-Wodarz, C. d. S., Lehr, C. M. P. aeruginosa Infected 3D Co-Culture of Bronchial Epithelial Cells and Macrophages at Air-Liquid Interface for Preclinical Evaluation of Anti-Infectives. J. Vis. Exp. (160), e61069, doi:10.3791/61069 (2020) [137]

3.3.5 Comparing ALI and submerse conditions on treatment success

Modelling *in vitro* systems of lung cells and especially the interaction of particles with lung mucosa is preferably done at ALI and has proven to be different[64,123], as being presented in more detail in chapter 1.3.2.1. and chapter 2. Also, the effect of cells on treatment of bacteria has been evaluated, e.g. by Anderson et al.[5] with more detail given in following chapters. Even so, the effect of ALI conditions on treatment of bacteria in terms of barrier and number of bacteria was not shown yet. Additionally, cells could have an influence on treatment success[112]. Here, the hypothesis was tested,

if treatment of bacteria at ALI differs from treatment of bacteria on an abiotic surface and if treatment success differs when cultivated under submerse conditions (as done in[4]).

First, cells were infected and treated with the 1x dose of tobramycin or cells were just treated with the vehicle (KRB) and incubated for 24h (general procedure, as explained in Figure 3.14). As comparison, blank Transwell® inserts were infected with transferred biofilm and treated likewise. Figure 3.24 shows that untreated CFU did not change compared to plastic maintaining approx. 10 $\log_{10}$ CFU/mL. Likewise, CFU is not influenced in general by cells. Nevertheless, treatment with tobramycin reduced amount of CFU on cells to 2.6 $\log_{10}$ CFU/mL, whereas the same treatment completely eradicated all bacteria on plastic wells (Figure 3.24 A). Bacteria on cells seem to be less prone to eradication. A comparable finding was made by Rodriguez-Sevilla et al., that showed the efficacy of clarithromycin to be reduced by 3D-lung cells[112]. Most prominently, a here often times cited very detailed study by Anderson et al. showed already some time ago, that most analyzed genes are differently up- or downregulated when treatment of *P. aeruginosa* is done under planktonic conditions on abiotic surface compared to planktonic bacteria grown on cells, indicating different behaviour[5]. Most eminently, Garcia-Medina et al. showed that *P. aeruginosa* invades in cells during acute infection and cells led to persistence of these bacteria for up to 3 days even with treatment, with cells apparently conveying resistance to bacteria that use the cells as protection[171].

To evaluate the effect of submerse conditions for infection and treatment outcome, samples of both compared test groups were infected (and treated) the same way, as described. After treatment with either tobramycin or vehicle, one group was submerged in medium, whereas the other group was left at ALI conditions. After 24h, resulting number of CFU changed significantly comparing both treated and non-treated CFU (Figure 3.24 A). Whereas CFU at ALI stayed at approx. 10 $\log_{10}$ CFU/mL, CFU of submerged cultivated bacteria increased to 13 $\log_{10}$ CFU/mL. This is most probably due to the increased availability of nutrients, as e.g., glucose (0.6 g per liter of cell medium), whereas bacteria at ALI are mostly growing inside a meniscus of

medium and probably cell debris at the apical side of the Transwell® insert. Treated CFU is significantly elevated after 24h when cultured at submerse conditions (2.5 vs. 4.7 $\log_{10}$ CFU/mL, respectively, Figure 3.24 C) with a p value of <0.001. This is in concordance to other studies focusing on the elevated drug concentration on cell layers via application of aerosols, as Bur et al.[71] or Loret et al.[65] showing effects on cells in a lower dose than in LCC. On the cell layer, the concentration treating bacteria must be higher, since the same dose of tobramycin was applied, but diluted in 500 µL cell medium at submerse conditions. This effect is now proven to be significant. Comparing barrier integrity, basically the same results could be found. TEER of submerged cells is about three times higher as the ALI control (about 300 vs. 1000 Ω*cm^2), that is expectable and known[167]. Though, the TEER of infected and treated cells at submerse conditions is reduced down to 108 Ω*cm^2, whereas ALI treated cells are about 300 Ω*cm^2. This comes to a reduction to about 80% at ALI versus a reduction to about 10 % of control TEER at submerse conditions. Interestingly, infected cells in submerged conditions cannot be saved with treatment as good as in ALI conditions, which is in contrast to the TEER in uninfected state, being vice versa[167]. Notably, the control TEER values of ALI cultures as in subfigure B and D shown, differ from each other in some way. As it is a biological model, such differences between experimental sets done after months or years cannot be completely controlled. In future, tests could help to may find a better suited cell line.

The outcome after treatment of cells at ALI significantly differs from submerse conditions and needs to be considered in future with higher importance, even though the values need to be evaluated with necessary caution.

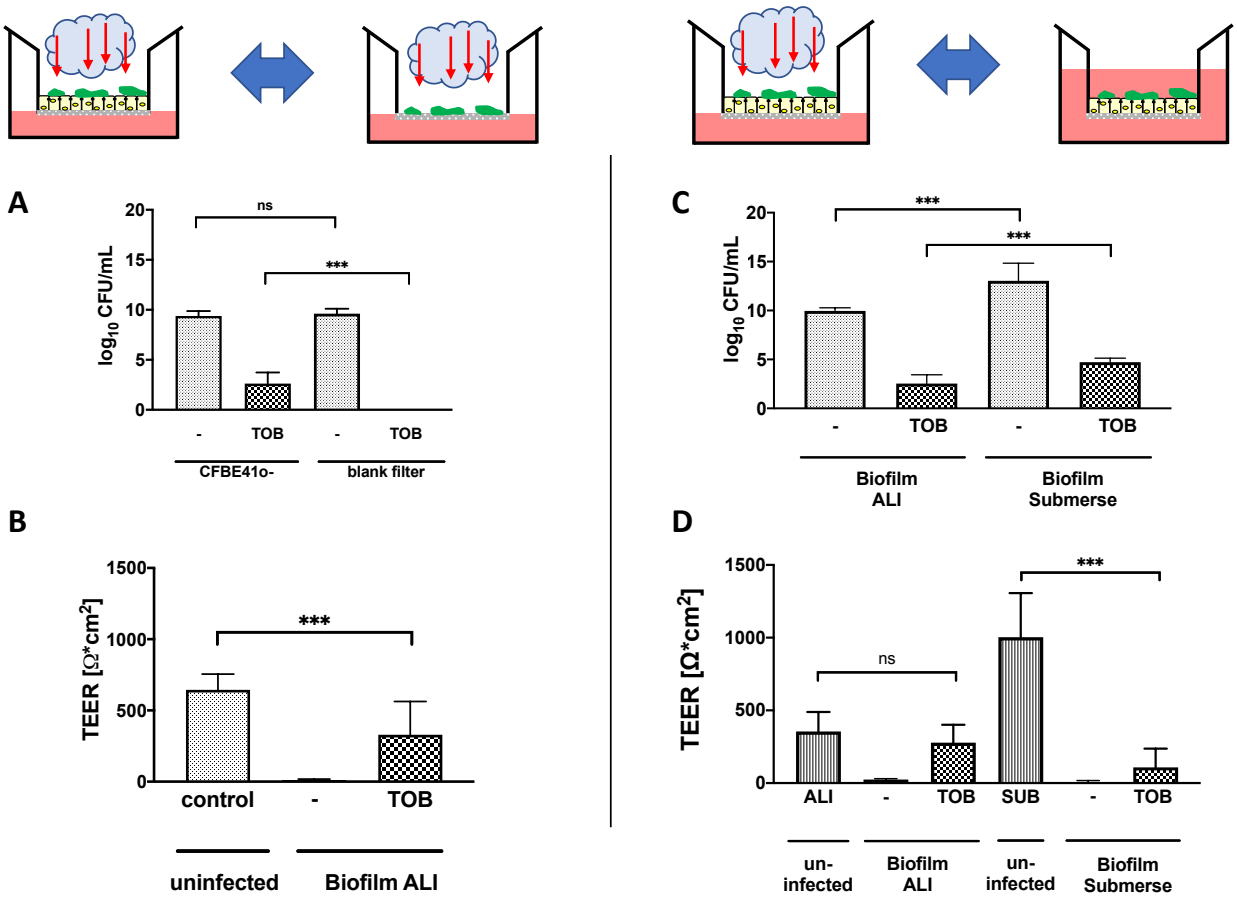

Figure 3.24: Comparison of culture conditions of infected and treated cell model after 24h incubation time. (A) Biofilm CFU on cells vs. on blank filter inserts. (B) TEER values of infected CFBE41o- cells at ALI (blank filter does not have TEER). (C) Biofilm CFU at ALI conditions and at submerse conditions. (D) TEER values at ALI conditions and at submerse (SUB) conditions. Control = uninfected control. One-Way ANOVA with Tukey´s multiple comparisons test, ns $p>0.12$; * $p<0.033$; ** $p<0.002$; *** $p<0.001$, N≥9 of ≥ 3 independent experiments. Subfigures A, C, D adapted with permission from [4]. ©2021, American Chemical Society.

3.3.6 Treatment of planktonic and biofilm bacteria on cell model

In Figure 3.13 it could be shown, that PAO1 biofilm is by far more resistant to tobramycin treatment compared to planktonic bacteria of same CFU. Chapter 3.3.3 dealt with the method of pre-treatment of biofilm and compared the outcome of infection of biofilm, pre-treated biofilm and planktonic bacteria on the cell model after 1 and 6h. Neither in CFU nor in TEER, a difference could be seen between biofilm and planktonic infection of cells, nevertheless, viability of CFBE41o- was increased when biofilm was pre-treated. Hence, it still is a matter of question if the infection of cells

with biofilm is different to infection with planktonic bacteria in terms of CFU and barrier, as these are important hallmarks.

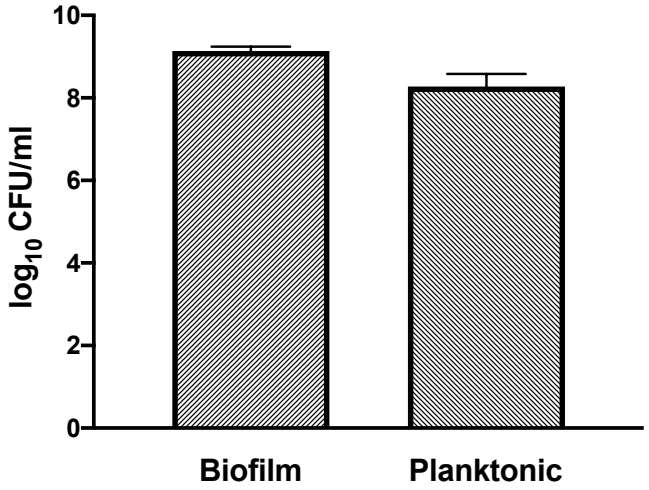

Figure 3.25: Comparison of CFU of transferred PAO1 biofilm and PAO1 planktonic bacteria that were used in the present study to infect epithelial cells. N=6 of three independent experiments. Error bar represent SD. Two-tailed t-test, P<0.0001.

As shown in Figure 3.13, cells grown at ALI conditions were infected with PAO1 biofilm as described. For comparison to planktonic bacteria, the same number of bacteria was given onto the cells as described in Materials and Methods. Figure 3.25 shows the amount of PAO1 CFU of both planktonic and biofilm bacteria. A two-tailed t-test showed that the used suspension of planktonic bacteria contains fewer living bacteria than biofilm suspension. Nevertheless, the difference is not higher than one logarithmic level (9.13 vs. 8.28 $\log_{10}$ CFU/mL), which is supposed to be still acceptable. To reach exactly a certain number of bacteria by diluting overnight cultures was trained with various techniques. Here, OC was diluted 10-fold wise, and thereafter counted to have a reproducible number of bacteria in each dilution. Though, it is still challenging to exactly match the number and the method further needs to be optimized.

After 1h, (infected) cells were treated with described 1-fold tobramycin dose at ALI conditions and incubated further 23h. Interestingly and in contrast to aforementioned earlier studies on the susceptibility of biofilm, no difference in number of CFU of planktonic or biofilm bacteria on either infected or infected treated cells can be found (both p>0.99, Figure 3.26 A). Analyzing barrier integrity, there is only a tendency

towards lower TEER values when being infected with planktonic bacteria and treated thereafter (Figure 3.26 B). This is a rather disappointing result, but it has to be kept in mind, that there is a proven difference between biofilm and planktonic PAO1, as thoroughly explained earlier (chapter 3.3.1.4 and 3.3.1.5). As a tendency towards lower TEER values is visible in Figure 3.26 B, one can hypothesize that an inoculum being some 2 logarithm steps higher concentrated than the actual used planktonic inoculum would cause higher damage to the cells making the difference statistically significant, without questioning the higher inoculum, as it is still then comparable to the biofilm inoculum CFU. Literature has proven the effect of biofilm form of growth on mammalian cells, as Bowler et al. showing less cytotoxic effects of PAO1 biofilm bacteria to epithelial cells in comparison to planktonic PAO1, as well as higher IL-8 release induced by biofilm[113]. Unfortunately, most other groups focused on the effect of biofilm on cells without comparing biofilm state or planktonic state in a comparable setup as done here[5,117]. Apparently, the direct comparison of planktonic and biofilm bacteria in the context of infection of cells at ALI conditions is a completely underrepresented area and needs therefore further investigation on the host-pathogen interaction of cells. In the following, the biofilm suspension is anyhow used, since it has been proven to be different to planktonic state *in vitro* on abiotic surface and it is hypothesized, that biofilm is different concerning genetic changes, as described[5]. This is a matter for further investigation, especially in the present setup.

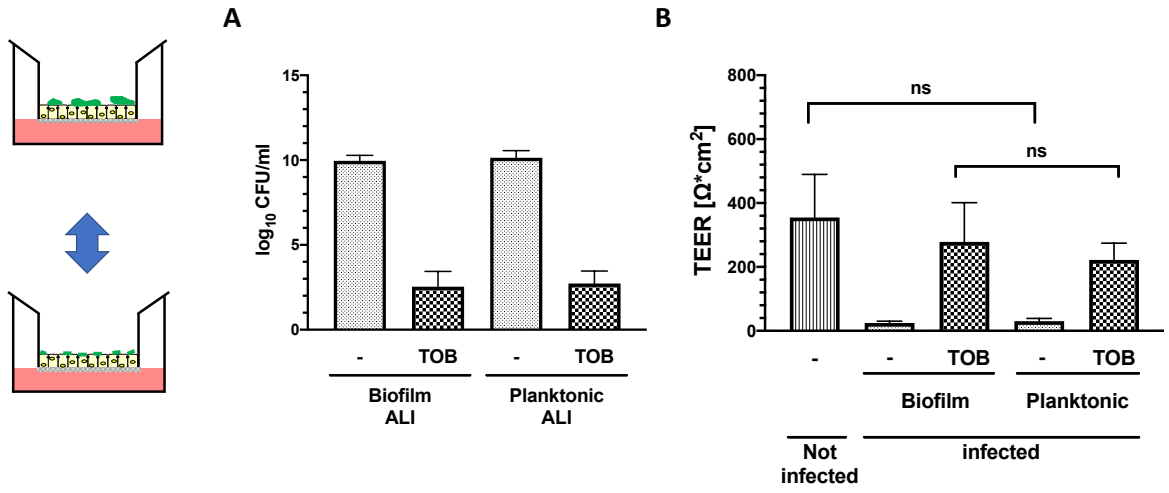

Figure 3.26: CFU of PAO1 biofilm and planktonic bacteria on infected cells and corresponding TEER values after 24h incubation time. (A) CFU on apical side of permeable supports. (B) TEER values of infected cells. One-Way ANOVA with Tukey´s multiple comparisons test, ns $p>0.12$; * $p<0.033$; ** $p<0.002$; *** $p<0.001$, $N\geq9$ of ≥ 3 independent experiments.

3.3.7 Effect of deposited antibiotics on infected cell model at different timepoints

3.3.7.1 Analysis of CFU, barrier function, cytokines and viability after 4/24h post infection

After having characterized ideal culture conditions for testing antibiotics on the presented infected co-culture, it is next to evaluate the influence of time regarding the state of cells and bacteria.

The following tests are done with ideal culture conditions as evaluated on Chapter 3 so far. This is 1) use of a transferred biofilm instead of planktonic bacteria, 2) assessment of biofilm in presence of epithelial cells, 3) treatment with a dose of tobramycin of 14.8 ± 0.16 µg and 4) analysis of CFU and TEER at ALI conditions. By doing so, it is straightforward to first assess the difference of a rather short incubation (4h) to the already assessed longer incubation (24h). CFU, TEER, viability and the release of IL-8 was analyzed to prove the effect of nebulized tobramycin, as done in[4].

CFU on epithelial cells was reduced as expected. Interestingly, the total number of CFU increased in the course of time independently from treatment (8.1 vs. 9.4 $\log_{10}$ CFU/mL

and 1.4 vs. 2.6 log_{10} CFU/mL, respectively, Figure 3.27 A). This is both statistically significant (p=0.002). At the same time, TEER values were reduced to baseline when cells were infected and not treated (Figure 3.27 B). Nebulized treatment could save TEER values at either 4 and 24h, whereas the control TEER and TEER of infected treated cells decreased in the course of time (952 vs. 589 Ω*cm^2 and 410 vs. 268 Ω*cm^2). Anyway, a TEER of 268 Ω*cm^2 is still comparable to TEER of rabbit bronchial airways as *in vivo* comparison[169], but still a bit lower than comparable bronchial epithelial primary cells[170]. After 4h infection time, TEER is fallen to nearly 0. Since cells were still visible (for images see chapter 3.3.7.3), a study to detect LDH release was done to finally proof the survival of cells. 41.4 % of cells are still viable after 4h (Figure 3.27 C), which is increased to 93.2 % when tobramycin is applied. After 24h, untreated cells are gone as proven by imaging and LDH release cannot be assessed due to the overgrown PAO1 bacteria (as described in materials and methods). Due to the treatment, LDH is still detectable after 24h showing 80.6 % viability, which is a significant decrease from control but still in an acceptable range. Tobramycin is not known as an anti-inflammatory drug per se, and PAO1 should induce an inflammation of epithelium. Hence it was tested if IL-8 as a known pro-inflammatory cytokine in the context of bronchial diseases and CF[172–174] is released in the following setup as described by an initial model of Bowler et al[113]. Here, IL-8 could be assessed in a far higher level than in untreated control (Figure 3.27 D) as CF cells are known to release IL-8 in higher amounts[137,175]. After 4h, IL-8 could be detected on treated and untreated wells without showing any difference in release (p=0.97). After 24h, IL-8 release is at the same level of the 4h value, indicating a chronic, not exacerbating infection. Treatment with tobramycin might exert reduction of virulence via other pathways, as via OMV-mediated reduction of virulence factors[143]. In clinics, tobramycin is shown to reduce inflammation via reducing blood neutrophils[176]. In concordance to viability, IL-8 was not measurable on infected samples. This is most probably due to pH-changes of the medium and due to bacterial lytic enzymes, that are abundant after 24h infection, comparable to a study investigating the fate of LDH in presence of bacteria[138]. Also, the cells were destroyed by bacteria, so that no new IL-8 could be formed.

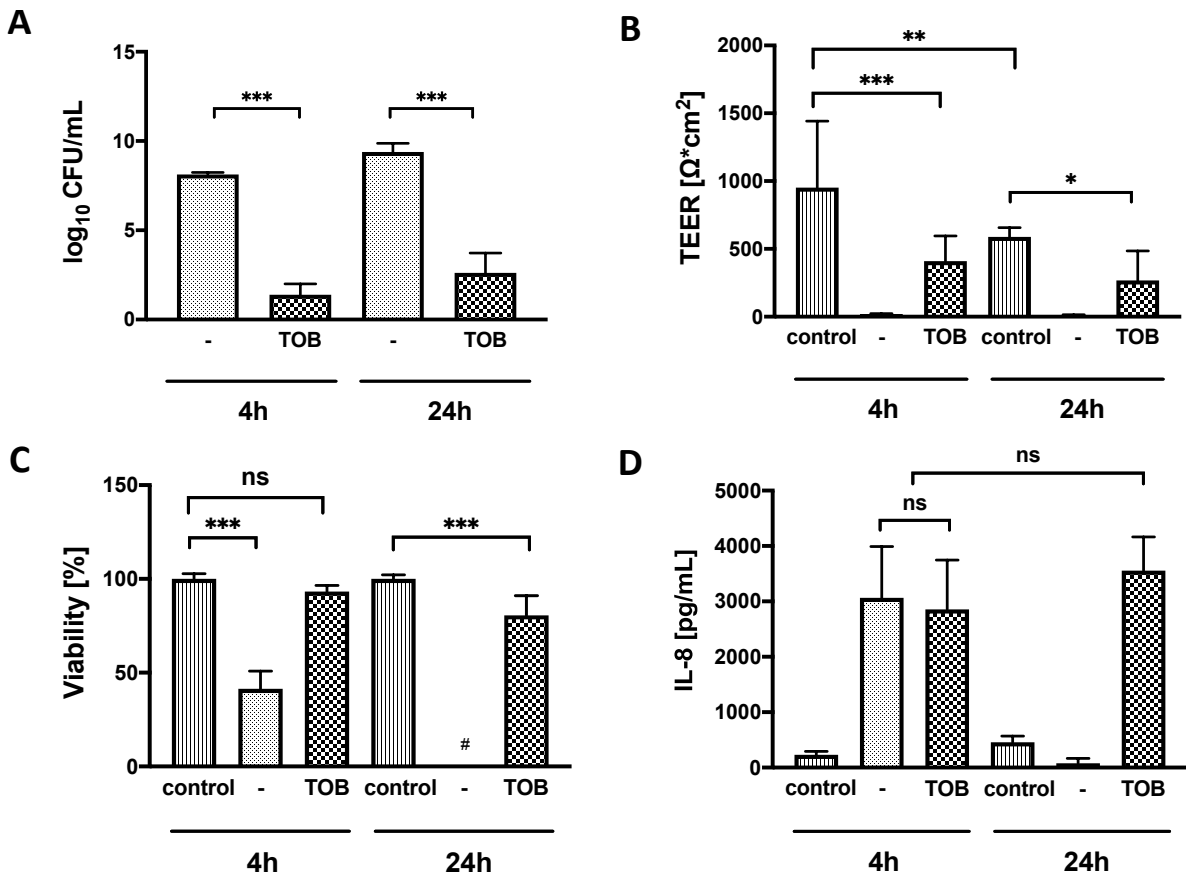

Figure 3.27: Analysis of infected cells at ALI comparing 4h and 24h post-infection time. A) CFU of apical PAO1 on infected cells. B) TEER of test system after 4 and 24h. C) Viability of cells in comparison to uninfected control via LDH release. D) IL-8 on basolateral side of Transwell® inserts in comparison to uninfected control. # LDH detection could not be done due to overgrowth of bacteria, lysed cells confirmed with light microscope. Control = uninfected control. One-Way ANOVA, Tukey´s multiple comparison test, ns $p>0.12$; * $p<0.033$; ** $p<0.002$; *** $p<0.001$. N ≥ 9 of ≥ 3 independent experiments. Adapted with permission from [4]. ©2021, American Chemical Society.

Summarizing, infection is not stopped via a single application of tobramycin. This is initially wanted, since a co-culture of cells and bacteria is possible thereby, nevertheless, CFU is increasing in the course of time. This is most probably due to persister cells that are not to eradicate as described[28,177]. As shown in chapter 3.3.5, mammalian cells seem to have an influence on antibiotic tolerant bacteria. Additionally, it is quite probable, that tobramycin is transported through the cells to the basolateral medium, decreasing its amount on the apical side of cells in the course

of time. By diluting its dose, PAO1 can re-grow again. This is a very important aspect of the ALI condition, as no apical washing step was artificially applied to remove bacteria (to mimic the *in vivo* system). Likewise, TEER apparently drops from around 400 to 300 Ω*cm^2 from 4h to 24h even with treatment, also viability further decreased by approximately 10 % (Figure 3.27). Infection of cells was not cured by tobramycin, but was maintained at a level of around 3000 pg/mL, showing the need of longer incubation times by treatment[137]. In future, anti-inflammatory drugs used in clinics could be employed to test reduction of inflammation on a sophisticated *in vitro* model[176].

3.3.7.2 Analysis of CFU, barrier function and cytokines after 24, 48 and 72h

Studies of cells and bacteria after 4 and 24h infection revealed in particular an increase of PAO1 and a reduction in TEER, while viability and infection (measured as release of IL-8) was about to be maintained with treatment (previous chapter). It is hypothesized, that bacteria could be eradicated by adding another dose, while cells receiving only one dose would maintain their level of CFU or would be slightly increasing, since some antibiotic must still be present on the cell layer. With reduction of bacteria, TEER values and viability could be thereby mostly saved. Most comparable studies concentrated on a single treatment of infected cells[117–119,148]. The reason could be, that submerse conditions are not ideal for re-treatment, as a given antibiotic needs to be removed with a pipette and replaced again, which causes a partial destruction and removal of bacteria, not to mention to risk cells being damaged. Repeated deposition was realized by application of up to two further doses applied on the apical side via deposition (Figure 3.14, as in[4]). In order to supply cells with adequate amount of nutrients and in order to simulate transport processes in the lung, basolateral medium was changed every 24h (as described).

Interestingly, CFU was not eradicated 24h after application of a second dose of tobramycin (24-48h, Figure 3.28) but even increased a bit (2.6 vs. 3.9 $\log_{10}$ CFU/mL). A

third dose did also not decrease biofilm burden (4.1 $\log_{10}$ CFU/mL). It could be shown, that a repeated dose is necessary to maintain CFU at a low level, while not eradicating bacteria. On the contrary, missing a second or a third dose or even missing only the third dose has tremendous impact on re-growth of CFU. Without direct treatment at least 24h before analysis, no difference can be seen comparing to the non-treated control (Figure 3.28, $p>0.12$). In contrast to the findings at timepoint 4 and 24h (previous chapter), CFU of the infected control wells is not increased any more in the course of time even though basolateral medium and sugar supply is renewed (Figure 3.28). This is in concordance to the CFU growth curve of PAO1 that is facing a plateau phase after some time (about 24h, Figure 3.1). Apparently, the small area on top of Transwell® inserts plus the liquid of the meniscus of medium limits the growth of bacteria as well. There is evidence, that bacterial cells and especially *P. aeruginosa* develops tolerance *in vivo*[178]*,* that has to be discriminated to well-known resistance of bacteria[28]. Tolerance of *P. aeruginosa* to antibiotics has been shown also *in vitro*[146], with cells most certainly being in a dormant state of growth that reduces its ability to grow, but on the other hand being not prone any more to antibiotics interfering with the cell division of bacteria as tobramycin[26,177]. Here, the reason for bacteria not being eradicated is most probably the emergence of tolerance of PAO1, which requires an initial dose of antibiotic that is not high enough to completely eradicate all bacterial cells (compare Figure 3.13, which is the volitional case in this model). Nevertheless, it was hoped to eradicate nearly all bacteria by adding a second or third dose. This dose is most probably diluted by being transported to the basolateral side through the slightly damaged cell layer. After changing the basolateral medium, the antibiotic is removed, modelling the lungs transporting the API via the blood flow or the mucociliary clearance[14,17].

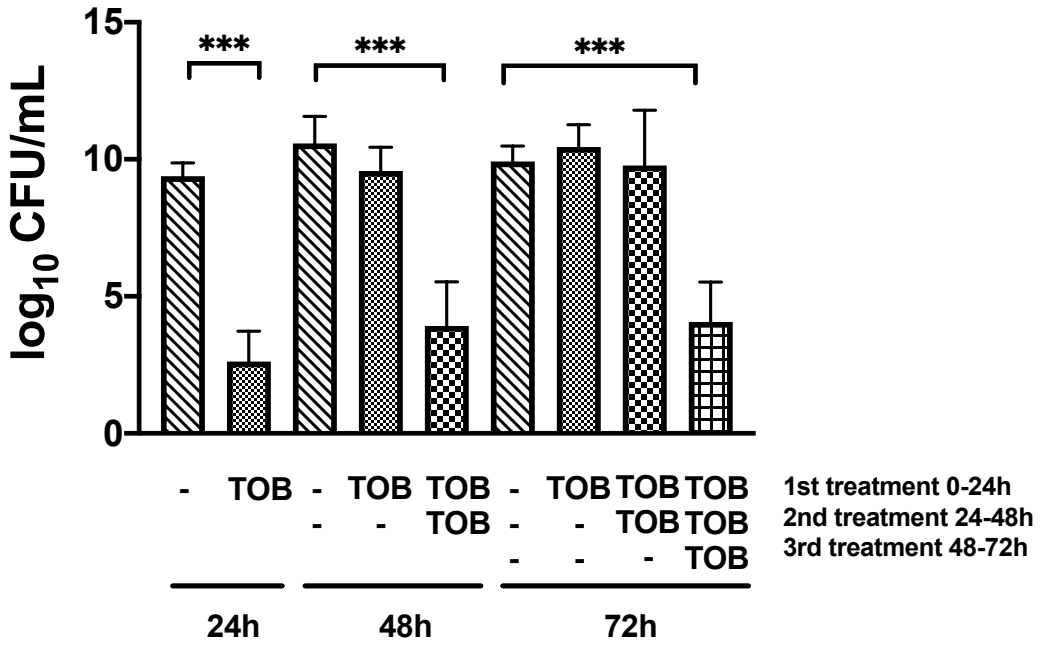

Figure 3.28: Multiple and repeated deposition of tobramycin leads to reduction, but not eradication of PAO1 on epithelial cells. One-Way ANOVA with Tukey´s multiple comparison test, ns $p>0.12$; * $p<0.033$; ** $p<0.002$; *** $p<0.001$. $N \geq 9$ of ≥ 3 independent experiments. Adapted with permission from [4]. ©2021, American Chemical Society.

The establishment of a complete model requires the host-response, which stands for the patient in this test system. Ideally, treatment with antibiotics would save the patient for a longer time period. By application of an antibiotic as tobramycin, not all patients can be saved, patients possibly decease even though an optimal treatment happened, due to resistant or tolerant bacterial biofilms in CF[39,177,179]. One of the important parameters to test the healthy state of barrier forming cells is the TEER value. Here it could be shown, that cells are only partially recovering from infection as shown by TEER (Figure 3.29 and in[4]). With increasing time, the uninfected controls are losing its TEER values, which could be partially explained with senescence[139]. In-process controls of medium did not uncover any contamination, as controlled via testing drops of medium on microscope slides under light microscope. Contamination with Mycoplasma was excluded on a regularly, 3 months basis as part of a standard DDEL

laboratory procedure. As shown before, TEER is not measurable of all infected cells beginning timepoint 4h. Inversely to CFU results (Figure 3.28), the TEER values (control and infected treated samples) of timepoints 24, 48 and 72h are decreasing (Figure 3.29). After 24h, infected and treated samples show 347 Ω*cm^2, which is significantly less than its control (612 Ω*cm^2). After 48h, this value is further reduced to 183 Ω*cm^2 with the control having a resistance of 449 Ω*cm^2. Inversely to CFU, giving only one dose of tobramycin leads to decrease to 50 Ω*cm^2, which is perceived a bit more than the baseline having no barrier any more. After 72h, the control further sank to 320 Ω*cm^2, infected and treated samples (dosing after t=1, 24 and 48h) do not have a barrier any more (102 Ω*cm^2), thus not showing any significant difference to the control (p=0.13).

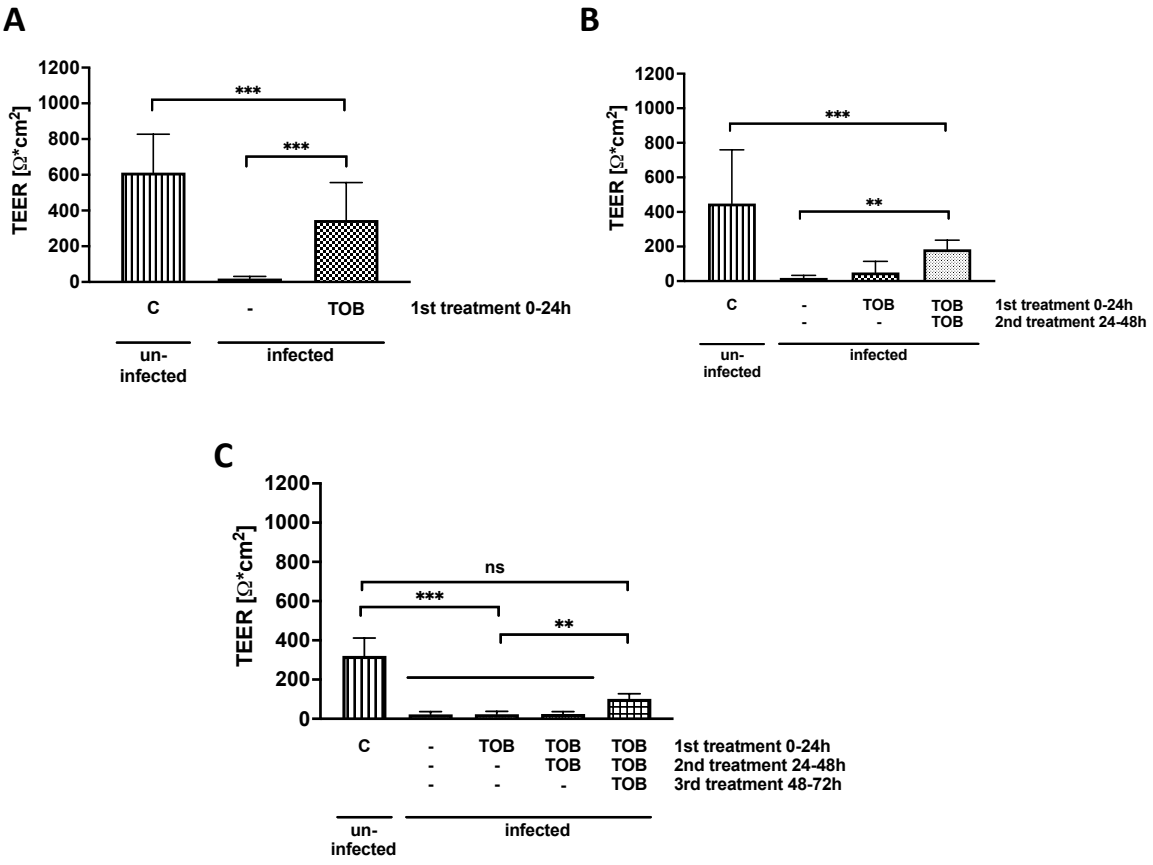

Figure 3.29: Barrier integrity as TEER of test system being repeatedly treated with aerosolized tobramycin dose plus respective controls for up to 72h. A: After 24h, B: After 48h, C: After 72h incubation. C = uninfected control. N ≥ 9 of ≥ 3 independent experiments. Adapted with permission from [4]. ©2021, American Chemical Society.

Interestingly, the detection of viability draws a different conclusion on the fate of host cells after infection and treatment.

Since detection of LDH is not possible or not completely possible if high inoculi of bacterial cells are present (about < 5 $\log_{10}$ CFU/mL[137,138]), only the infected samples treated completely (i.e. 2x in case of 48h or 3x in case of 72h) were compared to the controls (Figure 3.30 and [4]). A drop to 82 % viability is observed after 24h, compared to a drop to around 60% of control TEER (Figure 3.29). After 48h, 72% of cells are viable compared to control (compared to around 40% of control TEER). After 72h, even 88% of infected and treated cells are found in good health, which is far more than indicated by TEER (about 30%, Figure 3.29 C). Relatively and objectively, cells seem to be in far better health than expected by TEER. There has been evidence, that TEER is a more precise indicator for monolayer integrity, as bacteria attack the tight junction proteins first, causing subsequent TEER drop[137,180]. Some studies of long-term infection of cells on permeable supports have been done, but with other bacteria, as Haemophilus influenzae or Staphylococcus aureus, that are apparently less cytotoxic than PAO1 and therefore not comparable[121,181]. Recently, a study uncovered the effect of ciprofloxacin treatment (4 µg/mL) on Calu-3 cells on PAO1 infected cells for up to 72h, generally confirming the results of this study, though highlighting bacteriophage treatment[122]. Single treatment after 6h infection decreased apical CFU to 6 log CFU/well, whereas TEER could be maintained at the value of the control (around 300 Ω*cm^2). After 72h, CFU raised to around 9 log per well, whereas the TEER value decreased to about baseline[122]. No re-treatment was done, samples were only one-time treated. The authors stated ALI conditions, but apparently used small permeable supports of the size of 0.3 cm^2 with 20 µL pipetted apical volume, which leads to a visible amount of liquid on top of cells[122]. This might be the reason that authors could not induce re-treatment, as this is only fully realizable having true ALI conditions and a deposition device as described here.

All in all, epithelial cells are attacked by PAO1 and lose viability, nevertheless, around 80% viability can be seen when cells are treated. With increasing infection time, TEER

is objectively and relatively decreasing, whereas viability stays constant. CFU of treated samples is not eradicated, but maintains a level of 3-5 $\log_{10}$ CFU/mL, with CFU raising to the level of untreated samples (about 10 $\log_{10}$ CFU/mL) after not receiving a subsequent dose.

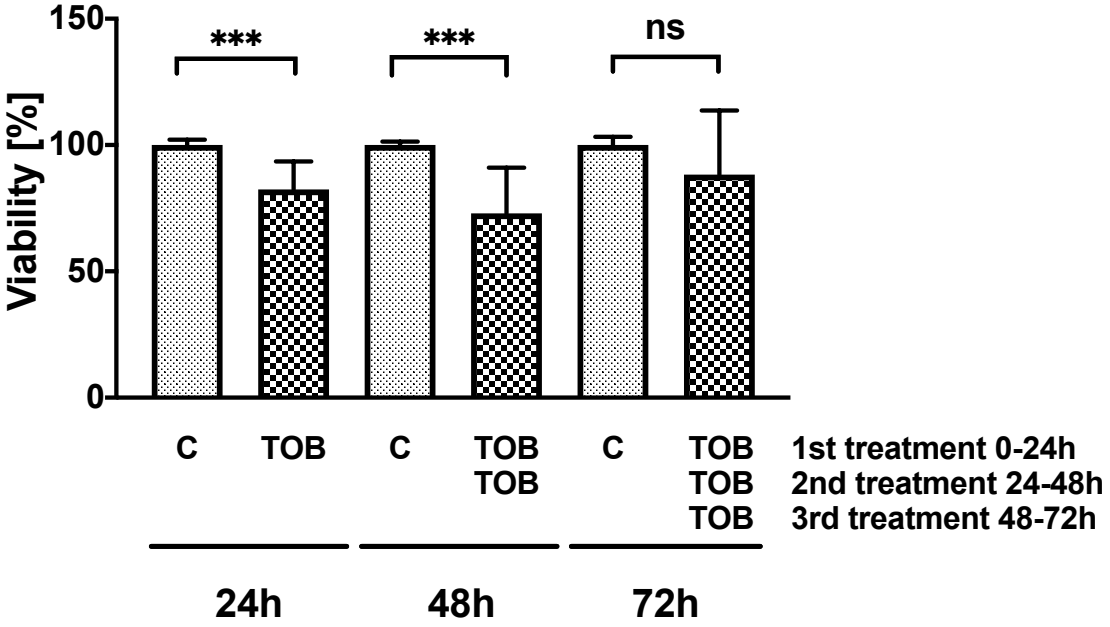

Figure 3.30: Viability of CFBE41o- cells after infection of co-culture with PAO1 biofilm. Basolateral supernatants were used and the viability was calculated from LDH release as described in material and methods. C = uninfected control. One-Way ANOVA and Tukey´s multiple comparison test, ns $p>0.12$; * $p<0.033$; ** $p<0.002$; *** $p<0.001$, N ≥ 9 of ≥ 3 independent experiments. Adapted with permission from [4]. ©2021, American Chemical Society.

3.3.7.3 CLSM and SEM imaging of the infected cell model

Chapter 3.3.8 already showed the results of infecting CFBE41o- cells with pre-formed biofilm for different time points. Even so, detailed images of the infected model would answer important questions. Still, there is no visual information about the process after infection and after infection and treatment in the course of time. The influence of a tobramycin dose on a culture treated thereafter with KRB (as after 48 or 72h incubation time, chapter 3.3.7.2) is not completely clear, since bacteria are already growing too

fast again to apply an LDH kit. Barrier measurement is very precise, since it detects already little holes in the membrane with fast reduction in TEER. Therefore, it is to argue, if stepwise addition of tobramycin prevents at least partly the complete destruction of cells. To prove this, SEM images were taken after the end of 4, 24, 48 and 72h incubation time of infected cultures. In order to control the results, the images were also obtained via CLSM imaging.

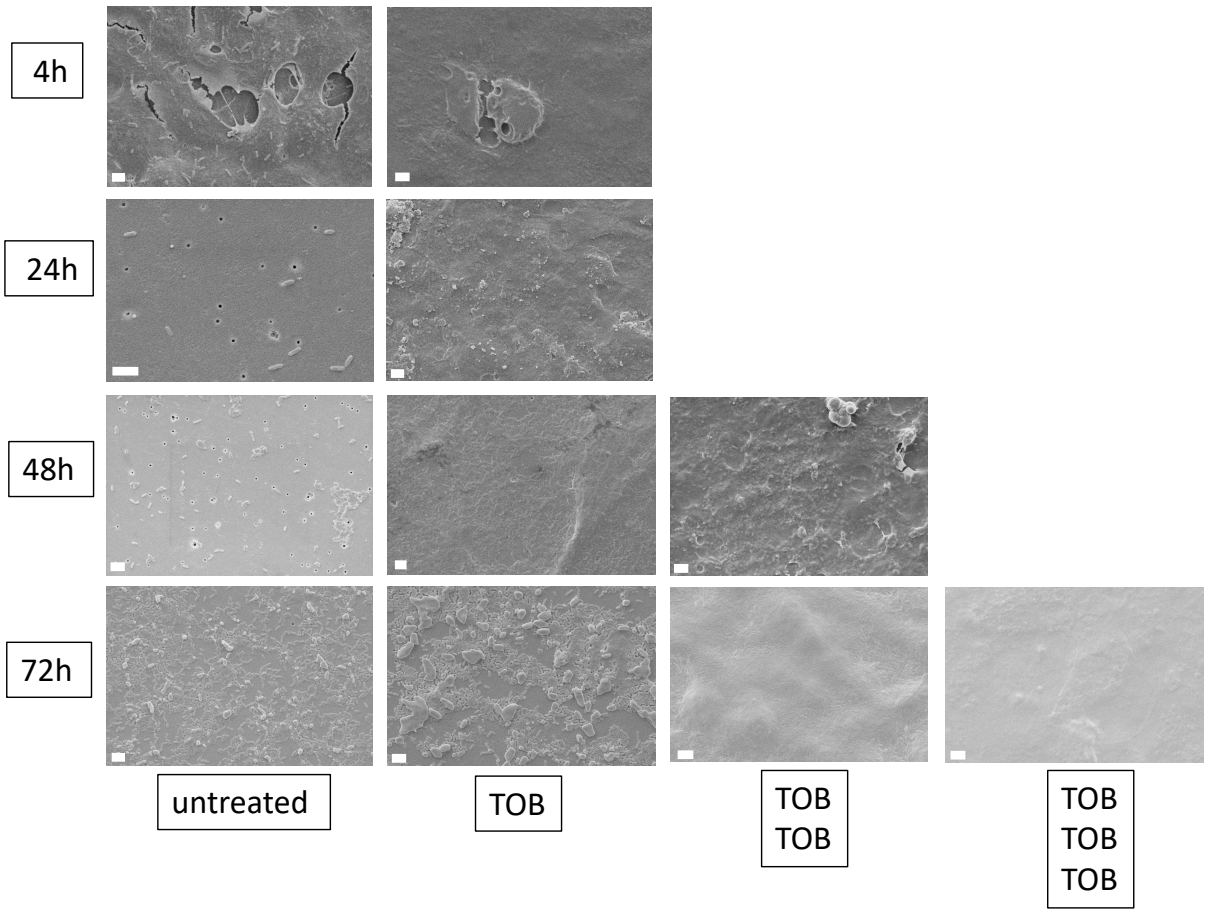

Figure 3.31: SEM images of pre-formed 72h PAO1 biofilm infected CFBE41o- cells after 4, 24, 48 and 72h incubation. Biofilm bacteria attacking cells without treatment lead to total destruction of epithelial barrier after 24, 48 and 72h timepoints. After 4h, remnants of epithelial cells can still be seen, but bacteria have formed holes in the barrier already. Tobramycin treatment saves cells after 4h and 24h, but not after 48 and 72h, since biofilm bacteria are clearly seen. 2x tobramycin treatment does not save cells after 72h. Interestingly, biofilm bacteria have already destroyed the complete cell material (untreated 24, 48 and 72h), whereas samples that received at least one dose of tobramycin do still show remnants of former cell material (48h TOB, 72h TOB and 72h TOB TOB). Scale bar shows 3 µm.

Figure 3.31 describes the state of the co-culture after respective treatment regimens (no tobramycin, tobramycin followed by KRB after further 24h (TOB), tobramycin followed by tobramycin after 24h and further KRB after 24h (TOB TOB) and three consecutive treatments with tobramycin (TOB TOB TOB)). The culture was exactly prepared as described in chapter 3.3.2 and tested in chapter 3.3.7.2.

No treatment does result in total loss of cells, but also of most of the biofilm, which is explained by the apical washing step to remove remaining water with alcohol. The biofilm has most probably no possibility to attach to a structure, as cells are already completely disrupted, and the plastic surface might be too flat to attach. A single treatment with tobramycin prevents loss of TEER and viability after 4 and 24h as already seen by aforementioned data, which is now confirmed by SEM imaging, visualizing a healthy cell layer. But most interestingly, a single tobramycin dose followed by no treatment does not simply result in total loss of cells, but creates a bacteria covered cell debris (48h TOB and 72h TOB/TOB TOB). Even when tobramycin was applied at t=1h and image was obtained after 72h (72h TOB), a little cell debris is still visible, which is not the case when no treatment was applied (Figure 3.31). This could be partly explained by the fact, that biofilm had more time to use the cells as a scaffold to grow in, resulting in a more stable conformation, that prevented being washed from the inserts.

The same holds true, when PAO1-GFP pre-grown biofilm was used instead of PAO1 for confocal imaging (Figure 3.32). Technically, it was very challenging to obtain these images, as the CFBE41o- cells had to be initially stained with Hoechst 33342, which was partly absorbed by the membrane of the Transwell® insert. This phenomenon was most problematic at images of timepoints 4, 24 and 48h (except the last treated sample each at the right side).

Imaging via confocal microscope generally confirms the results imaged via SEM, though, confocal image preparation does not need vigorous washing steps. This leads to have more biofilm structure left, especially noting the not-treated samples. Interestingly, these colocalize with former cell structures (48h untreated), most probably the rest of the biofilm was washed away and structures around cells were

physically more stable to attach to the plastic surface. The blue structures in 4, 24h and 48h untreated as well as in 48h treated 1x with tobramycin are no cells, but the blue stained membrane. Interestingly, we still see bacteria on top of cells, even if treated (4h TOB, 24h TOB, 48h TOB TOB, 72h TOB TOB TOB). This confirms CFU results from figure 3.28 showing bacteria even after treatment, that result in re-growth if not treated again.

This is in contrast to a former study done in the DDEL group of HIPS, detecting PAO1-GFP on confocal images, but not in CFU count[137]. This could be an artefact of CFU analysis, which was done in the present study with very fresh samples directly after end of the experiment.

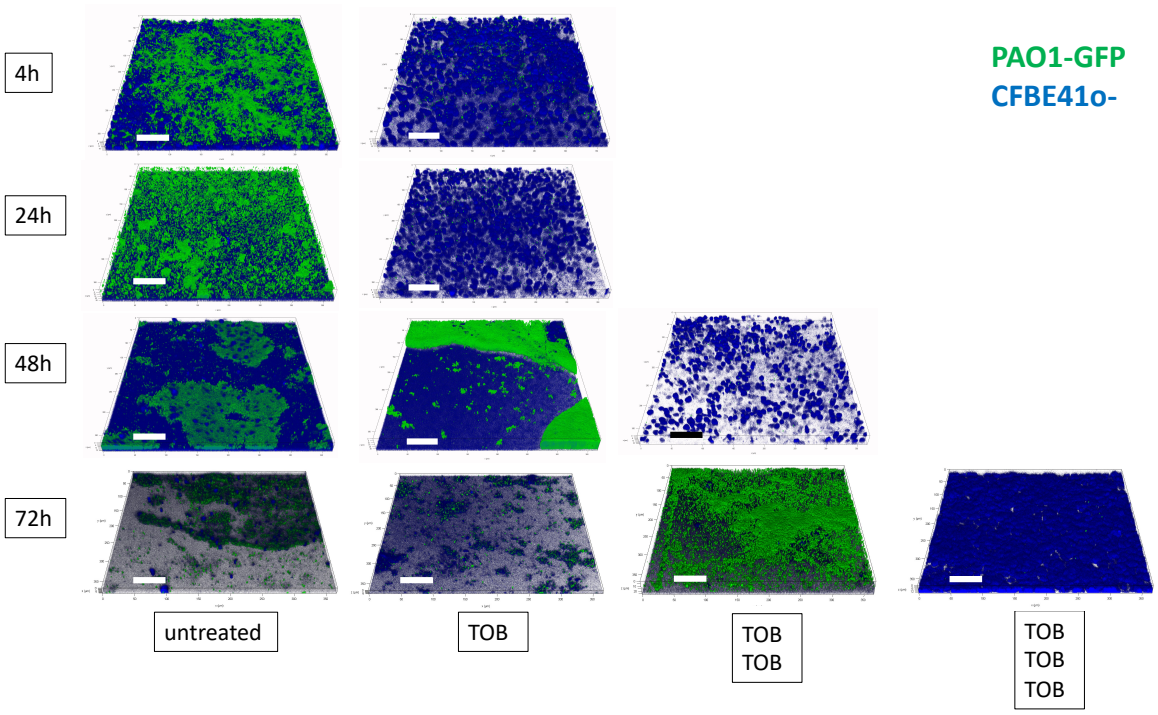

Figure 3.32: CLSM images of pre-formed 72h PAO1 biofilm infected CFBE41o- cells after 4, 24, 48 and 72h incubation. Experiment was done as shown in figure 3.14. PAO1-GFP biofilm shown in green, CFBE41o- cells pre-stained with Hoechst 33342 (blue). Scale bar: 50 µm.

3.3.7.4 Transport of sodium fluorescein across infected epithelium

Barrier integrity of biofilm infected and treated cells was reduced significantly (40% of control after 48h), but viability was maintained at about 80% throughout all infection times (chapter 3.3.7.2). This was more than initially expected; therefore, further tests should prove, if the barrier is really as compromised as shown by TEER. As an example, the 48h timepoint was chosen, because TEER was analyzed to be below the threshold of 300 $\Omega*cm^2$ even after repeated administration of tobramycin (183 $\Omega*cm^2$).

Cells were again infected and treated (with untreated controls) as depicted in Figure 3.14 for 48h (treated samples receiving in this case two consecutive tobramycin doses after 24 and 48h). After the 48h, the transport experiment itself was started and infected samples were compared to uninfected samples and samples receiving EDTA as control without TEER. As visible in Figure 3.33, TEER values are comparable to the TEER values obtained in previous experiments as already shown (chapter 3.3.7.2). After 4h of transport experiment, that cells had been stored under submerse conditions in KRB, the TEER values have risen as observed in preliminary experiments with cell medium (data not shown). Application of 16 mM EDTA drops TEER to baseline, as expected, and therefore serves as control to the non-treated infected samples.

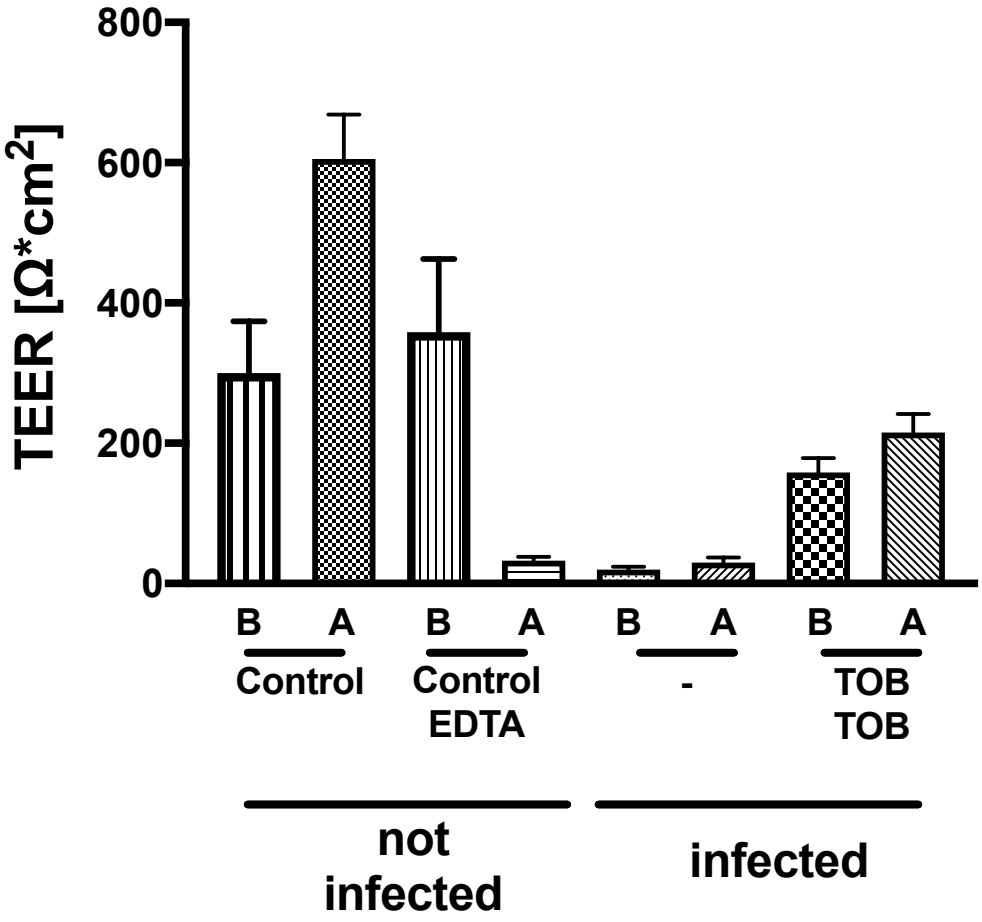

Figure 3.33: TEER values of CFBE41o- cells that have been incubated or infected for 48h before (B) and after (A) the transport experiment. Cells were incubated in medium for 1h first, then incubated for another hour in KRB, then the transport experiment has been done (>4h) and TEER was evaluated again. Data showing mean and SD. N=6 of two independent experiments.

Cells were subjected to 10 µg/mL sodium fluorescein solution, as this is often used and easy to detect via fluorescence[139,141,182]. It is expected, that uninfected control shows least transport and the biofilm control enables total diffusion of sodium fluorescein, as there are no cells visible after infection. After 4h transport, as shown in figure 3.34, apparent permeability values were calculated as described in materials and methods. It may be assumed that the higher the permeability, the leakier is the membrane. Control shows 8.8 x 10^{-7} cm/s, which is in range of literature (about 3 x 10^{-7})[141]. With addition of EDTA 16mM, permeability is increased (8.9 x 10^{-6} cm/s) as shown by TEER (Figure 3.33). Interestingly, infected and infected treated samples differ not as much

as expected (3.3 vs. 2.2 x 10^{-6}, respectively, Figure 3.34). Not treated samples show higher transport than treated samples, nevertheless, it was expectable to have a value comparable to the EDTA control (at least). Possibly, the biofilm that has formed on the insert in the incubation time of 48h hinders the flux of sodium fluorescein. The pH-sensitivity of sodium-fluorescein[183] is most probably not a concern in this setting, as Krebs-Ringer buffer is buffered at pH 7.4 and bacteria were thoroughly washed away before, plus the addition of 10 µg/mL tobramycin for the time of the transport experiment prevented re-growth. A study done by Thorn et al. with the very same infected cell model using a comparable transport protocol showed P_{app} values of infected barrier of 2 x 10^{-5} cm*s^{-1} and values of about 0.5 x 10^{-6} for transport across infected and treated as well as healthy epithelium, that did not show significant differences from each other[184]. The P_{app} value of healthy cells matches the here shown data, nevertheless, infected epithelium shows way higher values in the study of Thorn et al., whereas the treated cells show comparable values to the control.

The transport experiments could have been a more defined and specified way to analyze barrier integrity. By now, the rather discouraging results cannot be explained and also have to be evaluated with caution, since only 2 independent experiments were done. Definitively, more experiments need to be done to evaluate the effect of untreated cells on the transport, as for example a comparison to other compounds or extended studies on the role of biofilm as physical obstacle for drug transport studies across permeable supports. Even so, the study of Thorn et al. has already shown the general applicability of transport studies across infected epithelium to prove the efficacy of anti-infective drugs as another surrogate for TEER values.

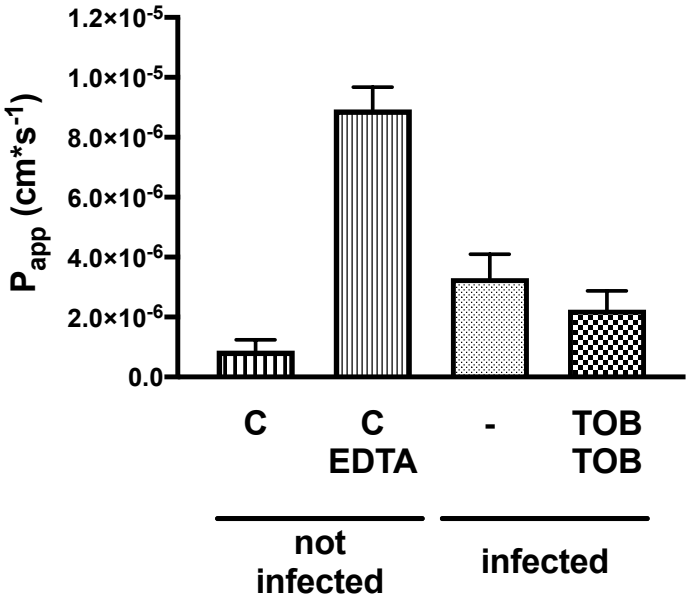

Figure 3.34: P_{app} values of CFBE41o- cells after 48h incubation with or without PAO1 biofilm. Transport of sodium-fluorescein was evaluated over 4h. C = control. Data show mean and standard deviation. N=6 of two independent experiments.

3.3.7.5 Analysis of E-cadherin in infected model

As transport experiments could not answer the question, if treatment helps to save barrier integrity after several days and to prove the discrepancy of rather high viability values in contrast to rather low TEER, an analysis of proteins that are involved in barrier formation is advisable. Therefore, the study focused on the well-known adhesion protein E-cadherin that is expressed also by CFBE41o- cell line[167]. As transmembrane protein, it is responsible for intercellular cohesion and cell signalling[185,186]. It is hypothesized, that the protein will still be present when treatment occurred for 3 subsequent times after 72h and that infection with biofilm will destroy the protein. Basically, this method is expected to be an alternative to test TEER or viability measurement of samples without complete treatment, as LDH measurement is not possible with high bacterial load and TEER measurement is very sensitive to infection (see chapter 3.3.7.2).

In order to analyze the mass of protein instead of just staining E-cadherin on cell layers, as already done[167], western blots were done after infection timepoints 24, 48 and 72h

according to already done experiments. The cells being used for TEER and viability measurements of chapter 3.3.7.2 were frozen and re-thawed to obtain the proteins for western blot. Each three Transwell® inserts were pooled per experiment, and three experiments per timepoint were combined. Figure 3.35 shows resulting exemplary western blots per timepoint (as done in[4]).

After 24h, control and control tobramycin not being infected show strong bands at 120 kDa that show about same intensity, whereas 100 and 37 kDa are discussed to be cleaved forms. Triton-X controls do only show a slight bar, indicating nearly complete loss of protein. Infected cells to not even show a shadow, indicating total protein disruption. Treated and infected cells feature a strong band, comparable to the control and control with tobramycin on the left (Figure 3.35 A).

Control cells after 48h show again strong bars, that are vanished with application of Triton-X, PAO1 or even PAO1 with only one treatment (Figure 3.35 B). Only the application of two treatments seem to rescue E-cadherin. After 72h, the same picture is visible, but a slight shadow shows at samples being treated only for two subsequent times and not three times (Figure 3.35 C). E-cadherin alone is not only responsible for barrier functionality, as there is a huge number of involved proteins as Occludin, for example[3,139]. These studies give a hint towards a new method analyzing treatment success via analysis of protein mass.

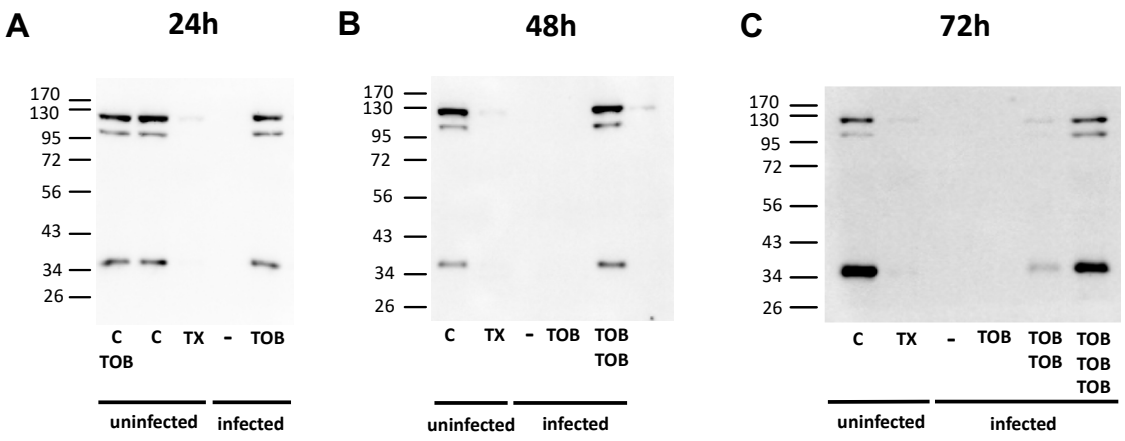

Figure 3.35: Western blots of E-cadherin (120 kDa) showing adherence protein E-cadherin to be destroyed by infection and saved by treatment. (A) after 24 h (B) after 48h (C) after 72 h incubation. C = uninfected control, C TOB = uninfected control treated with tobramycin, TX = Triton-X treated control. Representative images of 3 independent experiments. Adapted with permission from [4]. ©2021, American Chemical Society.

To verify the single images, intensity of the triplicates was blotted relatively to the intensity of the controls at each experiment (Figure 3.36, as in[4]). The controls treated with tobramycin are at 80% of control untreated, yet this is still acceptable. Triton-X treated cells do nearly not show any of the protein any more. Thoroughly treated and infected samples after 24, 48 and 72h show 105 ±35, 138 ±97 and 81 ±27 % of the control intensity, respectively (Figure 3.36). Even though the standard deviation is very high and therefore, this analysis might not be perceived as accurate, it may be beneficial together with TEER analysis and LDH release (chapter 3.3.7.2). Analyzing the effect of two consecutive doses of tobramycin leaving out the third dose, the test shows about 12% resulting E-cadherin, which is not possible to see with TEER, as the values are already too low to discriminate. LDH is not possible to detect, since the values are not trustable any more due to the high bacterial inoculum. Macroscopically seen at the time of the experiment, some of the infected and two times treated wells are still clear after waiting another 24h until t=72h. Apparently, at some samples, there are less persistent bacteria that are better to eradicate. This again shows the usefulness of repeated administration of antibiotics and the necessity of at least 3 replicates of 3 individual experiments when analyzing bacteria. This might be the

reason, that in total some 12% E-cadherin is still visible. All in all, repeated administration of tobramycin maintains E-cadherin abundance after 72h and serves as another proof of a chronic infected cell model to be successfully established.

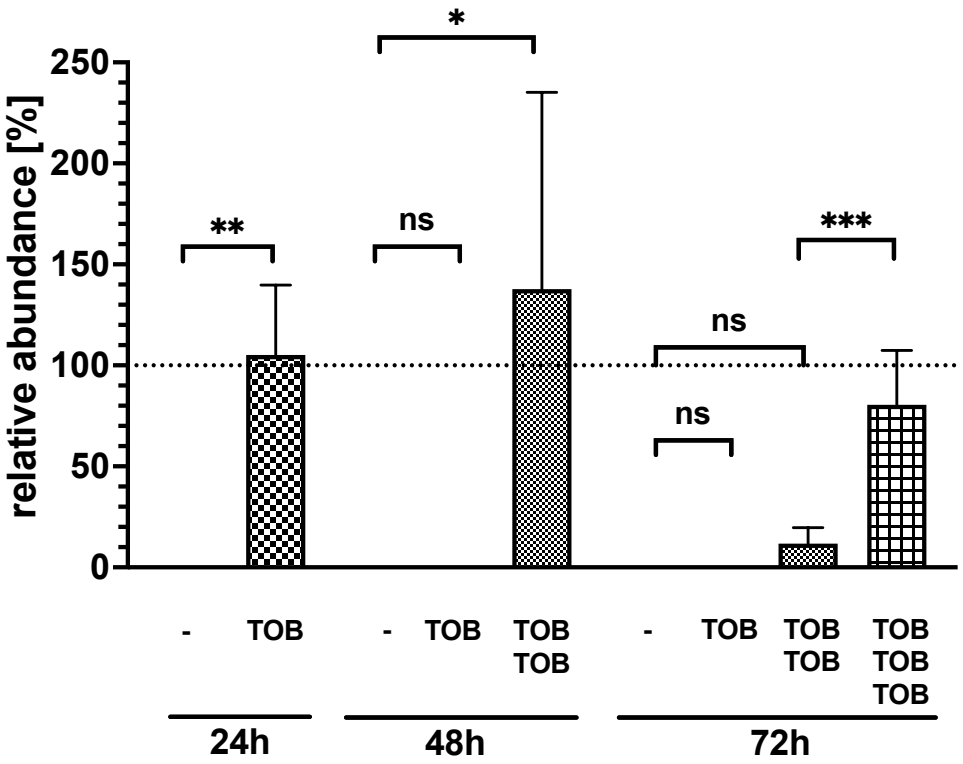

Figure 3.36: Intensities of E-cadherin (120 kDa) as imaged by western blots normalized to control in %. Control tobramycin and control for Triton-X were made (not shown, see [4]). Each replicate is merged value of 3 Transwell® replicates (see Material and Methods). Rest N=3 of 3 independent experiments (infected 48h N=2 of 2 experiments). Adapted with permission from [4]. ©2021, American Chemical Society.

3.3.8 Evaluation of quorum sensing inhibitors on complete model

3.3.8.1 Cytotoxicity and TEER of QS inhibitor on CFBE41o-

The complete infected model, as thoroughly described and characterized from chapter 3.3.2 onwards, was tested only using tobramycin sulfate so far. There are multiple examples in literature though, that tested the influence of various agents that at least support the efficacy of antibiotics on infected co-cultures, as already described in the

introduction part of this thesis[117–119]. By best knowledge, no one so far tested the influence of QS inhibitor like a novel dual pqsR inverse agonist on a comparable infected cell model as described recently[7]. This chemical molecule is able to reduce pyocyanin as well as eDNA secretion and biofilm formation with concentrations in the nano- to micromolar region. It is also described to act better against *P. aeruginosa* in mice applied together with tobramycin in an inhalable, novel co-loaded squalenyl nanoparticle formulation[7]. As this is a very promising approach, it is self-evident to prove this effect also on infected CFBE41o- infected complete model. This would have the advantage to prove the effect of such drugs easier, cheaper and, most importantly, ethically justifiable.

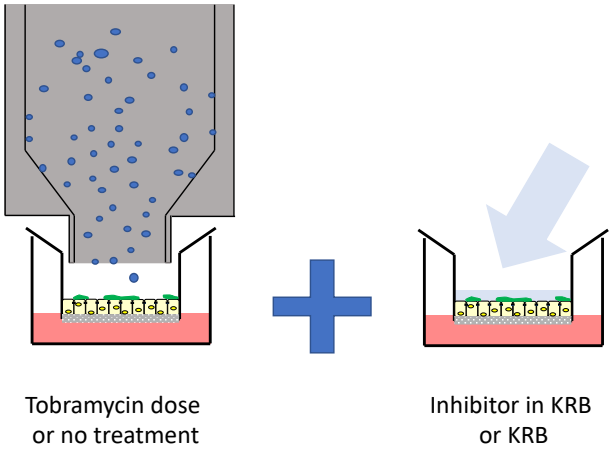

Figure 3.37: Concept of testing a novel QS inhibitor on infected model. Tobramycin sulfate was deposited on infected cells as described in methods section. In case of an additional treatment with the pqsR inverse agonist, 10 µM of inhibitor in 100 µL KRB was added on cells right after deposition of tobramycin. Treatment with tobramycin could be omitted – in this case only the inhibitor was applied.

The problem of the present substance is its limited solubility of 7.7 x 10^{-6} M as described[7]. The inventors of the inhibitor recommended a maximum concentration of 10 µM in KRB. When 200 µL are nebulized, only about 3-4 % reaches the cells (see Chapter 2). To this time, it was still not clear, if the resulting mass on the cells would have an effect on biofilms together with tobramycin. Hence it was decided to start initial tests with the highest possible dose by adding the solution directly on the cells,

but being still somewhat comparable to ALI conditions, since only 100 µL were used. Nevertheless, the main advantage of this model, enabling complete air-liquid interface treatment, must be circumvented for doing such initial studies proving the effect of this inhibitor.

The substance was tested for its influence on CFBE41o- cells. In order to get as close as possible to the experimental conditions, Transwell® inserts with 500 µL medium on the basolateral side were used, and the inhibitor was tested on the apical side (Figure 3.37). This also enables the testing of barrier properties via TEER, as this is a secondary hint at cell survival.

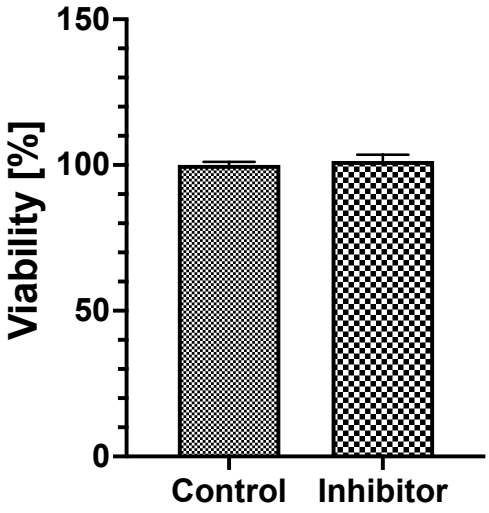

Figure 3.38: Viability of CFBE41o- cells grown on Transwell® inserts after addition of QS Inhibitor and incubation for 48h. 100 µL KRB (0.5% DMSO) vs. 100 µL Inhibitor 10 µM (containing 0.5% DMSO). No statistically significant difference (unpaired t-test, two-tailed, p=0.15). N=7 of 3 independent experiments.

The inhibitor does not show any adverse effect on CFBE41o- cells after 48h (Figure 3.38). This is better than in the publication of the inhibitor. The authors incubated the inhibitor also for 48h, but on 24-well plates and on hepatic HepG2 cells. 55% viability was found at 25 µM concentration[7]. Most probably, the different culture conditions explain the higher viability. Cells on the well inserts receive medium from the basolateral side, whereas the inhibitor in KRB is only on the apical side. The Hep2G cells were incubated with inhibitor in medium, but with 1 % final DMSO concentration,

whereas the KRB on the apical side contains only 0.5 % DMSO. It is well-known that different cell lines react more or less sensitive to noxae, therefore it seems pivotal to only compare same cell lines. This is the reason, why this test was done with the same cell line in same culture conditions.

As illustrated further above in chapter 3, the TEER values are mostly more sensitive to viability changes of cells grown on Transwell® inserts. Hence, also the barrier properties were measured (Figure 3.39). It is expected to be same for treated and untreated cells, since the viability is not changed at all.

The result is quite interesting: CFBE41o- cells treated with inhibitor showed more than double the TEER value as the control (Figure 3.39). This phenomenon is completely unclear. Other researcher could find substances, that increase TEER values, as Lippmann et al. finding retinoic acid to increase Occludin and Cadherin[187]. The phenomenon of increasing TEER of CFBE41o- cells, however, could not be investigated unfortunately in the frame of this PhD project. Nevertheless, this could be the origin in the search of a possible cell-protective element.

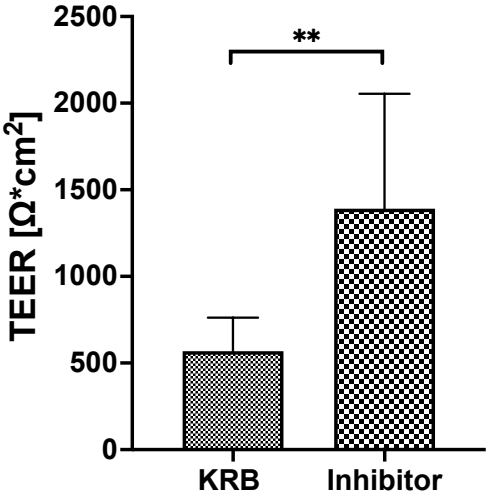

Figure 3.39: TEER of CFBE41o- cells grown on Transwell® inserts after addition of pqsR inverse agonist and incubation for 48h. 100 µL KRB (Krebs-Ringer buffer, supplemented with 0.5% DMSO) vs. 100 µL Inhibitor 10 µM (containing 0.5% DMSO). Statistically significant difference between the two groups (unpaired t-test, two-tailed, p=0.02). N=9-10 of 4 independent experiments.

3.3.8.2 Analysis of CFU

Since the inhibitor is not toxic, and shows even possible cell-protective properties, the substance could be tested on the complete infected model (Figure 3.14). The first question was, if a combination of inhibitor and deposited treatment with tobramycin may be advantageous in contrast to tobramycin without inhibitor.

This hypothesis was tested by infecting cells for 24h without treatment compared with tobramycin, inhibitor and the combination by counting CFU first (Figure 3.40). No significant difference could be found between KRB and inhibitor and the combination tobramycin and inhibitor ($p=0.59$ and $p>0.99$, respectively). It was not expected, that the inhibitor alone could suppress the infection, since it is not antibiotic per se. Nevertheless, Schütz et al. found a reduction in CFU in a mouse model by only applying the inhibitor alone, which was explained with the immune system taking advantage of the impact of the inhibitor on biofilm formation, LasB expression and pyocyanin reduction[7]. Although the authors used three subsequent applications of inhibitor for 72h, the main difference is the absence of an immune system in the present *in vitro* experiment. Likewise, there is strong evidence, that a combination of tobramycin and inhibitor is more effective than tobramycin alone, and this effect was even improved when applying both in a co-loaded squalenyl nanoparticle formulation[7]. The authors used an MBEC biofilm model of *P. aeruginosa* PA14 strain, without the use of ALI conditions and of cells, but also for a time range of 24h.

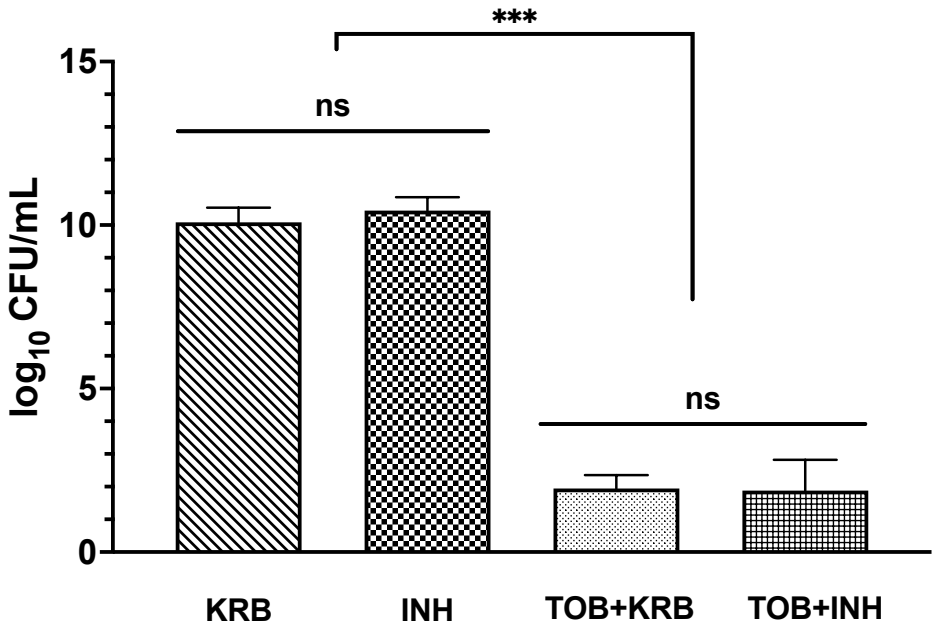

Figure 3.40: CFU on infected model after 24h infection. INH=100 µL inhibitor as described[7]. KRB=Krebs-Ringer buffer (with 0.5 % DMSO). TOB=Tobramycin sulfate applied as deposited dose as described in Materials and Methods. One-Way ANOVA and Tukey´s multiple comparison test, ns $p>0.12$; *** $p<0.001$, N = 9 of 3 independent experiments.

Since the effects of the inhibitor on biofilm did not match the observations of the publication of Schütz et al., we hypothesized, that the infected model may only be applicable for longer time periods, as done with the 72h *in vivo* infection model of Schütz et al., proving the inhibitor efficacy[7]. May the synergistical effect of the biofilm reducing inhibitor and the antibiotic tobramycin can only be seen on this model, when applied as a subsequent treatment for a time period of at least 48h. Therefore, tobramycin was applied on all tested wells after infection, as it has been proven, that re-infection will take place immediately otherwise (chapter 3.3.7.2 and following). The inhibitor was compared to KRB alone, and was either applied directly with the first tobramycin deposition or was added after 24h or both (see figure 3.41).

A tendency towards reduction of CFU is observable when inhibitor was applied after 24h compared to KRB alone (Figure 3.41). Nevertheless, this effect is not statistically significant ($p=0.15$). Interestingly, a significant difference in CFU after 48h could be seen between infected wells and infected wells treated with tobramycin for the first 24h, which was not significant in experimental sets before (Chapter 3.3.7.2). When

tobramycin was applied twice, the number of bacteria was further reduced as seen before, leading to an infected, but stable system. Combining inhibitor and tobramycin led to the lowest number of CFU on cells after 48h of all done experiments (1 $\log_{10}$ CFU/mL). Even if there is no significant difference compared to the tobramycin control without inhibitor ($p=0.69$), a significant difference can be seen compared to the control that did not receive a second dose of tobramycin, but a second dose of inhibitor (Figure 3.41, $p<0.001$).

Given the fact, that significantly less PAO1 bacteria are found on wells that received a first treatment with tobramycin, but not a second, compared to the wells that did not receive any treatment (vs. the results in chapter 3.3.7.2) no reasonable explanation for this phenomenon is available. It is more probable, that *P. aeruginosa* bacteria were more vulnerable to the initial treatment with tobramycin than in the experimental setups before, even though all preparation steps were kept same and same stocks of different containers were used to avoid re-freeze effects. Controls with tobramycin treatment in the time period of the inhibitor experiments gave a hint, that the number of bacteria 24h after treatment was less than in the experimental setups done before (about 2 vs. about 3 $\log_{10}$ CFU/mL). The reasons could be manifold, as we face a complex biological system comprising of mammalian and bacterial cells, that are challenging to reproducibly generate robust outcome. Mammalian cells can have an influence on the efficacy of tobramycin, for example by changing the pathogen´s resistance to tobramycin or by physical interactions, which may has been more pronounced before for some reason[5,112,171]. Also, *P. aeruginosa* was found to have changed behavior after freeze-thaw cycles[188]. Although these freeze-thaw cycles of stock *P. aeruginosa* were tried to be avoided as much as possible, this factor cannot be excluded. A sudden increase in the efficacy of tobramycin, due to increase in purity for example, is assessed to be rather unprobeable due to quality controls of the supplier.

Application of a second dose of inhibitor was not proven to be more effective on the biofilm model. Nevertheless, both, the single application of inhibitor after 24h and the combination of tobramycin and inhibitor, that was repeated after 24h, showed a

tendency towards lower CFU numbers on cells, that confirm the results of the publication of Schütz et al.[7].

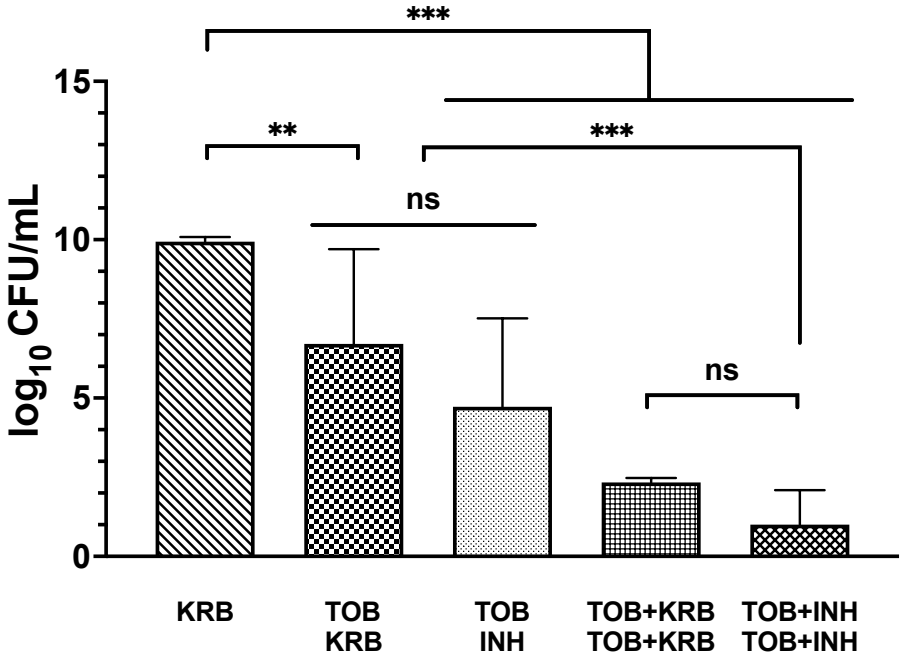

Figure 3.41: CFU on infected model after 48h infection. INH=100 µL inhibitor as described[7]. TOB=Tobramycin sulfate applied as deposited dose. KRB=Krebs-Ringer buffer (with 0.5 % DMSO). First line represents treatment from 1-24h, second line represents treatment from 24-48h. One-Way ANOVA and Tukey´s multiple comparison test, ns $p>0.12$; ** $p<0.002$; *** $p<0.001$, N = 9-15 of 3-5 independent experiments.

3.3.8.3 Barrier function and viability

As the inhibitor was proven to enlarge TEER values, it was tested, if this effect is maintained with infection or if it is just an artefact on healthy cell lines.

The setup was kept same as described, but the 48h infected model was tested only, since the effects of the inhibitor could be shown more precisely. TEER values were measured thereafter by submerging cells with medium for one further hour as described. Results are shown in figure 3.42.

Infecting cells without treatment led, as before, to baseline TEER value. Yet, the not treated cells showed quite high TEER values. The positive effect of the inhibitor on cells (Figure 3.39) was also measurable when cells were infected. Wells, that received at least one dose with inhibitor, showed a tendency towards higher TEER values. The effect of the inhibitor increasing TEER values is comparable to the uninfected controls in Figure 3.39, which is roughly about the double the TEER value. Again, there is a general effect seen, that TEER values are higher compared to the experiments done before (Chapter 3.3.7.2). This corresponds to the lower CFU numbers found in the previous chapter. With lower CFU numbers, the TEER values have dramatically changed. Even without inhibitor, that further increased TEER values, the combination tobramycin (24h), then KRB (48h) led to a TEER of about 300 $\Omega*cm^2$ (Figure 3.42). In contrast, TEER of the same condition was nearly not measurable in the experiment before (Figure 3.29 B), following the same protocol, only using 100 µL KRB here instead of ALI due to technical reasons. In this experiment, the treatment with tobramycin for 24 and 48h even increased TEER to about 600 $\Omega*cm^2$, compared to roughly 200 $\Omega*cm^2$ in Chapter 3.3.7.2.

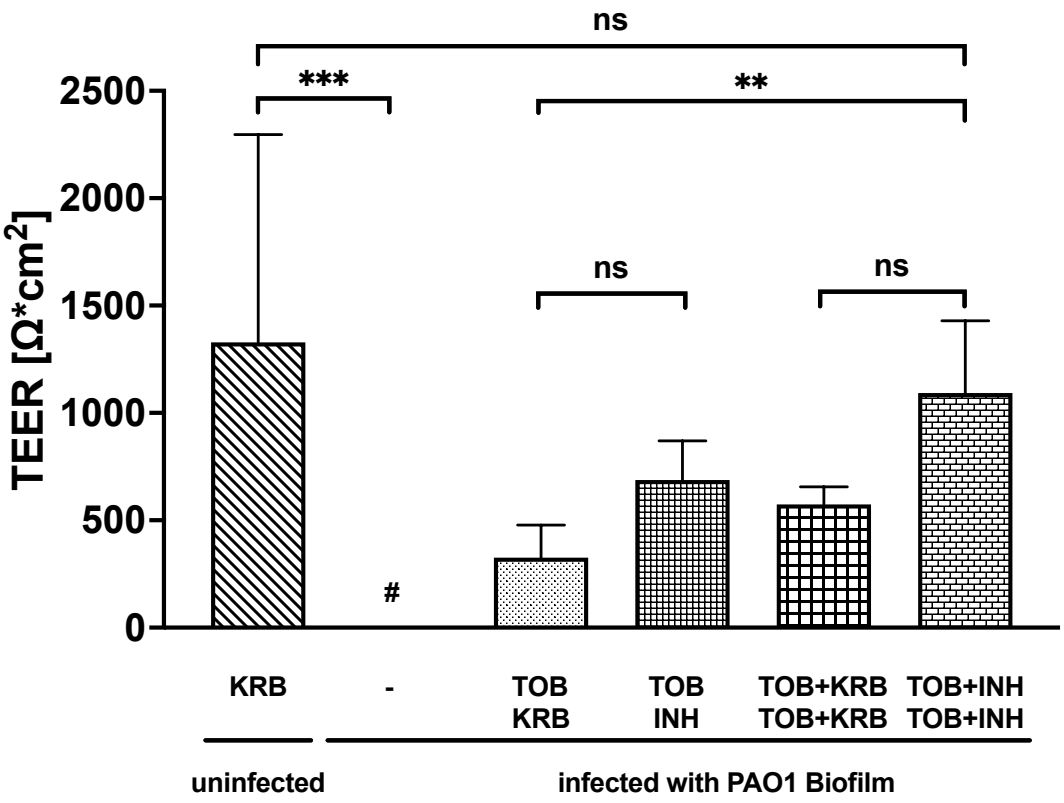

Figure 3.42: Barrier properties measured as TEER of infected model after 48h infection. INH=100 µL inhibitor as described[7]. TOB=Tobramycin sulfate applied as deposited dose. KRB=100µL KRB (supplemented with 0.5% DMSO). First line represents treatment from 1-24h, second line represents treatment from 24-48h. # lysed cells confirmed with light microscope. One-Way ANOVA and Tukey´s multiple comparison test, ns $p>0.12$; ** $p<0.002$; *** $p<0.001$, N = 9-15 of 3-5 independent experiments.

Having a look on the respective viability of cells at the same time, a comparable observation could be made. In contrast to chapter 3.3.7.2, viability values are around 100 % at all conditions (in this case all after 48h), meaning, that only few cells must have been eliminated by the infection (Figure 3.43). Even the combination tobramycin for 24h and KRB for the 48h led to a measurable sample, since bacteria did not overgrow. Therefore, pathogenicity was measurable via LDH, which was not possible before (Figure 3.43). This is all explainable with PAO1 being more eradicated during treatment with tobramycin and probably more prone to treatment, as previously discussed.

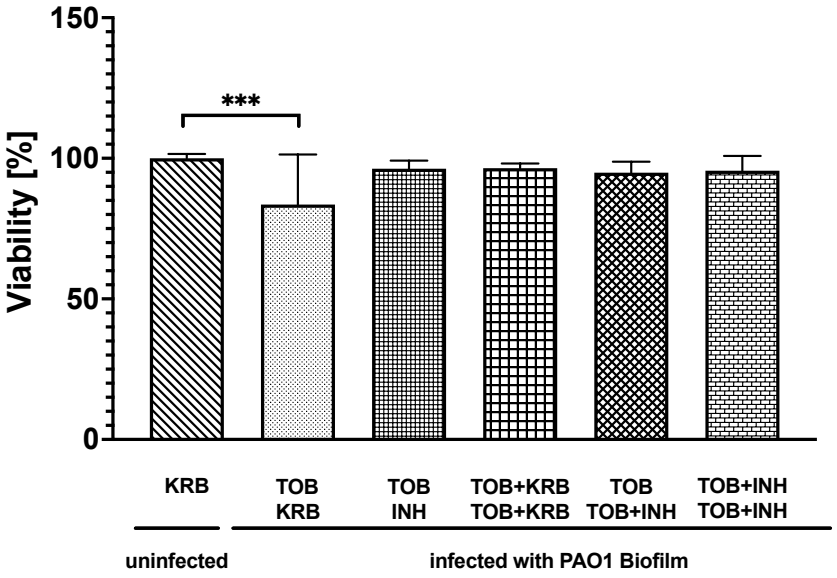

Figure 3.43: Viability of infected CFBE41o- cells after 48h infection. INH=100 µL inhibitor as described[7]. TOB=Tobramycin sulfate applied as deposited dose. KRB=100 µL KRB (supplemented with 0.5% DMSO). Basolateral supernatants were used to calculate LDH release and the viability was calculated by subtracting values from 100% viability. One-Way ANOVA and Tukey´s multiple comparison test, ns $p>0.12$; ** $p<0.002$; *** $p<0.001$, N = 9-15 of 3-5 independent experiments.

3.3.8.4 Analysis of QS molecules after 48 on infected model

Tobramycin has been shown not only to kill bacteria, but also to reduce its virulence in sub-inhibitory concentrations[5,168]. Also, the here described inverse pqsR agonist has the ability to reduce *P. aeruginosa* quorum sensing molecules as PQS and HHQ[7]. These tests have been conducted so far on bacteria without the presence of cells[7,30,189].

The success of treatment on the complete model was measured via CFU reduction and barrier properties mainly. Nevertheless, it would be an advantage to see the effect of tobramycin and novel anti-infectives on the model by quantifying the amount of quorum sensing molecules simultaneously, as partly published by the author of this thesis[4].

Quorum sensing molecules were either assessed using the apical or basolateral supernatant. Using the basolateral medium, even a simultaneous analysis of CFU

(apical side), LDH (using medium of the basolateral side) and QS molecules (rest of basolateral medium) is possible. PQS and HHQ activate the pqsR[7], as explained in the introduction of this thesis. This receptor controls the production of other factors as 2-AA, DHQ and HQNO[189]. 2-AA, for example, induces oxidative stress, apoptosis and has immunomodulatory features[190,191].

Nevertheless, it was not the intention to uncover the exact mechanism of QS molecules, but rather check the presence of aforementioned molecules to have a complete picture of excreted bacterial substances, that are more or less influenced by treatment. Figure 3.44 shows an overview of the amount of all measured molecules after 48h incubation with either no treatment, tobramycin, inhibitor or both, with the combinations as done previously. The 48h timepoint was here decided for, since it offers the possibility to combine treatments and no treatments (as depicted in chapter 3.3.7.2).

It is interesting, that generally higher concentrations of alkylquinolones are found in the basolateral side of the insert, although the infection takes place at the apical part, and less volume was present at the apical side compared to the basolateral (300 vs. 500 µL, after addition of KRB to the end of the experiment). This is probably due to the available nutrition of the media, that serve for better growth conditions in comparison to the apical part with few amounts of KRB present. At both apical and basolateral side, HQNO and PQS are most abundant with up to 30 µM concentration of HQNO in the basolateral side (Figure 3.44). Interestingly, the relative amount of HQNO and PQS is different when measured apically and on the basolateral side. On the apical side, no statistically significant difference between untreated samples can be found ($p>0.99$), whereas on the basolateral side, this difference is very significant ($p<0.001$). To date, no explanation can be found describing this phenomenon and needs further investigation.

Adding treatment, either with or without tobramycin, decreases the concentration of AQs to nearly zero, whereas CFU number is still accessible (compare chapter 3.3.7.2 and 3.3.8.2). Thereby, a much more detailed answer of the state of infection is possible, as it is easier to formulate a yes/no answer on the success of treatment rather

than guessing the threshold of bacteria still present and a simultaneous check of CFU/AQs can be done with novel anti-infectives. This is really important concerning host-pathogen interaction[1,192].

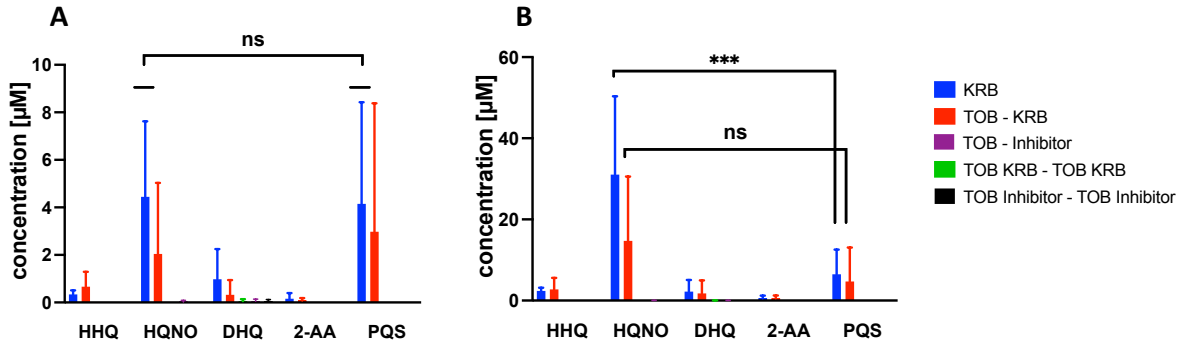

Figure 3.44: Concentration of quorum sensing molecules detected on infected model after 48h. A: Molecules on apical side of Transwell® inserts. B: Molecules on basolateral side, in the medium, values partly published in [4]. "TOB" = Tobramycin sulfate, deposited dose as described, "Inhibitor"= QS inhibitor[7]. Two-Way ANOVA and Tukey´s multiple comparison test, ns $p>0.12$; *** $p<0.001$, N=9 of 3 experiments, "TOB Inhibitor – TOB Inhibitor" N = 6 of 2 independent experiments.

3.3.9 Evaluation of the addition of mucus to the model

3.3.9.1 Human mucus vs. artificial mucus

It has been shown, that the interplay of human cells and bacteria is important to test novel anti-infectives, as well as the ALI conditions. Nonetheless, one last factor was not assessed so far. CFBE41o- does not produce mucus, even though this is a crucial problem of CF patients, as explained in the beginning of this chapter[8]. The thesis of Dr. Jenny Juntke deals with how to solve this problem. It could be shown, that adding human mucus to the cells at ALI conditions, the barrier properties and resilience of cells to infection could be increased[8,9]. This thesis was meant to further develop this idea, albeit the availability of human mucus to produce sterile disks was very limited. Therefore, experiments were conducted first without the addition of mucus, which has been successfully shown so far in this chapter 3.

Nevertheless, the idea of adding external mucus on cells is very interesting and showed some promising results[8,9]. In order to increase the availability of mucus, ideas were made in the group of Claus-Michael Lehr to modify an artificial mucus with poly(acrylic) acid, that was originally invented by Sriramulu et al. and modified by Huck et al.[16,193]. By adding poly(acrylic) acid, viscoelastic properties were improved and come close to human lung mucus[16]. This surrogate was thereafter called “modified artificial sputum medium” (ASM_{mod}). It was proven that ASM_{mod} is a well comparable surrogate for human mucus in terms of permeation of antibiotics and growth of biofilm[194].

It has been shown, that TEER values of CFBE41o- equipped with human mucus differed from their unequipped counterpart, at least in the ALI setup of Dr. Jenny Juntke, not in the work of Dr. Xabier Murgia[8,9,141]. Nevertheless, it was not clear, if this is reproducible by another researcher, and, if there is a comparable effect seen with ASM_{mod}. The hypothesis is, that human mucus provokes higher TEER values than its artificial counterpart, as TEER with mucus has been shown to be about sevenfold higher than without mucus[8,9].

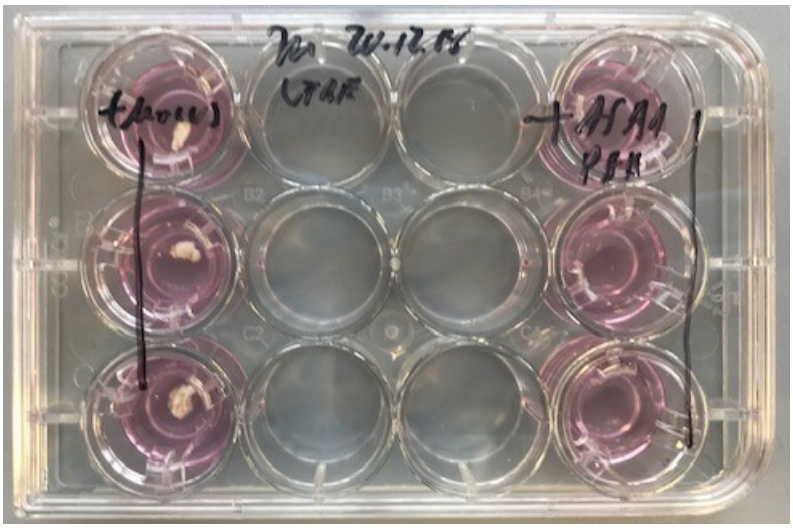

Figure 3.45: Image of the Transwell® inserts that received a human mucus disk (left) and ASM_{mod} (right). The mucus discs were partly not flat and did not cover the whole epithelium, which was technically not possible. Meanwhile, the ASM_{mod} spread quite well over the cell surface. Image was taken before overnight incubation.

Therefore, barrier properties of CFBE41o- cells were measured after the addition of human mucus, ASM_{mod}, medium control and ALI control after overnight incubation (Materials and methods, Figure 3.45 and 3.46). The idea was to simulate the day of infection and to decide for the best alternative.

Without doubts, cells having been incubated with human mucus showed highest TEER values (ca. 1000 Ω*cm^2, SD about 500 Ω*cm^2, Figure 3.46). Interestingly, cells equipped with ASM_{mod} showed significant increase in comparison to ALI culture with about 750 Ω*cm^2. No statistical significance is noted to TEER of cells with human mucus (p=0.55). Addition of a small amount of medium (50 µL) increases the TEER value after overnight incubation, but not as high as with mucus (p=0.04) or ASM_{mod} (ns).

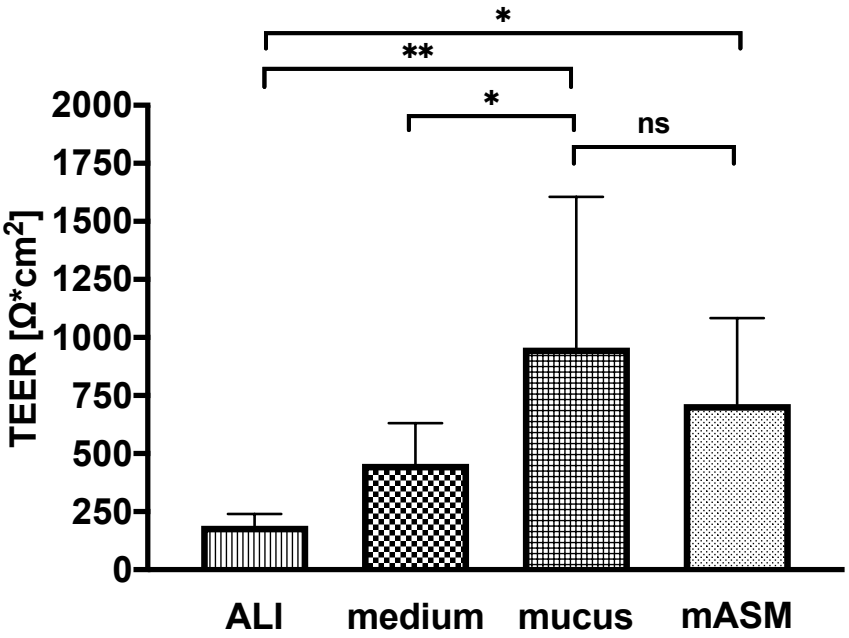

Figure 3.46: Barrier properties of CFBE41o- cells that were incubated over night at ALI, cells at ALI covered with 50 µL medium, cells with human mucus and cells with modified artificial sputum medium (ASM_{mod}). One-Way ANOVA and Tukey´s multiple comparison test, ns p>0.12; * p<0.033; ** p<0.002; *** p<0.001, N = 9 of 3 independent experiments.

This small study reveals, that ASM_{mod} could be indeed a surrogate for mucus in cell-based infection experiments, at least regarding cell barrier integrity, even though it

provokes by tendency smaller TEER values (Figure 3.46). It is of note, that human mucus (chapter 1.1) also contains a strong variating amount of growth factors and hormones, that could be the reason for higher TEER values[15]. The original ASM was not considered a cell medium, but a growth medium for bacteria[193]. Even though it could be a very cell compatible mucus surrogate on Transwell® inserts, particularly due to its defined composition[16].

3.3.9.2 Infection and treatment of the model featuring artificial mucus

After having identified ASM_{mod} as a possible alternative to the limited human mucus, a short experimental study was done to identify, if the mucus conveys a certain resilience to CFBE41o- cells, or if the mucus just serves as a scaffold for growing bacteria.

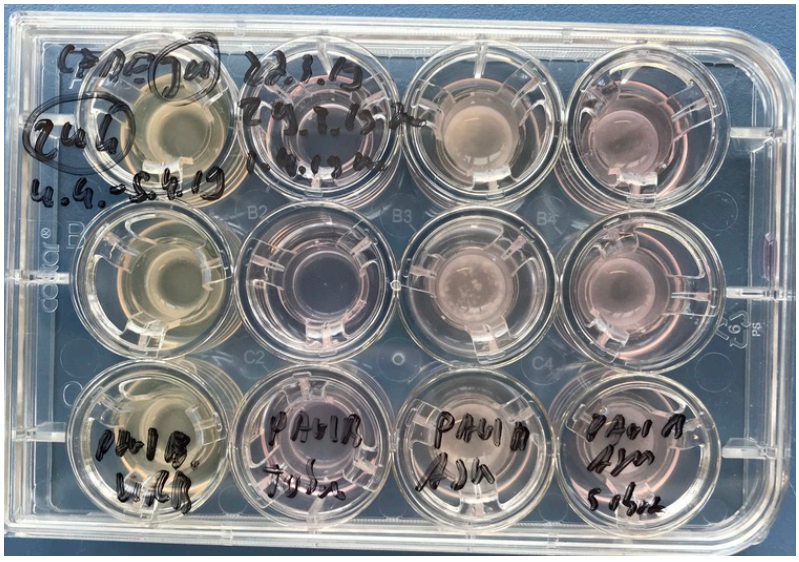

Figure 3.47: Image of PAO1 infected CFBE41o- cells in Transwell® inserts after 24h. From left to right (per column of 3 inserts): Infected cells, infected and with tobramycin treated cells, infected cells with ASM_{mod}, infected cells with ASM_{mod} treated with tobramycin.

Either 200 µL sterile ASM_{mod} was added at day 7 on cells grown at ALI or cells were kept at ALI as described. Pre-grown PAO1 biofilm was added on the ASM_{mod} and liquid

remnants were removed after 1h, but not the whole ASM_{mod} layer, due to technical reasons.

Addition of ASM_{mod} leads to an about 2mm thick layer on the cells, which could be perceived as being not ALI conditions any more. Nevertheless, 200 µL were chosen, because the former protocol of biofilm transfer described 200 µL biofilm suspension, and because the ASM_{mod} needs to be transferred in a volume, that is able to be transferred in a pipette (Figure 3.47). Initial experiments have shown, that the addition of a biofilm suspension of 200 µL in KRB on a 200 µL ASM_{mod} layer on cells diluted the ASM_{mod}, so that the liquid could not be removed anymore and the properties on the artificial mucus might change by dilution. CFU were not detected in this experiment, since the focus was set to the viability of the cells and the reaction to infection, rather the effect of treatment on CFU. Nevertheless, CFU of biofilm inoculum of pure PAO1 biofilm suspension and PAO1 biofilm in ASM_{mod} after 1h was counted and did not differ more than about 1 log (data not shown).

After 4h, viability of all conditions was maintained in a range of about 80-100%, only cells infected at ALI without treatment lost viability to a value of about 40 % as described (Figure 3.48 A). This could lead to the perception, that ASM_{mod} protects cells from the bacteria. After 24h incubation though, infected cells either with and without ASM_{mod} were completely destroyed. Tobramycin treatment saved cells at ALI better than with ASM_{mod} (Figure 3.48 B). Control ASM_{mod} even showed viability values of >100%. This fact cannot be explained so far. Nevertheless, this effect was only seen after 24h, not after 4h, whereas the ASM_{mod} treated cells had higher viability as their ALI counterpart (Figure 3.48 B). The ASM_{mod} might could have served as a certain barrier, delaying direct contact of all bacteria with the epithelial cells. Due to growth of bacteria in the ASM_{mod}, this effect did not last long. Tobramycin treatment also might not have reached the bacteria so well as directly on cells at ALI conditions. These values have to be considered carefully, since only two biological replicates could be done.

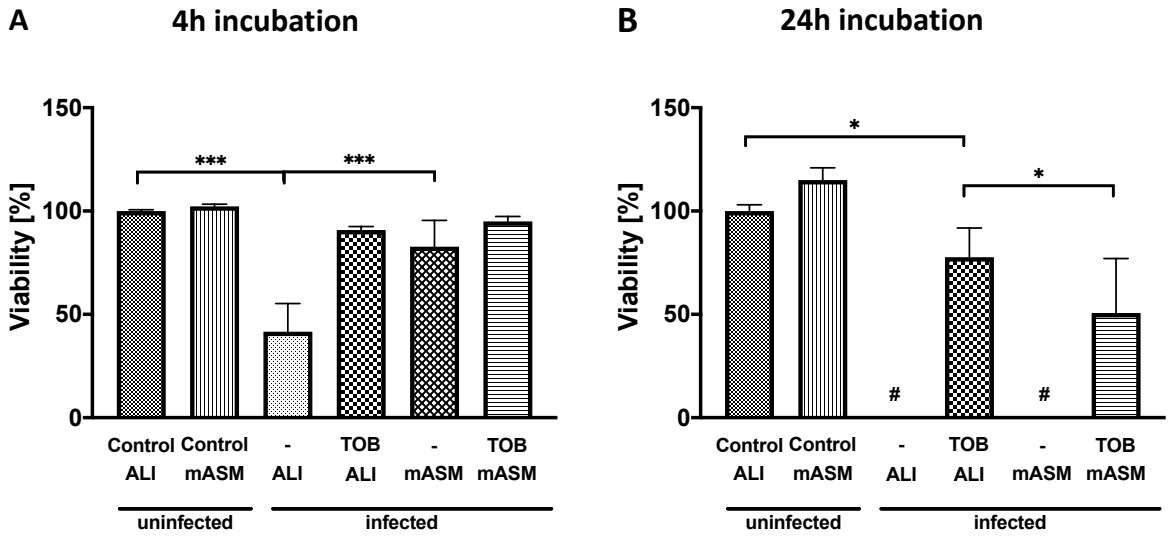

Figure 3.48: Viability of uninfected and infected CFBE41o- cells. LDH release was measured and calculated back to viability. ASM_{mod}: modified artificial sputum medium, TOB: deposited tobramycin dose. # LDH detection could not be done due to overgrowth of bacteria, lysed cells confirmed with light microscope. One-Way ANOVA and Tukey´s multiple comparison test, ns $p>0.12$; * $p<0.033$; ** $p<0.002$; *** $p<0.001$, N = 6 of 2 independent experiments.

TEER values of infected cells and even of cells treated with tobramycin when ASM_{mod} was present completely dropped already after 4h (Figure 3.49 A). As detected in earlier experiments, treatment of cells at ALI results in maintaining TEER values of >300 $\Omega*cm^2$. Interestingly, TEER values of ASM_{mod} control decreased drastically in comparison to the control measured at ALI, that is in this case unexpectedly high (but only two independent experiments were done). Nevertheless, a TEER value of about 500 $\Omega*cm^2$ could be maintained (Figure 3.49 A). This could be explained with a certain adaption time of cells to the not cell physiological mucus medium. After 24h incubation, both controls maintain a TEER of about 500 $\Omega*cm^2$ and tobramycin treated cells show still measurable TEER values, whereas all other samples stayed at a TEER value of about zero.

In contrast to viability, TEER values revealed, that ASM_{mod} did not have a protective role for cells, as TEER values of infected and infected treated cells were lost already after 4h. Nevertheless, TEER values have to be considered carefully concerning the fact, that only two biological replicates could be made.

To summarize, adding artificial mucus to CFBE41o- cells changes the outcome in regard to viability and TEER values after 4 and 24h infection time with and without infection. Likewise, ASM_{mod} might hide bacteria from treatment and can only protect cells from infection for a limited time of about 4h. Therefore, using ASM_{mod} instead of human mucus cannot be recommended, nevertheless, further studies, as CFU detection and a structured search for the best volume of ASM_{mod} on cells and its technique for transfer have to be found to have a final answer on this question.

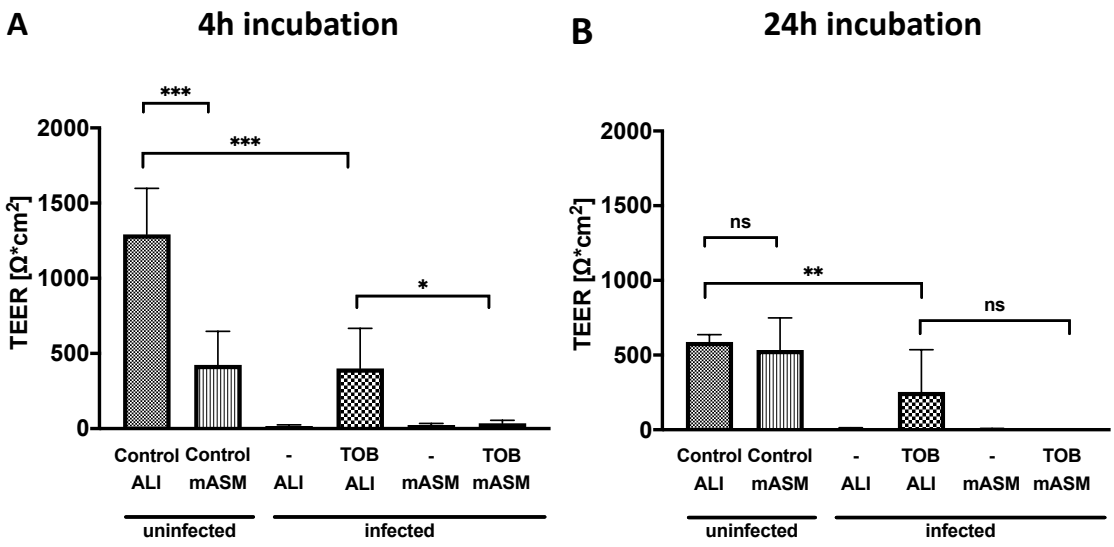

Figure 3.49: Barrier properties of uninfected and infected CFBE41o- cells. ASM_{mod}: modified artificial sputum medium, TOB: deposited tobramycin dose. One-Way ANOVA and Tukey´s multiple comparison test, ns $p>0.12$; * $p<0.033$; ** $p<0.002$; *** $p<0.001$, N = 6 of 2 independent experiments.

3.4 Conclusion

In this chapter, the development of a novel biofilm infected model could be presented, as already partly published[4]. *P. aeruginosa* PAO1, that was selected as most promising model strain, was used to build a 72h plastic-grown biofilm, that was transferred onto CFBE41o- cells. The bacteria were proven to be less susceptible to tobramycin treatment as expected even after transfer, which also serves as indirect proof of biofilm presence. Metabolomic studies further verified this assumption. In order to find the best conditions to model a chronic infected patient *in vitro*, several pre-studies were done to elucidate the effect of ALI conditions and CFBE41o- cells on the outcome of tests, as well as the possible pre-treatment with ciprofloxacin. As a result, ALI conditions were proven to be completely different to submerse, which was expected. It is assumed, that cells have thereby a protective element for bacteria against treatment, which has to be further verified. Ciprofloxacin pre-treatment of biofilm influences it being less virulent, but the effect is only modest.

The goal thereafter was to maintain a chronic infection *in vitro*. As previous studies already uncovered the devastating effect of PAO1 on CFBE41o- cells, only treatment with a high dose of tobramycin could stop the bacteria eradicating mammalian cells. A dose was chosen, that keeps the epithelial cells alive, whereas bacteria are still present directly on cells, so that a chronic infection can be modelled. Interestingly, bacteria could not be eradicated even with several doses of tobramycin given every 24h. In contrast, bacteria rather increased over a period of 72h with treatment, from about 2 to about 4 $\log_{10}$ CFU/mL. While viability is still satisfying after 72h, TEER values have been decreasing to values under 300 $\Omega*cm^2$ after 72h. TEER values are maintained until about 48h after infection, which was further thought to be supported by transport experiments, that unfortunately could not finally verify barrier integrity due to unsolved technical questions. Imaging proved cells and bacteria being for 72h in co-culture, while adherence protein E-cadherin was maintained in infected and treated cells until 72h, serving as an indirect proof of healthy epithelial cells.

Finally, a novel quorum sensing inhibitor was added in order to prove the model´s predictability. Unfortunately, the effects of the combination with tobramycin could not be reproduced with the model, since no statistically significant effect could be shown. Nevertheless, it could be shown, that the inhibitor had a positive influence on TEER values, as well as to exert a tendency towards lower CFU numbers in combination with tobramycin (2 vs. 1 $\log_{10}$ CFU/mL). Finally, the principal idea of the first study by Dr. Jenny Junkte was revisited[8,9]. Adding human mucus on CFBE41o- cells rises TEER values, but with no significant difference to adding artificial mucus, which paves the way for future applications. Nevertheless, artificial mucus can save epithelial cells at most for some hours, but reducing TEER completely as soon as an infection takes place. Therefore, addition of artificial mucus is rated as not to be an alternative to ALI conditions or the addition of human mucus, but more experiments have to be done.

4 Summary and Outlook

The present doctoral thesis consists of 3 chapters, parts of which also have been already published as research papers and book chapters[3,4,10,11]. Whereas chapter 1 is an introductory review that summarizes the disease background and the possibilities to model such diseases *in vitro*, the actual results forthcoming from this thesis are described in chapter 2 and 3. The present scientific work consists of 2 chapters, that are combined to build a realistic and currently lacking *in vitro* model of the infected bronchial epithelium. In the first chapter (chapter 2 of this thesis), the basis of the development of a realistic *in vitro* model is presented, that is a novel device facilitating the deposition of all kind of excipients onto cell culture inserts at the ALI conditions. Initially designed by members of the DDEL group at HIPS, it has been used by Graef et al. and Juntke et al., before it was completely described and analyzed as published by the author of this thesis[8–10,124]. This device is especially suited for S2 laboratory conditions. It is cost-efficient and the production of many devices realize the use of several pre-cleaned, sanitized columns, that facilitate the experiments under laminar flow conditions. The device allows reproducible and precise dosing of excipients and formulations onto cell culture inserts while being non-toxic for epithelial cells, that is premise for testing efficiency of excipients[10].

The second chapter (chapter 3 of this thesis) presents the idea and development of a cell based, *P. aeruginosa* infected model at ALI conditions, allowing to realistically model a chronic bacterial biofilm infected patient, that was partly published by the author of this thesis[4]. The test system receives anti-infective treatment as in clinics[21,22]. The lung and bacteria in the biofilm mode of growth are thereby the major hallmark of design. By transferring a whole biofilm instead of planktonic bacteria, major differences in their susceptibility and metabolomic configuration were detected. Whereas pre-treatment with sub-inhibitory concentrations of ciprofloxacin could decrease virulence of the biofilm, the effect was not strong enough to model a chronic infected epithelium. The deposition of a metered dose of tobramycin was needed to permit the viability and measurement of barrier properties of epithelial cells after 4

and 24h. Thereby, it could not only be shown, that biofilm bacteria are different to planktonic bacteria, but also, that the culture conditions of cells play an important role when infected with bacteria. The results of *in vitro* testing of tobramycin were significantly different when done at the submerse culture conditions, that did not allow a chronic model to be built. Nevertheless, ALI infected and treated cells could even be treated consecutively every 24h until 72h with doses of tobramycin and thereby kept their viability. Whereas TEER values dropped in the course of time, the abundance of E-cadherin, an important adhesion protein, could be maintained until 72h post-infection, underlining the efficiency of tobramycin. Transport studies could basically reveal tightness of infected and treated barrier 48h post-infection (except some technical challenges, that have to be taken care of in future), which is principally confirmed by a recent study with the same model employed[184]. In order to further prolong the time of chronic infection, treatment with a novel anti-infective QS Inhibitor[7] was done. Positive trends of CFU reduction and a drastically increased TEER value could be shown, as well as efficient reduction of QS molecules measured on the model, explaining and confirming CFU reduction on the well inserts. Even so, the inhibitor could not be proven to act significantly more efficient on the model, as described on plastic[7]. Last but not least, the influence of an alternative to human mucus, that has been shown to be beneficial for viability of human cells[8,9], was tested in order to have positive effects for epithelial cells as an alternative to this precious source. Unfortunately, ASM_{mod} was not able to protect cells from infection, nevertheless, it could be shown, that it increases TEER values in the magnitude of original human mucus, leaving perspectives for further tests.

All in all, a valid and reproducible model of the chronic infected (CF) lung is presented, that could be pathbreaking for testing novel anti-infectives at the ALI conditions. Future scientists could prove the reliability of the cell line CFBE41o- at long term infection of 72h and contrast it to Calu-3 cells or other CF relevant cell lines, as CuFi[195]. While the model in is present state has already successfully been tested with free tobramycin, a promising study showing efficacy of novel anti-infective formulations on this model was already done[184]. The next step could be the testing of sustained release

formulations, that keep the bacterial load as low as possible enabling mammalian cells to survive for longer than 24h, facilitating anti-infective treatment for patients. The use of attenuated bacterial strains thereby could increase the infection time, as shortly outlined in chapter 3.3.1.3. Last but not least, a direct comparison of testing results of antibiotics in mice and the present model could show, how far this system could even replace animal experiments in future.

5 References

1. Bhagirath, A. Y. *et al.* Cystic fibrosis lung environment and Pseudomonas aeruginosa infection. *BMC Pulmonary Medicine* **16**, 1–22 (2016).
2. Maselli, D. J., Keyt, H. & Restrepo, M. I. Inhaled antibiotic therapy in chronic respiratory diseases. *International Journal of Molecular Sciences* **18**, (2017).
3. Carius, P., Horstmann, J. C., de Souza Carvalho-Wodarz, C. & Lehr, C.-M. Disease Models: Lung Models for Testing Drugs Against Inflammation and Infection. in *Handbook of Experimental Pharmacology* (Springer, Berlin, Heidelberg, 2020).
4. Horstmann, J. C. *et al.* Transferring Microclusters of P. aeruginosa Biofilms to the Air–Liquid Interface of Bronchial Epithelial Cells for Repeated Deposition of Aerosolized Tobramycin. *ACS Infectious Diseases* **8**, 137–149 (2022).
5. Anderson, G. G., Moreau-Marquis, S., Stanton, B. A. & O'Toole, G. A. In vitro analysis of tobramycin-treated Pseudomonas aeruginosa biofilms on cystic fibrosis-derived airway epithelial cells. *Infection and Immunity* **76**, 1423–1433 (2008).
6. Cystic Fibrosis Foundation Bethesda USA. *2018 Patient Registry Annual Data Report*. (2019).
7. Schütz, C. *et al.* A New PqsR Inverse Agonist Potentiates Tobramycin Efficacy to Eradicate Pseudomonas aeruginosa Biofilms. *Advanced Science* **8**, (2021).
8. Juntke, J. A novel co-culture model of human bronchial epithelial cells and Pseudomonas aeruginosa biofilms to mimic chronic lung infections in cystic fibrosis. (Saarland University, 2019).
9. Juntke, J. *et al.* Testing of aerosolized ciprofloxacin nanocarriers on cystic fibrosis airway cells infected with P. aeruginosa biofilms. *Drug Delivery and Translational Research* **11**, 1752–1765 (2021).
10. Horstmann, J. C. *et al.* A Custom-Made Device for Reproducibly Depositing Pre-metered Doses of Nebulized Drugs on Pulmonary Cells in vitro. *Frontiers in Bioengineering and Biotechnology* **9**, 1–12 (2021).
11. Schneider-Daum, N., Carius, P., Horstmann, J.C., Lehr, C. M. Reconstituted 2D Cell and Tissue Models. in *Pharmaceutical Inhalation Aerosol Technology* (eds. Hickey, A. J. & da Rocha, S. R. P.) 25 (CRC Press, 2019).
12. Lavelle, G. M., White, M. M., Browne, N., McElvaney, N. G. & Reeves, E. P. Animal Models of Cystic Fibrosis Pathology: Phenotypic Parallels and Divergences. *BioMed Research International* 1–14 (2016).
13. Saint-Criq, V. & Gray, M. A. Role of CFTR in epithelial physiology. *Cellular and Molecular Life Sciences* **74**, 93–115 (2017).
14. Button, B. *et al.* A periciliary brush promotes the lung health by separating the mucus layer from airway epithelia. *Science* **337**, 937–941 (2012).
15. Bansil, R. & Turner, B. S. Mucin structure, aggregation, physiological functions and biomedical applications. *Current Opinion in Colloid and Interface Science* **11**, 164–170 (2006).
16. Huck, B. C. *et al.* Macro- And Microrheological Properties of Mucus Surrogates in Comparison to Native Intestinal and Pulmonary Mucus. *Biomacromolecules* **20**, 3504–3512 (2019).
17. Sheppard, D. N. & Davis, A. P. Pore-forming small molecules offer a promising way to tackle cystic fibrosis. *Nature* **567**, 315–317 (2019).

18. Torres, A. *et al.* International ERS/ESICM/ESCMID/ALAT guidelines for the management of hospital-acquired pneumonia and ventilator-associated pneumonia. *European Respiratory Journal* **50**, (2017).
19. Prina, E., Ranzani, O. T. & Torres, A. Community-acquired pneumonia. *The Lancet* **386**, 1097–1108 (2015).
20. Knapp, S., Schultz, M. J. & Van Der Poll, T. Pneumonia models and innate immunity to respiratory bacterial pathogens. *Shock* **24**, 12–18 (2005).
21. Høiby, N., Ciofu, O. & Bjarnsholt, T. Pseudomonas aeruginosa biofilms in cystic fibrosis. *Future Microbiology* **5**, 1663–1674 (2010).
22. Bjarnsholt, T. *et al.* The in vivo biofilm. *Trends in Microbiology* **21**, 466–474 (2013).
23. Stoodley, P., Sauer, K., Davies, D. G. & Costerton, J. W. Biofilms as complex differentiated communities. *Annual Review of Microbiology* **56**, 187–209 (2002).
24. Alhede, M., Bjarnsholt, T., Givskov, M. & Alhede, M. Pseudomonas aeruginosa Biofilms. in *Advances in Applied Microbiology* vol. 86 1–40 (Elsevier Inc., 2014).
25. Van Duuren, J. B. J. H. *et al.* Use of Single-Frequency Impedance Spectroscopy to Characterize the Growth Dynamics of Biofilm Formation in Pseudomonas aeruginosa. *Scientific Reports* **7**, 1–11 (2017).
26. Barraud, N., Buson, A., Jarolimek, W. & Rice, S. A. Mannitol enhances antibiotic sensitivity of persister bacteria in Pseudomonas aeruginosa biofilms. *PLoS ONE* **8**, 1–13 (2013).
27. Macià, M. D., Rojo-Molinero, E. & Oliver, A. Antimicrobial susceptibility testing in biofilm-growing bacteria. *Clinical Microbiology and Infection* **20**, 981–990 (2014).
28. Ciofu, O. & Tolker-Nielsen, T. Tolerance and resistance of Pseudomonas aeruginosa biofilms to antimicrobial agents - how P. aeruginosa can escape antibiotics. *Frontiers in Microbiology* **10**, (2019).
29. Johnson, P. A. Novel understandings of host cell mechanisms involved in chronic lung infection: Pseudomonas aeruginosa in the cystic fibrotic lung. *Journal of Infection and Public Health* **12**, 242–246 (2019).
30. Thomann, A., De Mello Martins, A. G. G., Brengel, C., Empting, M. & Hartmann, R. W. Application of Dual Inhibition Concept within Looped Autoregulatory Systems toward Antivirulence Agents against Pseudomonas aeruginosa Infections. *ACS Chemical Biology* **11**, 1279–1286 (2016).
31. Ho, D. K. *et al.* Squalenyl Hydrogen Sulfate Nanoparticles for Simultaneous Delivery of Tobramycin and an Alkylquinolone Quorum Sensing Inhibitor Enable the Eradication of P. aeruginosa Biofilm Infections. *Angewandte Chemie - International Edition* **59**, 10292–10296 (2020).
32. Hall, C. W. & Mah, T. F. Molecular mechanisms of biofilm-based antibiotic resistance and tolerance in pathogenic bacteria. *FEMS Microbiology Reviews* **41**, 276–301 (2017).
33. Malhotra, S., Hayes, D. & Wozniak, D. J. Cystic Fibrosis and Pseudomonas aeruginosa : the Host-Microbe Interface. *Clinical Microbiology Reviews* **32**, 814–817 (2019).
34. Billings, N. *et al.* The Extracellular Matrix Component Psl Provides Fast-Acting Antibiotic Defense in Pseudomonas aeruginosa Biofilms. *PLoS Pathogens* **9**, (2013).
35. Pang, Z., Raudonis, R., Glick, B. R., Lin, T. J. & Cheng, Z. Antibiotic resistance in Pseudomonas aeruginosa: mechanisms and alternative therapeutic strategies. *Biotechnology Advances* **37**, 177–192 (2019).
36. Airway clearance techniques CFF (access date 2022-02-21). https://www.cff.org/managing-cf/airway-clearance.
37. Wilson, L. M., Morrison, L. & Robinson, K. A. Airway clearance techniques for cystic

fibrosis: An overview of Cochrane systematic reviews. *Cochrane Database of Systematic Reviews* **1**, (2019).
38. Velino, C. *et al.* Nanomedicine Approaches for the Pulmonary Treatment of Cystic Fibrosis. *Frontiers in Bioengineering and Biotechnology* **7**, (2019).
39. Brown, S. D., White, R. & Tobin, P. Keep them breathing: Cystic fibrosis pathophysiology, diagnosis, and treatment. *Journal of the American Academy of Physician Assistants* **30**, 23–27 (2017).
40. Veit, G. *et al.* Allosteric folding correction of F508del and rare CFTR mutants by elexacaftor-tezacaftor-ivacaftor (Trikafta) combination. *JCI Insight* **5**, 1–14 (2020).
41. Elborn, J. S. Cystic fibrosis. *The Lancet* **388**, 2519–2531 (2016).
42. Quon, B. S., Goss, C. H. & Ramsey, B. W. Inhaled antibiotics for lower airway infections. *Annals of the American Thoracic Society* **11**, 425–434 (2014).
43. Ho, D. K. *et al.* Challenges and strategies in drug delivery systems for treatment of pulmonary infections. *European Journal of Pharmaceutics and Biopharmaceutics* **144**, 110–124 (2019).
44. McKinzie, C. J. *et al.* Off-label use of intravenous antimicrobials for inhalation in patients with cystic fibrosis. *Pediatric Pulmonology* **54**, S27–S45 (2019).
45. Schütz, C. & Empting, M. Targeting the Pseudomonas quinolone signal quorum sensing system for the discovery of novel anti-infective pathoblockers. *Beilstein Journal of Organic Chemistry* **14**, 2627–2645 (2018).
46. Sommer, R. *et al.* Glycomimetic, Orally Bioavailable LecB Inhibitors Block Biofilm Formation of Pseudomonas aeruginosa. *Journal of the American Chemical Society* **140**, 2537–2545 (2018).
47. Wagner, S. *et al.* Novel Strategies for the Treatment of Pseudomonas aeruginosa Infections. *Journal of Medicinal Chemistry* **59**, 5929–5969 (2016).
48. Skariyachan, S., Sridhar, V. S., Packirisamy, S., Kumargowda, S. T. & Challapilli, S. B. Recent perspectives on the molecular basis of biofilm formation by Pseudomonas aeruginosa and approaches for treatment and biofilm dispersal. *Folia Microbiologica* **63**, 413–432 (2018).
49. Hoffmann, N. *et al.* Novel Mouse Model of Chronic Pseudomonas aeruginosa Lung Infection Mimicking Cystic Fibrosis. *Infection and Immunity* **73**, 5290–5290 (2005).
50. Van Heeckeren, A. M. & Schluchter, M. D. Murine models of chronic Pseudomonas aeruginosa lung infection. *Laboratory Animals* **36**, 291–312 (2002).
51. Semaniakou, A., Croll, R. P. & Chappe, V. Animal models in the pathophysiology of cystic fibrosis. *Frontiers in Pharmacology* **9**, 1–16 (2019).
52. Movia, D. & Prina-Mello, A. Preclinical development of orally inhaled drugs (Oids)—are animal models predictive or shall we move towards in vitro non-animal models? *Animals* **10**, 1–16 (2020).
53. Leist, M. & Hartung, T. Inflammatory findings on species extrapolations: Humans are definitely no 70-kg mice. *Archives of Toxicology* **87**, 563–567 (2013).
54. Tannenbaum, J. & Bennett, B. T. Russell and Burch's 3Rs then and now: The need for clarity in definition and purpose. *Journal of the American Association for Laboratory Animal Science* **54**, 120–132 (2015).
55. Castellani, S., Di Gioia, S., di Toma, L. & Conese, M. Human cellular models for the investigation of lung inflammation and mucus production in cystic fibrosis. *Analytical Cellular Pathology* **2018**, (2018).
56. Pulskamp, K., Diabaté, S. & Krug, H. F. Carbon nanotubes show no sign of acute toxicity but induce intracellular reactive oxygen species in dependence on

contaminants. *Toxicology Letters* **168**, 58–74 (2007).
57. Metz, J. K. *et al.* Safety assessment of excipients (SAFE) for orally inhaled drug products. *Altex* **37**, 275–286 (2020).
58. Rothen-Rutishauser, B., Mühlfeld, C., Blank, F., Musso, C. & Gehr, P. Translocation of particles and inflammatory responses after exposure to fine particles and nanoparticles in an epithelial airway model. *Particle and Fibre Toxicology* **4**, 1–9 (2007).
59. Darquenne, C. Aerosol deposition in health and disease. *Journal of Aerosol Medicine and Pulmonary Drug Delivery* **25**, 140–147 (2012).
60. Bastacky, J. *et al.* Alveolar lining layer is thin and continuous: Low-temperature scanning electron microscopy of rat lung. *Journal of Applied Physiology* **79**, 1615–1628 (1995).
61. Brandenberger, C. *et al.* Effects and uptake of gold nanoparticles deposited at the air-liquid interface of a human epithelial airway model. *Toxicology and Applied Pharmacology* **242**, 56–65 (2010).
62. Paur, H. R. *et al.* In-vitro cell exposure studies for the assessment of nanoparticle toxicity in the lung-A dialog between aerosol science and biology. *Journal of Aerosol Science* **42**, 668–692 (2011).
63. Upadhyay, S. & Palmberg, L. Air-liquid interface: Relevant in vitro models for investigating air pollutant-induced pulmonary toxicity. *Toxicological Sciences* **164**, 21–30 (2018).
64. Bur, M., Huwer, H., Muys, L. & Lehr, C.-M. Drug Transport Across Pulmonary Epithelial Cell Monolayers. *Journal of Aerosol Medicine and Pulmonary Drug Delivery* **23**, 119–127 (2010).
65. Loret, T. *et al.* Air-liquid interface exposure to aerosols of poorly soluble nanomaterials induces different biological activation levels compared to exposure to suspensions. *Particle and Fibre Toxicology* **13**, (2016).
66. Lenz, A. G. *et al.* Efficient bioactive delivery of aerosolized drugs to human pulmonary epithelial cells cultured in air-liquid interface conditions. *American Journal of Respiratory Cell and Molecular Biology* **51**, 526–535 (2014).
67. Blank, F., Rothen-Rutishauser, B. M., Schurch, S. & Gehr, P. An optimized in vitro model of the respiratory tract wall to study particle cell interactions. **19**, 392–405 (2006).
68. PennCentury® (access date 2022-01-30). https://penncentury.com.
69. Meindl, C. *et al.* Permeation of therapeutic drugs in different formulations across the airway epithelium in vitro. *PLoS ONE* **10**, 1–19 (2015).
70. Hickey, A. J. Controlled delivery of inhaled therapeutic agents. *Journal of Controlled Release* **190**, 182–188 (2014).
71. Bur, M., Rothen-Rutishauser, B., Huwer, H. & Lehr, C. M. A novel cell compatible impingement system to study in vitro drug absorption from dry powder aerosol formulations. *European Journal of Pharmaceutics and Biopharmaceutics* **72**, 350–357 (2009).
72. Grainger, C. I., Greenwell, L. L., Martin, G. P. & Forbes, B. The permeability of large molecular weight solutes following particle delivery to air-interfaced cells that model the respiratory mucosa. *European Journal of Pharmaceutics and Biopharmaceutics* **71**, 318–324 (2009).
73. Haghi, M., Traini, D., Bebawy, M. & Young, P. M. Deposition, diffusion and transport mechanism of dry powder microparticulate salbutamol, at the respiratory epithelia.

Molecular Pharmaceutics **9**, 1717–1726 (2012).
74. Ong, H. X. *et al.* Is the cellular uptake of respiratory aerosols delivered from different devices equivalent? *European Journal of Pharmaceutics and Biopharmaceutics* **93**, 320–327 (2015).
75. Cooney, D. J., Kazantseva, M. & Hickey, A. J. Development of a size-dependent aerosol deposition model utilising human airway epithelial cells for evaluating aerosol drug delivery. *ATLA Alternatives to Laboratory Animals* **32**, 581–590 (2004).
76. Jeannet, N. *et al.* Acute toxicity of silver and carbon nanoaerosols to normal and cystic fibrosis human bronchial epithelial cells. *Nanotoxicology* **10**, 279–291 (2016).
77. Frijns, E. *et al.* A Novel Exposure System Termed NAVETTA for in Vitro Laminar Flow Electrodeposition of Nanoaerosol and Evaluation of Immune Effects in Human Lung Reporter Cells. *Environmental Science and Technology* **51**, 5259–5269 (2017).
78. Yu, Z., Jang, M., Sabo-Attwood, T., Robinson, S. E. & Jiang, H. Prediction of delivery of organic aerosols onto air-liquid interface cells in vitro using an electrostatic precipitator. *Toxicology in Vitro* **42**, 319–328 (2017).
79. Aufderheide, M. & Mohr, U. CULTEX - An alternative technique for cultivation and exposure of cells of the respiratory tract to airborne pollutants at the air/liquid interface. *Experimental and Toxicologic Pathology* **52**, 265–270 (2000).
80. Aufderheide, M. & Mohr, U. CULTEX - A new system and technique for the cultivation and exposure of cells at the air/liquid interface. *Experimental and Toxicologic Pathology* **51**, 489–490 (1999).
81. Aufderheide, M., Ritter, D., Knebel, J. W. & Scherer, G. A method for in vitro analysis of the biological activity of complex mixtures such as sidestream cigarette smoke. *Experimental and Toxicologic Pathology* **53**, 141–152 (2001).
82. Ritter, D., Knebel, J. W. & Aufderheide, M. In vitro exposure of isolated cells to native gaseous compounds - Development and validation of an optimized system for human lung cells. *Experimental and Toxicologic Pathology* **53**, 373–386 (2001).
83. Knebel, J. W., Ritter, D. & Aufderheide, M. Exposure of human lung cells to native diesel motor exhaust - Development of an optimized in vitro test strategy. *Toxicology in Vitro* **16**, 185–192 (2002).
84. Aufderheide, M., Heller, W. D., Krischenowski, O., Möhle, N. & Hochrainer, D. Improvement of the CULTEX® exposure technology by radial distribution of the test aerosol. *Experimental and Toxicologic Pathology* **69**, 359–365 (2017).
85. Aufderheide, M. & Emura, M. Phenotypical changes in a differentiating immortalized bronchial epithelial cell line after exposure to mainstream cigarette smoke and e-cigarette vapor. *Experimental and Toxicologic Pathology* **69**, 393–401 (2017).
86. Lenz, A. G. *et al.* A dose-controlled system for air-liquid interface cell exposure and application to zinc oxide nanoparticles. *Particle and Fibre Toxicology* **6**, 1–17 (2009).
87. VITROCELL® Cloud Systems (access date 2022-01-30). https://www.vitrocell.com/inhalation-toxicology/exposure-systems/vitrocell-cloud-system.
88. Chortarea, S. *et al.* Human Asthmatic Bronchial Cells Are More Susceptible to Subchronic Repeated Exposures of Aerosolized Carbon Nanotubes at Occupationally Relevant Doses Than Healthy Cells. *ACS Nano* **11**, 7615–7625 (2017).
89. He, R. W. *et al.* Comparative toxicity of ultrafine particles around a major airport in human bronchial epithelial (Calu-3) cell model at the air–liquid interface. *Toxicology in Vitro* **68**, 104950 (2020).
90. Röhm, M. *et al.* A comprehensive screening platform for aerosolizable protein

formulations for intranasal and pulmonary drug delivery. *International Journal of Pharmaceutics* **532**, 537–546 (2017).
91. D'Angelo, I. *et al.* Hybrid lipid/polymer nanoparticles for pulmonary delivery of siRNA: Development and fate upon in vitro deposition on the human epithelial airway barrier. *Journal of Aerosol Medicine and Pulmonary Drug Delivery* **31**, 170–181 (2018).
92. Cei, D. *et al.* Development of a dynamic in vitro stretch model of the alveolar interface with aerosol delivery. *Biotechnology and Bioengineering* **118**, 690–702 (2021).
93. Hein, S. *et al.* The Pharmaceutical Aerosol Deposition Device on Cell Cultures (PADDOCC) in vitro system: Design and experimental protocol. *ATLA Alternatives to Laboratory Animals* **38**, 285–295 (2010).
94. Hein, S., Bur, M., Schaefer, U. F. & Lehr, C. M. A new Pharmaceutical Aerosol Deposition Device on Cell Cultures (PADDOCC) to evaluate pulmonary drug absorption for metered dose dry powder formulations. *European Journal of Pharmaceutics and Biopharmaceutics* **77**, 132–138 (2011).
95. Hittinger, M. *et al.* Autologous co-culture of primary human alveolar macrophages and epithelial cells for investigating aerosol medicines. Part I: Model Characterisation. *ATLA Alternatives to Laboratory Animals* **44**, 337–347 (2016).
96. Hittinger, M. *et al.* Autologous Co-culture of Primary Human Alveolar Macrophages and Epithelial Cells for Investigating Aerosol Medicines. Part II: Evaluation of IL-10-loaded Microparticles for the Treatment of Lung Inflammation. *ATLA Alternatives to Laboratory Animals* **4**, 349–360 (2016).
97. Dimer, F., De Souza Carvalho-Wodarz, C., Haupenthal, J., Hartmann, R. & Lehr, C. M. Inhalable Clarithromycin Microparticles for Treatment of Respiratory Infections. *Pharmaceutical Research* **32**, 3850–3861 (2015).
98. Hittinger M Siebenbürger L, Zäh K, Gress A, Guenther S, Wiegand B, Boerger C, Berger M, Krebs T, Groß H, Lehr C., B. S. Proof of Concept of the VITROCELL Dry Powder Chamber: A New In Vitro Test System for the Controlled Deposition of Aerosol Formulations. *RDD Europe 2017* **2**, 283–288 (2017).
99. Fiegel, J., Ehrhardt, C., Schaefer, U. F., Lehr, C. M. & Hanes, J. Large porous particle impingement on lung epithelial cell monolayers - Toward improved particle characterization in the lung. *Pharmaceutical Research* **20**, 788–796 (2003).
100. Neilson, L. *et al.* Development of an in vitro cytotoxicity model for aerosol exposure using 3D reconstructed human airway tissue; application for assessment of e-cigarette aerosol. *Toxicology in Vitro* **29**, 1952–1962 (2015).
101. Fröhlich, E. *et al.* Comparison of two in vitro systems to assess cellular effects of nanoparticles-containing aerosols. *Toxicology in vitro : an international journal published in association with BIBRA* **27**, 409–417 (2013).
102. Vitrocell® Powder Chamber (access date 2022-01-30). https://www.vitrocell.com/inhalation-toxicology/exposure-systems/vitrocell-powder-chamber.
103. Ceri, H. *et al.* The MBEC assay system: Multiple equivalent biofilms for antibiotic and biocide susceptibility testing. *Methods in Enzymology* **337**, 377–385 (2001).
104. Conlon, B. P. *et al.* Activated ClpP kills persisters and eradicates a chronic biofilm infection. *Nature* **503**, 365–370 (2013).
105. Ceri, H. *et al.* The Calgary Biofilm Device: New technology for rapid determination of antibiotic susceptibilities of bacterial biofilms. *Journal of Clinical Microbiology* **37**, 1771–1776 (1999).
106. Harrison, J. J. *et al.* The use of microscopy and three-dimensional visualization to

evaluate the structure of microbial biofilms cultivated in the Calgary biofilm device. *Biological Procedures Online* **8**, 194–213 (2006).
107. Chen, X., Thomsen, T. R., Winkler, H. & Xu, Y. Influence of biofilm growth age, media, antibiotic concentration and exposure time on Staphylococcus aureus and Pseudomonas aeruginosa biofilm removal in vitro. *BMC Microbiology* **20**, 264 (2020).
108. Forbes, B. *et al.* In Vitro Testing for Orally Inhaled Products: Developments in Science-Based Regulatory Approaches. *AAPS Journal* **17**, 837–852 (2015).
109. Loo, C. Y. *et al.* Sweetening Inhaled Antibiotic Treatment for Eradication of Chronic Respiratory Biofilm Infection. *Pharmaceutical Research* **35**, (2018).
110. Müller, L. *et al.* Human airway mucus alters susceptibility of Pseudomonas aeruginosa biofilms to tobramycin, but not colistin. *Journal of Antimicrobial Chemotherapy* **73**, 2762–2769 (2018).
111. Wheeler, K. M. *et al.* Mucin glycans attenuate the virulence of Pseudomonas aeruginosa in infection. *Nature Microbiology* **4**, 2146–2154 (2019).
112. Rodríguez-Sevilla, G. *et al.* Influence of three-dimensional lung epithelial cells and interspecies interactions on antibiotic efficacy against Mycobacterium abscessus and Pseudomonas aeruginosa. *Pathogens and Disease* **76**, 1–8 (2018).
113. Bowler, L. L., Ball, T. B. & Saward, L. L. A novel in vitro co-culture system allows the concurrent analysis of mature biofilm and planktonic bacteria with human lung epithelia. *Journal of Microbiological Methods* **101**, 49–55 (2014).
114. Montefusco-Pereira, C. V. *et al.* Decoding (patho-)physiology of the lung by advanced in vitro models for developing novel anti-infectives therapies. *Drug Discovery Today* **26**, 148–163 (2021).
115. Moreau-Marquis, S. *et al.* The ΔF508-CFTR mutation results in increased biofilm formation by Pseudomonas aeruginosa by increasing iron availability. *American Journal of Physiology - Lung Cellular and Molecular Physiology* **295**, 25–37 (2008).
116. Moreau-Marquis, S., Redelman, C. V., Stanton, B. A. & Anderson, G. G. Co-culture Models of Pseudomonas aeruginosa Biofilms Grown on Live Human Airway Cells. *Journal of Visualized Experiments* 2–5 (2010).
117. Moreau-Marquis, S., Coutermarsh, B. & Stanton, B. A. Combination of hypothiocyanite and lactoferrin (ALX-109) enhances the ability of tobramycin and aztreonam to eliminate Pseudomonas aeruginosa biofilms growing on cystic fibrosis airway epithelial cells. *Journal of Antimicrobial Chemotherapy* **70**, 160–166 (2015).
118. Lashua, L. P. *et al.* Engineered cationic antimicrobial peptide (eCAP) prevents Pseudomonas aeruginosa biofilm growth on airway epithelial cells. *Journal of Antimicrobial Chemotherapy* **71**, 2200–2207 (2016).
119. Price, K. E. *et al.* Mannitol does not enhance tobramycin killing of Pseudomonas aeruginosa in a cystic fibrosis model system of biofilm formation. *PLoS ONE* **10**, 1–9 (2015).
120. Tan, N. C. W. *et al.* Small-colony variants and phenotype switching of intracellular Staphylococcus aureus in chronic rhinosinusitis. *Allergy: European Journal of Allergy and Clinical Immunology* **69**, 1364–1371 (2014).
121. Starner, T. D., Zhang, N., Kim, G. H., Apicella, M. A. & McCray, P. B. Haemophilus influenzae forms biofilms on airway epithelia: Implications in cystic fibrosis. *American Journal of Respiratory and Critical Care Medicine* **174**, 213–220 (2006).
122. Luscher, A. *et al.* Combined Bacteriophage and Antibiotic Treatment Prevents Pseudomonas aeruginosa Infection of Wild Type and cftr- Epithelial Cells. *Frontiers in Microbiology* **11**, (2020).

123. Hiemstra, P. S., Grootaers, G., van der Does, A. M., Krul, C. A. M. & Kooter, I. M. Human lung epithelial cell cultures for analysis of inhaled toxicants: Lessons learned and future directions. *Toxicology in Vitro* **47**, 137–146 (2018).
124. Graef, F. *et al.* In Vitro Model of the Gram-Negative Bacterial Cell Envelope for Investigation of Anti-Infective Permeation Kinetics. *ACS Infectious Diseases* **4**, 1188–1196 (2018).
125. Aerogen® (access date 2022-01-30). https://www.aerogen.com/.
126. Thorn, C. R., Clulow, A. J., Boyd, B. J., Prestidge, C. A. & Thomas, N. Bacterial lipase triggers the release of antibiotics from digestible liquid crystal nanoparticles. *Journal of Controlled Release* **319**, 168–182 (2020).
127. Roche® Cytotoxicity Detection Kit (access date 2022-01-30). https://www.sigmaaldrich.com/content/dam/sigma-aldrich/docs/Roche/Bulletin/1/11644793001bul.pdf.
128. Dolovich, M. B. & Dhand, R. Aerosol drug delivery: Developments in device design and clinical use. *The Lancet* **377**, 1032–1045 (2011).
129. Di Cristo, L. *et al.* Repeated exposure to aerosolized graphene oxide mediates autophagy inhibition and inflammation in a three-dimensional human airway model. *Materials Today Bio* **6**, (2020).
130. Di Cristo, L. *et al.* Towards the identification of an in vitro tool for assessing the biological behavior of aerosol supplied nanomaterials. *International Journal of Environmental Research and Public Health* **15**, (2018).
131. Foster, K. A., Avery, M. L., Yazdanian, M. & Audus, K. L. Characterization of the Calu-3 cell line as a tool to screen pulmonary drug delivery. *International Journal of Pharmaceutics* **208**, 1–11 (2000).
132. Barosova, H. *et al.* Use of EpiAlveolar Lung Model to Predict Fibrotic Potential of Multiwalled Carbon Nanotubes. *ACS Nano* **14**, 3941–3956 (2020).
133. Sauer, K., Camper, A. K., Ehrlich, G. D., Costerton, J. W. & Davies, D. G. Pseudomonas aeruginosa displays multiple phenotypes during development as a biofilm. *Journal of Bacteriology* **184**, 1140–1154 (2002).
134. Lacroix, G. *et al.* Air-Liquid Interface in Vitro Models for Respiratory Toxicology Research: Consensus Workshop and Recommendations. *Applied In Vitro Toxicology* **4**, 91–106 (2018).
135. ATCC® PAO1-GFP (access date 2022-01-30). https://www.lgcstandards-atcc.org/products/all/10145GFP.aspx?geo_country=de.
136. O'Toole, G. A. Microtiter Dish Biofilm Formation Assay. *Journal of Visualized Experiments* 10–11 (2011).
137. Montefusco-Pereira, C. V. *et al.* P. Aeruginosa infected 3D co-culture of bronchial epithelial cells and macrophages at air-liquid interface for preclinical evaluation of anti-infectives. *Journal of Visualized Experiments* **2020**, 1–20 (2020).
138. Van den Bossche, S., Vandeplassche, E., Ostyn, L., Coenye, T. & Crabbé, A. Bacterial Interference With Lactate Dehydrogenase Assay Leads to an Underestimation of Cytotoxicity. *Frontiers in Cellular and Infection Microbiology* **10**, 1–11 (2020).
139. Ehrhardt, C. *et al.* Influence of apical fluid volume on the development of functional intercellular junctions in the human epithelial cell line 16HBE14o-: Implications for the use of this cell line as an in vitro model for bronchial drug absorption studies. *Cell and Tissue Research* **308**, 391–400 (2002).
140. Robert Richter. Predicting Bacterial Accumulation of Anti-infectives by Measuring Permeability across Surrogates of the Gram-negative Bacterial Cell Envelope.

(Saarland University, 2020).
141. Murgia, X. *et al.* Modelling the bronchial barrier in pulmonary drug delivery: A human bronchial epithelial cell line supplemented with human tracheal mucus. *European Journal of Pharmaceutics and Biopharmaceutics* **118**, 79–88 (2017).
142. Halldorsson, S. *et al.* Azithromycin maintains airway epithelial integrity during Pseudomonas aeruginosa infection. *American Journal of Respiratory Cell and Molecular Biology* **42**, 62–68 (2010).
143. Koeppen, K. *et al.* Tobramycin reduces key virulence determinants in the proteome of Pseudomonas aeruginosa outer membrane vesicles. *PLoS ONE* **14**, 1–14 (2019).
144. Stover, C. K. *et al.* Complete genome sequence of Pseudomonas aeruginosa PAO1, an opportunistic pathogen. *Nature* **406**, 959–964 (2000).
145. PAO1 DSM 22644 (date accessed 2022-01-30). https://www.dsmz.de/collection/catalogue/details/culture/DSM-22644.
146. Sultana, S. T., Call, D. R. & Beyenal, H. Eradication of Pseudomonas aeruginosa biofilms and persister cells using an electrochemical scaffold and enhanced antibiotic susceptibility. *npj Biofilms and Microbiomes* **2**, 2 (2016).
147. Periasamy, S. *et al.* Pseudomonas aeruginosa PAO1 exopolysaccharides are important for mixed species biofilm community development and stress tolerance. *Frontiers in Microbiology* **6**, 1–10 (2015).
148. Zemke, A. C., Kocak, B. R. & Bomberger, J. M. Sodium nitrite inhibits killing of Pseudomonas aeruginosa biofilms by ciprofloxacin. *Antimicrobial Agents and Chemotherapy* **61**, 16–19 (2017).
149. Friedman, L. & Kolter, R. Genes involved in matrix formation in Pseudomonas aeruginosa PA14 biofilms. *Molecular Microbiology* **51**, 675–690 (2004).
150. Wang, L., Fan, D., Chen, W. & Terentjev, E. M. Bacterial growth, detachment and cell size control on polyethylene terephthalate surfaces. *Scientific Reports* **5**, 1–11 (2015).
151. Woodworth, B. A., Tamashiro, E., Bhargave, G., Cohen, N. A. & Palmer, J. N. An in vitro model of Pseudomonas aeruginosa biofilms on viable airway epithelial cell monolayers. *American Journal of Rhinology* **22**, 235–238 (2008).
152. Castaneda, P., McLaren, A., Tavaziva, G. & Overstreet, D. Biofilm Antimicrobial Susceptibility Increases With Antimicrobial Exposure Time. *Clinical Orthopaedics and Related Research* **474**, 1659–1664 (2016).
153. van Gennip, M. *et al.* Interactions between polymorphonuclear leukocytes and Pseudomonas aeruginosa biofilms on silicone implants in vivo. *Infection and Immunity* **80**, 2601–2607 (2012).
154. Binder incubators (date accessed 2022-01-30). https://www.binder-world.com/de/produkte/co2-inkubatoren/.
155. Hoechst 33342 (date accessed 2022-01-30). https://www.thermofisher.com/order/catalog/product/H3570.
156. Lee, V. T., Smith, R. S., Tümmler, B. & Lory, S. Activities of Pseudomonas aeruginosa Effectors Secreted by the Type III Secretion System In Vitro and during Infection. *Infection and Immunity* **73**, 1695–1705 (2005).
157. Jyot, J. *et al.* Type II secretion system of pseudomonas aeruginosa: In vivo evidence of a significant role in death due to lung infection. *Journal of Infectious Diseases* **203**, 1369–1377 (2011).
158. Hoang, T. T., Karkhoff-Schweizer, R. R., Kutchma, A. J. & Schweizer, H. P. A broad-host-range Flp-FRT recombination system for site-specific excision of chromosomally-located DNA sequences: application for isolation of unmarked Pseudomonas

aeruginosa mutants. *Gene* **212**, 77–86 (1998).
159. Guillon, A. *et al.* Pseudomonas aeruginosa proteolytically alters the interleukin 22-dependent lung mucosal defense. *Virulence* **8**, 810–820 (2017).
160. Dasgupta, N. *et al.* A four-tiered transcriptional regulatory circuit controls flagellar biogenesis in Pseudomonas aeruginosa. *Molecular Microbiology* **50**, 809–824 (2003).
161. Ma, L. *et al.* Assembly and development of the Pseudomonas aeruginosa biofilm matrix. *PLoS Pathogens* **5**, (2009).
162. Hoffmann, T., Krug, D., Hüttel, S. & Müller, R. Improving natural products identification through targeted LC-MS/MS in an untargeted secondary metabolomics workflow. *Analytical Chemistry* **86**, 10780–10788 (2014).
163. Krug, D. & Müller, R. Secondary metabolomics: The impact of mass spectrometry-based approaches on the discovery and characterization of microbial natural products. *Natural Product Reports* **31**, 768–783 (2014).
164. Krug, D. *et al.* Discovering the hidden secondary metabolome of Myxococcus xanthus: A study of intraspecific diversity. *Applied and Environmental Microbiology* **74**, 3058–3068 (2008).
165. Yang, L. *et al.* In situ growth rates and biofilm development of Pseudomonas aeruginosa populations in chronic lung infections. *Journal of Bacteriology* **190**, 2767–2776 (2008).
166. Gruenert, D. C., Willems, M., Cassiman, J. J. & Frizzell, R. A. Established cell lines used in cystic fibrosis research. *Journal of Cystic Fibrosis* **3**, 191–196 (2004).
167. Ehrhardt, C. *et al.* Towards an in vitro model of cystic fibrosis small airway epithelium: Characterisation of the human bronchial epithelial cell line CFBE41o-. *Cell and Tissue Research* **323**, 405–415 (2006).
168. Gupta, P., Chhibber, S. & Harjai, K. Subinhibitory concentration of ciprofloxacin targets quorum sensing system of pseudomonas aeruginosa causing inhibition of biofilm formation & reduction of virulence. *Indian Journal of Medical Research* **143**, 643–651 (2016).
169. Bhat, M. *et al.* Regulation of Tight Junction Permeability by Calcium Mediators and Cell Cytoskeleton in Rabbit Tracheal Epithelium. *Pharmaceutical Research: An Official Journal of the American Association of Pharmaceutical Scientists* vol. 10 991–997 (1993).
170. Haghi, M. *et al.* Mono- and Cocultures of Bronchial and Alveolar Epithelial Cells Respond Differently to Proinflammatory Stimuli and Their Modulation by Salbutamol and Budesonide. *Molecular Pharmaceutics* **12**, 2625–2632 (2015).
171. Garcia-Medina, R., Dunne, W. M., Singh, P. K. & Brody, S. L. Pseudomonas aeruginosa acquires biofilm-like properties within airway epithelial cells. *Infection and Immunity* **73**, 8298–8305 (2005).
172. Puchelle, E., Zahm, J. M., Tournier, J. M. & Coraux, C. Airway epithelial repair, regeneration, and remodeling after injury in chronic obstructive pulmonary disease. *Proceedings of the American Thoracic Society* **3**, 726–733 (2006).
173. Nichols, D. P. & Chmiel, J. F. Inflammation and its genesis in cystic fibrosis. *Pediatric Pulmonology* **50**, S39–S56 (2015).
174. Eisele, N. A. & Anderson, D. M. Host Defense and the Airway Epithelium: Frontline Responses That Protect against Bacterial Invasion and Pneumonia. *Journal of Pathogens* **2011**, 1–16 (2011).
175. Kube, D., Sontich, U., Fletcher, D., Davis, P. B. & Sontich, U. T. E. Infection in Human Airway Epithelial Cell Lines. *Molecular Physiology* **4948**, 493–502 (2010).

176. Cantin, A. M., Hartl, D., Konstan, M. W. & Chmiel, J. F. Inflammation in cystic fibrosis lung disease: Pathogenesis and therapy. *Journal of Cystic Fibrosis* **14**, 419–430 (2015).
177. Lewis, K. Persister cells, dormancy and infectious disease. *Nature Reviews Microbiology* **5**, 48–56 (2007).
178. Dongari-Bagtzoglou, A. Pathogenesis of mucosal biofilm infections: Challenges and progress. *Expert Review of Anti-Infective Therapy* **6**, 201–208 (2008).
179. Vázquez-Espinosa, E. *et al.* Long-term safety and efficacy of tobramycin in the management of cystic fibrosis. *Therapeutics and Clinical Risk Management* **11**, 407–415 (2015).
180. Rejman, J., Di Gioia, S., Bragonzi, A. & Conese, M. Pseudomonas aeruginosa infection destroys the barrier function of lung epithelium and enhances polyplex-mediated transfection. *Human Gene Therapy* **18**, 642–652 (2007).
181. Ren, D. *et al.* Characterization of extended co-culture of non-typeable Haemophilus influenzae with primary human respiratory tissues. *Experimental Biology and Medicine* **237**, 540–547 (2012).
182. Grainger, C. I., Greenwell, L. L., Lockley, D. J., Martin, G. P. & Forbes, B. Culture of Calu-3 cells at the air interface provides a representative model of the airway epithelial barrier. *Pharmaceutical Research* **23**, 1482–1490 (2006).
183. Doughty, M. J. PH dependent spectral properties of sodium fluorescein ophthalmic solutions revisited. *Ophthalmic and Physiological Optics* **30**, 167–174 (2010).
184. Thorn, C. R. *et al.* Tobramycin Liquid Crystal Nanoparticles Eradicate Cystic Fibrosis-Related Pseudomonas aeruginosa Biofilms. *Small* **2100531**, 1–17 (2021).
185. Van Roy, F. & Berx, G. The cell-cell adhesion molecule E-cadherin. *Cellular and Molecular Life Sciences* **65**, 3756–3788 (2008).
186. Bhatt, T., Rizvi, A., Batta, S. P. R., Kataria, S. & Jamora, C. Signaling and mechanical roles of E-cadherin. *Cell Communication and Adhesion* **20**, 189–199 (2013).
187. Lippmann, E. S., Al-Ahmad, A., Azarin, S. M., Palecek, S. P. & Shusta, E. V. A retinoic acid-enhanced, multicellular human blood-brain barrier model derived from stem cell sources. *Scientific Reports* **4**, 1–10 (2014).
188. Hakimzadeh, A., Okshevsky, M., Maisuria, V., Déziel, E. & Tufenkji, N. Exposure to Freeze-Thaw Conditions Increases Virulence of Pseudomonas aeruginosa to Drosophila melanogaster. *Environmental Science and Technology* **52**, 14180–14186 (2018).
189. Allegretta, G. *et al.* In-depth profiling of MvfR-regulated small molecules in Pseudomonas aeruginosa after Quorum Sensing inhibitor treatment. *Frontiers in Microbiology* **8**, 1–12 (2017).
190. Bandyopadhaya, A. *et al.* Bacterial-excreted small volatile molecule 2-aminoacetophenone induces oxidative stress and apoptosis in murine skeletal muscle. *International Journal of Molecular Medicine* **37**, 867–878 (2016).
191. Bandyopadhaya, A., Tsurumi, A., Maura, D., Jeffrey, K. L. & Rahme, L. G. A quorum-sensing signal promotes host tolerance training through HDAC1-mediated epigenetic reprogramming. *Nature Microbiology* **1**, 1–9 (2016).
192. Hurley, M. N., Cámara, M. & Smyth, A. R. Novel approaches to the treatment of Pseudomonas aeruginosa infections in cystic fibrosis. *European Respiratory Journal* **40**, 1014–1023 (2012).
193. Sriramulu, D. D., Lünsdorf, H., Lam, J. S. & Römling, U. Microcolony formation: A novel biofilm model of Pseudomonas aeruginosa for the cystic fibrosis lung. *Journal of Medical Microbiology* **54**, 667–676 (2005).

194. Frisch, S. *et al.* A pulmonary mucus surrogate for investigating antibiotic permeation and activity against Pseudomonas aeruginosa biofilms. *Journal of Antimicrobial Chemotherapy* **76**, 1472–1479 (2021).
195. Zabner, J. *et al.* Development of cystic fibrosis and noncystic fibrosis airway cell lines. *American Journal of Physiology - Lung Cellular and Molecular Physiology* **284**, 844–854 (2003).

Scientific output

Peer-reviewed publications

Horstmann, J.C., Boese, A., Laric, A., Yildiz, D., Röhrig, T., Empting, M., Frank, N., Krug, D., Müller, R., Schneider-Daum, N., de Souza Carvalho-Wodarz, C. and Lehr, C.-M. (2022) Transferring microclusters of *P. aeruginosa* biofilms to the air-liquid Interface of bronchial epithelial cells for repeated deposition of aerosolized tobramycin. *ACS Infect. Dis*., 8 (1), 137-149. DOI 10.1021/acsinfecdis.1c00444

Thorn, C.R., De Souza Carvalho-Wodarz, C., **Horstmann, J.C.**, Lehr, C-M., Prestidge, C. A., Thomas, N. (2021) Tobramycin liquid crystal Nanoparticles eradicate Cystic Fibrosis-related *Pseudomonas aeruginosa* biofilms. *Small* 17 (24), 2100531. DOI 10.1002/smll.202100531.

Horstmann, J.C., Thorn, C.R., Carius, P., Graef, F., Murgia, X., De Souza Carvalho-Wodarz, C., Lehr, C-M. (2021) A custom-made device for reproducibly depositing pre-metered doses of nebulized drugs on pulmonary cells in vitro, *Front. Bioeng. Biotechnol*. 9, 9:643491. DOI 10.3389/fbioe.2021.643491

Schütz, C., Ho, D-K, Hamed, M.M., Abdelsamie, A.S., Röhrig, T., Herr, C., Kany, A.M., Rox, K., Schmelz, S., Siebenbürger, L., Wirth, M., Börger, C., Yahiaoui, S., Bals, R., Scrima, A., Blankenfeldt, W., **Horstmann, J.C.,** Christmann, R., Murgia, X., Koch, M., Berwanger, A., Loretz, B., Hirsch, A.K.H., Hartmann, R.W., Lehr, C-M., Empting, M. A (2021) New PqsR Inverse Agonist Potentiates Tobramycin Efficacy to Eradicate Pseudomonas aeruginosa Biofilms. *Adv. Sci.* 8 (12), 2004369. DOI: 10.1002/advs.202004369

Frisch, S., Boese, A., Huck, B., **Horstmann, J.C.,** Ho, D.K., Schwarzkopf, K., Murgia, X., Loretz, B., Carvalho-Wodarz, C., Lehr, C.M. (2021) A pulmonary mucus surrogate for investigating antibiotic permeation and activity against Pseudomonas aeruginosa biofilms, *J. Antimicrob. Chemother.* 76 (6), 1472–1479. DOI 10.1093/jac/dkab068

Montefusco-Pereira, C.V.*, **Horstmann, J.C.*,** Ebensen, T., Beisswenger, C., Bals, R., Guzmán, C.A., Schneider-Daum, N., Carvalho- Wodarz, C.S., Lehr, C.M. (2020) P. aeruginosa Infected 3D Co-Culture of Bronchial Epithelial Cells and Macrophages at Air-Liquid Interface for Preclinical Evaluation of Anti-Infectives. *J. Vis*. Exp. (160). DOI 10.3791/61069 **(*shared first authorship)**

Book chapters

Carius, P.*, **Horstmann, J.C.*,** de Souza Carvalho-Wodarz, C. Lehr, C.M. (2020) Disease Models: Lung Models for Testing Drugs Against Inflammation and Infection. In: Schäfer-Korting M., Stuchi Maria-Engler S., Landsiedel R. (eds) Organotypic Models in Drug Development. Handbook of Experimental Pharmacology. Springer, Cham. DOI 10.1007/164_2020_366 **(*shared first authorship)**

Schneider-Daum, N., Carius, P., **Horstmann, J.C.**, Lehr, C.M. (2020) Reconstituted 2D Cell and Tissue Models. In: Hickey, A. J. and da Rocha S.R. (Eds.), Pharmaceutical Inhalation Aerosol Technology, Third edition, CRC Press. DOI 10.1201/9780429055201

Poster

Carlos V. Montefusco-Pereira, Justus Horstmann, Jenny Juntke, Christine K. Maurer, Martin Empting, Rolf W. Hartmann, Cristiane Carvalho-Wodarz, Nicole Schneider-Daum, Claus-Michael Lehr

Novel *in-vitro* cystic fibrosis human bronchial epithelial cell co-culture models infected with *P. aeruginosa*

HIPS Symposium, June 2018, Saarbrücken, Germany

An Abstract was prepared in advance of the poster presentation.

Justus Horstmann, Carlos V. Montefusco-Pereira, Martin Empting, Rolf W. Hartmann, Cristiane Carvalho-Wodarz, Nicole Schneider-Daum, Claus-Michael Lehr

Novel *in vitro* cystic fibrosis co-culture model consisting of human bronchial epithelial cells infected with *P. aeruginosa* to study biofilm formation and host-pathogen interactions

12th International conference and workshop on biological barriers, August 2018, Saarbrücken, Germany

An Abstract was prepared in advance of the poster presentation.

Justus Horstmann, Carlos V. Montefusco-Pereira, Martin Empting, Rolf W. Hartmann, Cristiane Carvalho-Wodarz, Nicole Schneider-Daum, Claus-Michael Lehr

Novel *in vitro* cystic fibrosis co-culture model consisting of human bronchial epithelial cells infected with *P. aeruginosa* to study biofilm formation and host-pathogen interactions

5th Pulmonary Drug Delivery Workshop, September 2018, Dublin, Ireland

An Abstract was prepared in advance of the poster presentation.

Justus C. Horstmann, Carlos V. Montefusco-Pereira, Thomas Ebensen, Carlos A. Guzmán, Christian Schütz, Teresa Röhrig, Martin Empting, Rolf W. Hartmann, Cristiane Carvalho-

Wodarz, Nicole Schneider-Daum, Claus-Michael Lehr

***P. aeruginosa*-infected co-culture of human cystic fibrosis bronchial epithelial cells as a preclinical test system for anti-infectives**

HIPS Symposium, June 2019, Saarbrücken, Germany

An Abstract was prepared in advance of the poster presentation.

Justus C. Horstmann, Annette Boese, Sarah Frisch, Cristiane Carvalho-Wodarz, Nicole Schneider-Daum, Claus-Michael Lehr

Infection of CFBE41o- cells with pre-formed *P. aeruginosa* biofilm at Air-Liquid Interface as pre-clinical test system for anti-infectives

Doktorandentag der Naturwissenschaftlich-Technischen Fakultät der Universität des Saarlandes, November 2019, Saarbrücken, Germany

Oral presentations

Justus C. Horstmann, Cristiane Carvalho-Wodarz, Nicole Schneider-Daum, Claus-Michael Lehr

Cystic fibrosis bronchial epithelial cells infected with *P. aeruginosa* biofilm at air-liquid interface for new anti-infectives tests

19th Scientific Meeting Mukoviszidose e.V., September 2019 Montabaur, Germany

An Abstract was prepared in advance of the oral presentation.

Justus C. Horstmann, Cristiane Carvalho-Wodarz, Nicole Schneider-Daum, Claus-Michael Lehr

***P. aeruginosa* infected co-culture of human cystic fibrosis bronchial epithelial cells as a preclinical test system for anti-infectives**

22nd European Congress on Alternatives to Animal Testing, October 2019 Linz, Austria

An Abstract was prepared in advance of the oral presentation.

Justus C. Horstmann, Annette Boese, Nicole Schneider-Daum, Cristiane Carvalho-Wodarz, Claus-Michael Lehr

***P. aeruginosa* biofilm infected bronchial epithelium as test system for anti-infective aerosol formulations**

Planned on 12th World Meeting on Pharmaceutics, Biopharmaceutics and Pharmaceutical Technology, March 2020, Vienna, Austria, but cancelled due to Covid-19 pandemic

An Abstract was prepared in advance. Talk was taken over by Claus-Michael Lehr in May 2021 as virtual meeting.

Acknowledgements - Danksagung

Nach fast 3 ½ Jahren endet meine Zeit am HIPS in Saarbrücken. In dieser Zeit habe ich vor allem gelernt, wie ein Wissenschaftler zu denken und zu handeln. Der Erfolg ist mir in keiner Weise zugeflogen, sondern war von Anfang an hart erarbeitet. Das motiviert mich, auch kommende Projekte zu einem Erfolg zu führen, auch wenn sie noch so herausfordernd sind. Geduld und Nachhaltigkeit tragen irgendwann Früchte.

Allem voran möchte ich mich für das Vertrauen bedanken, das mein Doktorvater Prof. Dr. Claus-Michael Lehr in mich gesetzt hat. Vor allem ihm habe ich die interessante Stelle am Helmholtz-Institut für pharmazeutische Forschung Saarland zu verdanken. Er war es, der mich gelehrt hat, die richtigen Fragen zu stellen, um an eine wissenschaftliche Antwort zu kommen.

Ein großes Dankeschön geht auch an meine erste Betreuerin Frau Dr. Nicole Schneider-Daum und an meine darauffolgende Betreuerin Frau Dr. Cristiane Carvalho-Wodarz. Nicole hat mich gerade am Anfang darauf aufmerksam gemacht, wie wichtig es ist, genau zu arbeiten. Cristiane hat in besonderem Maße meine Begeisterung für das Thema geteilt. Sie hat mich beraten und unterstützt, einschließlich der letzten Publikation Ende 2021, noch lange über die Zeit am HIPS hinaus.

Zum Ende dieser langen Reise geht mein Dank natürlich auch an meinen wissenschaftlichen Begleiter Prof. Dr. Rolf Hartmann für seine Unterstützung, vor allem im Rahmen der Thesis Committee Meetings. Prof. Dr. Marc Schneider habe ich in unseren Blockseminaren sehr gut kennenlernen können und bedanke mich an dieser Stelle für seine freundliche Unterstützung.

Der Lung Club hat mich von Anfang an begleitet, von den ersten Versuchen einer wissenschaftlichen Präsentation im März/April 2017 bis zum Vorstellen meiner wissenschaftlichen Erfolge im Sommer 2020. Ich konnte während der ganzen Zeit von dem wissenschaftlichen Austausch sehr profitieren. Aber auch die gemeinsamen HIPS Events sind mir noch in guter Erinnerung, allem voran BioBarriers, als auch schon die erwähnten Blockseminare zusammen mit der Arbeitskreis Pharmazeutische Technologie mit Prof. Schneider. Auch möchte ich mich vor allem bei Frau Dr. Brigitta

Loretz bedanken, die mir immer mit einem offenen Ohr zur Verfügung stand und mich mit Ratschlägen unterstützt hat, bis zum Schluss.
Es gibt unzählige Weggefährten meiner Zeit in Saarbrücken, denen ich danken möchte, so viele, dass ich hoffentlich keine(n) vergesse.
Angefangen bei meinem langjährigen Büronachbarn Patrick, mit dem ich viel Zeit verbringen durfte und wir uns bei allen Fragen des Alltags bestens unterstützt haben. Carlos und Robert kenne ich schon seit den ersten Stunden unseres Lung Clubs, und zum Schluss haben wir uns alle ein Büro geteilt – das waren viele lustige Stunden, die ich sehr vermisse, vor allem Carlos´ speziellen Humor sowie die witzigen und wissenschaftlichen Unterhaltungen mit Robert. Sarah hat später Carlos´ Platz würdig eingenommen und es war mir eine Freude, mit Ihr wissenschaftlich zu arbeiten. Danke für Deine Unterstützung.
2019/2020 hat uns Chelsea aus Australien für einige Monate am HIPS besucht. Ihre Mithilfe an unserem Projekt haben entscheidend zum Erfolg beigetragen, nicht zuletzt durch die praktische Anwendung meines Modells, was mich sehr stolz macht. Vielen Dank für Deine Unterstützung!
Ich bedanke mich des Weiteren beim BION Team um Gregor, Kathrin, Eilien, Thomas, Mina, Adriely und Max für die gute Zusammenarbeit und die schöne und lustige Zeit.
Das gilt natürlich auch für alle anderen auf unserem langen Flur, viele kamen und gingen, aber man konnte sich mit allen gut austauschen und hat den Menschen im Kollegen kennen lernen können. Besonders erwähnen möchte ich Remi (die man meistens schon von weitem lachen hörte und für viel Stimmung sorgte), Sara Nasr, Lena, Lung Club Kollegen Alberto, Samy und Clémentine, Thiago, Benedikt (mit dem ich mit Adriely meine Liebe zu den Gators teile), Olga und natürlich Rebekka (mit der ich seit dem ersten Tag des Pharmaziestudiums Analysen gekocht habe und mit der ich meinen letzten Tag am HIPS verbracht habe – unglaublich!).
Besonders hervorheben möchte ich auch die tolle Arbeit unserer wissenschaftlichen Mitarbeiter(innen) Jana, Petra, Annette und Pascal. Ohne euch hätte ich gerade zum Schluss meine Zellen kaum versorgen können. Annette konnte mich in meiner Arbeit zum Biofilm gut unterstützen und Pascal hat mich mit vielen LC – MS Analysen

unterstützt sowie am SEM. Im Büro war immer eine professionelle, aber gelöste Stimmung. Auch Sarah Müller, Annette Herkströter, und natürlich Karin Groß danke ich sehr für die gesamte administrative Unterstützung – bis zum Schluss. Ich habe mich immer gefreut, bei euch vorbeizukommen☺

Auch außerhalb unseres Institutes gab es viele Menschen, die mein Leben und meine Arbeit in Saarbrücken zu einem schönen Lebensabschnitt gemacht haben. Danke Marcel, Thorben, Johannes und Aljoscha - ich bin euch für die gemeinsame Zeit in Saarbrücken sehr dankbar.

Danke auch an meine Gator Kollegin Katharina, die, wie der Zufall es wollte, auch in Saarbrücken gelandet war, für die vielen Treffen auch außerhalb von Orlando;) Nicht zuletzt aber danke ich meinem guten Freund Tarek, den ich, wie die Rebekka, schon seit der ersten Stunde des Pharmaziestudiums kenne und mit dem ich viel erlebt habe. Unsere Wohnungen lagen nur einen Steinwurf entfernt, wir waren viel unterwegs und haben uns gegenseitig immer wieder motiviert. Danke Dir für alles, ohne dich wäre Saarbrücken nur halb so schön gewesen!

Zum Schluss möchte ich meiner Mutter und meiner Schwester danken, die immer an mich geglaubt haben und dafür, dass ich bei euch einfach ich sein kann. Aber allem voran geht der größte Dank an meine Frau Nadine, die mich bis heute immer wieder mental unterstützt hat, wenn es nicht ganz so rund lief – damit hat sie einen entscheidenden Beitrag zum Erfolg des Projekts geleistet. Gerade in der Anfangszeit meiner Promotion gab es viele Gelegenheiten dazu. Ich freue mich sehr auf die kommende Zeit mit Dir. Ich liebe Dich!